# A THREE-BODY SCATTERING MODEL USING DELTA SHELL INTERACTIONS

by

K. J. Nieukerke
Natuurkundig Ingenieur, Delft

A thesis submitted in accordance with
the requirements of the degree of
Doctor of Philosophy

Department of Mathematical Physics,
University of Adelaide

August, 1979

*To Vivian*

ABSTRACT

A model is presented for the rearrangement scattering of heavy ions. The two ions scatter either elastically or by the exchange of a valence particle between the otherwise identical cores. This becomes a three-body problem when the internal degrees of freedom in the cores are ignored. In the Faddeev formalism the two scattering processes are treated in a coherent manner. The model assumes delta shell interactions between all particles. This potential permits the reduction of the three-body equations to equivalent two-body equations with effective potentials. The core-core interaction can contribute at three levels of sophistication to the effective potential in the integral equation for the half-on-shell amplitude. The calculations are carried out for a vanishing core-core potential.

Singularities off the real axis at infinity prevent using the standard solution method of contour rotation. The integration path along the real line crosses a number of singular points contained in the kernel. The treatment of these points is discussed in detail.

The interactions do not correspond to physical potentials. A different theoretical approach enables the testing of the numerical calculations. Its base lies in the expansion in Sturmian states of the wave function for the core-valence particle subsystem . This adiabatic model leads to a differential equation in the static limit . A formal proof of the identity of both approaches is presented for zero range interactions.

Calculations for s-state to s-state scattering are carried out at various energies above the three-body threshold. The effects of the approxmations in the "Sturmian" approach are compared with the exact results.

STATEMENT

This thesis contains no material which has been accepted for the award of any other degree or diploma in any University and, to the best of the candidate's knowledge and belief, the thesis contains no material previously published or written by any other person, except where due reference is made in the text of the thesis.

K. J. Nieukerke

ACKNOWLEDGEMENTS

It gives me great pleasure to thank Lindsay Dodd for his support in the years of research. I especially appreciated his continuous criticism on the draft of this thesis.

My thanks also go to the members of the department for supplying a stimulating and friendly environment.

The financial assistance of a University Research Grant and a Commonwealth Postgraduate Research Award between 1974 and 1979 is gratefully acknowledged.

Last, but not least, I am indebted to Barbara Beilby for lending her expertise in typing the manuscript.

CONTENTS

Page No.

# CHAPTER 1

## INTRODUCTION

Rearrangement scattering between heavy ions is a many body reaction process. A much simpler picture, that keeps the essential features intact, is obtained when the interactions between the individual nucleons are replaced by potentials between the centres of mass of the three clusters that characterise the process: the two cores and the exchanged cluster. In other words: a three-body reaction is the minimal description that can be used to model this type of rearrangement process. Transfer reactions are most likely in grazing collisions and are treated theoretically as a direct reaction (1 - 3). Calculations are often based on the distorted wave Born approximation (DWBA) (4 - 6). However, there are many instances where the DWBA fails to fit the experimental data (7 and ref. therein).

In the past much attention has been paid to rearrangement reactions where only one heavy ion is involved, such as stripping and pick-up processes. There are some clear theoretical advantages over the scattering of two heavy ions. The relative angular momentum of the scatterers will be small even at energies above the Coulomb barrier. The DWBA is much simplified if terms proportional to the displacement in the centre of mass of the composite particle, due to the valence particle, are ignored (no recoil), or approximately taken into account (8, 9). The aim of some model calculations (10 - 13) has been to test the DWBA directly or via quantities that it predicts, such as the spectroscopic factor. A recent review is given by Redish (14). He states: "The comparison between an exact model, an exact DWBA and a realistic DWBA could be very useful in understanding whether the phenomenological freedom in relativistic DWBA's masks the true reaction mechanism."

We wish to present in this thesis a model for a transfer reaction between two heavy ions. The class of reactions of specific interest is exemplified by

$$C^{12} + C^{13} \rightarrow C^{12} + C^{13} \ . \qquad (1.1)$$

The reaction (1.1) has a number of interesting features. First of all, there are two coherent scattering processes that fall under the symbolic expression (1.1): the elastic scattering process

$$C^{13} \ (C^{12}, \ C^{12}) \ C^{13} \ , \qquad (1.2)$$

and the rearrangement scattering process

$$C^{13} \ (C^{12}, \ C^{13}) \ C^{12} \ . \qquad (1.3)$$

This suggests that a scattering amplitude should be obtained using the Faddeev formulation. Here the two scattering processes are coupled in a coherent manner. Secondly, the mass ratio of transferred particle and core is small, but not negligible. In an exact model calculation this can throw some light on the importance of the recoil effects. And finally, one can expect a simplification in the theoretical approach due to the identical cores.

Another way to calculate the scattering amplitude is with the DWBA, as has been done in the past for this particular reaction (15, 16). The DWBA makes a clear distinction between the elastic and the rearrangement scattering process. In the elastic process the amplitude consists of three parts: the direct elastic scattering due to the core-core potential, the direct elastic scattering due to the presence of the valence particle and a term caused by the symmetry in the process - the transfer scattering at an angle complementary to the elastic scattering (see Fig. 1.1). In the rearrangement scattering only the last two types will appear.

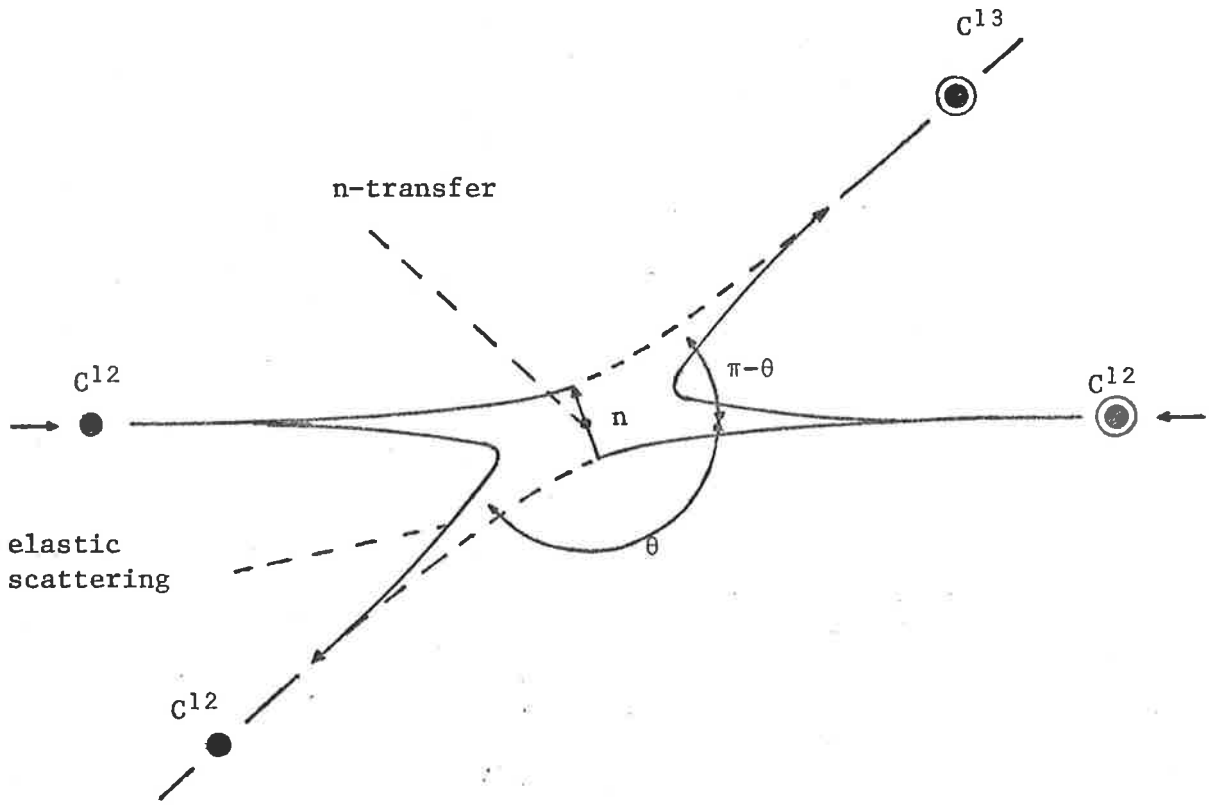


Fig. 1.1: $C^{12} + C^{13} \rightarrow C^{12} + C^{13}$ (from Ref. 16)

There are a number of other models which can also be used to describe the process (1.1). Gobbi et al (16) explained their experimental results successfully by a coherent addition of an elastic scattering amplitude, obtained by a smooth cut-off model, and a transition amplitude obtained from a semi-classical DWBA. Von Oetzen (17) developed a model based on the adiabatic assumption, using molecular wave functions in a two state approximation. In a slow scattering process the valence particle can rescatter several times between the cores during the time of interaction. This is in contrast with the DWBA, which describes an essentially one step process. In a comparison of these two methods by Bauer and Gelbke (18), no indication is

found for multiple scattering taking place. This might explain why the two methods are in good agreement in this case. However, often the exclusion of multi step processes is a factor in the failure of the DWBA to reproduce experimental results. Multi step processes may be included in the theory by explicit consideration of competing channels as in the coupled channel Born approximation (19). An exact model calculation would be very valuable in trying to answer many of the open questions mentioned so far.

Let us now consider the reasons for the choice of a delta shell potential to describe the interactions between particles in the model. It is a separable potential, which means that it is especially suited for the use in the Faddeev formulation (20, 21). The potential is also local. It follows that the interaction is specified in all angular momentum states by two parameters, the radius of the delta shell and the strength of the interaction. With the choice of the strength and the radius one can vary the number of bound states that can be supported by the potential. This provides a restriction on the number of open initial and final channels in the Faddeev equations.

The form factors, used in the description of the potential in momentum space, are a product of a spherical Bessel function and a spherical harmonic in each angular momentum state. Form factors, depending parametrically on the sum of two momenta, can consequently be factorised in form factors depending only on the separate single momentum variable. This brings an enormous advantage in the partial wave expansion of the integral equation for the scattering amplitude.

These convenient properties of the delta shell potential are somewhat offset by the fact that the standard methods to solve the integral equations cannot be applied. The spherical Bessel functions are entire functions, which become singular at infinity off the real axis, and hence prevent the

use of rotated contours in the solution process. This has proved to be the major technical obstacle in obtaining solutions for our model. In the past the delta potential has been used in the one-dimensional N-particle problem (22, 23), and in the one-dimensional, three-body problem with identical particles (24), and with arbitrary mass particles (25, 26). The δ-interaction in 3-dimensions is singular. The next simplest possibility is the δ-shell interaction, used by R. van Wageningen et al (27) in a three nucleon bound state study. The interaction formed by the combination of a Yamaguchi potential and a delta shell interaction is known in the literature as the Puff potential (28). In this separable, non-local potential the strength of the delta shell is usually taken to be positive infinite, providing for a repulsive hard shell (29, 30).

In Chapter 2 we will introduce the variables, give basic definitions and formulate the standard Faddeev equations. As stated above we are interested in the scattering process where the two heavy ions are identical. This means that the scattering amplitude must by symmetrized. The fact that the elastic and rearrangement scattering process are indistinguishable is used to reduce the number of coupled integral equations. Next it is realized that the core-core interaction can be incorporated into the model at three different levels of sophistication. In the intermediate level the amplitude, obtained with vanishing core-core interaction, is modified, requiring only the calculation of simple matrix elements and no further matrix inversions. The derivation, given in detail in Appendix B, relies on the separability of the effective core-core potential.

The model is restricted to delta shell interactions between all particles. Chapter 3 deals with the special properties of the form factors of this potential. It is the simple factorisation of the form factors, which depend parametrically on the sum of two momenta, that make the model extremely

suitable for the description of the scattering of two heavy ions. Higher total orbital angular momentum states, which one can expect to contribute considerably at energies above the Coulomb barrier, are easily handled by the model. They manifest themselves as constituents of the vector coupling coefficients and in the occurrence of higher order Legendre functions of the second kind.

The integral equation for the scattering amplitude has a kernel with moving singularities. As mentioned before, the spherical Bessel functions contained in the kernel, prevent the use of the standard solution method. We have chosen to integrate along the real axis and treat each of the singularities as it is met. Only the case with vanishing core-core interaction is studied numerically. The different types of singularities in the kernel are discussed at the start of Chapter 4, and their location in the real plane is established. This is followed by a detailed explanation of the treatment of the singular points in the numerical integration.

The method is an extension on the approach of Larson and Hetherington (31). Our set up allows a greater freedom in the location of the mesh points. We give a complete, mathematical discussion of treatment of the logarithmic singularity, including the handling of the physical limit. And it is shown how the occurrence of a square root branch point restricts the interpolation procedure for the amplitude near this point.

The choice of a delta shell potential to describe the interaction in the model means that the cross section obtained in the calculations cannot be compared directly with a physical experiment. It was therefore thought especially important to derive a different method to test our computed results. The spectator wave function can be expanded in a complete set of states that describe the subsystem consisting of one core and the valence particle. For the bound states in this set, the problem reduces to a set

of coupled equations of the Lippmann-Schwinger form (the close coupling scheme). This approach suggested that the completely discrete set, formed by the Sturmian states (which are the eigenstates of the kernel of a two-body Lippmann-Schwinger equation), would provide a more suitable basis for this type of expansion. This is worked out in the second part of Chapter 5. A new set of equations, equivalent to the Faddeev equations, is obtained. In the adiabatic limit the close coupling and Sturmian schemes are compared, indicating that the new expansion might be superior to calculations based on the close coupling approach.

The Sturmian expansion is then applied to the delta shell interaction. Using a Fourier transform a change is made from momentum to configuration space. As it turns out, the equations are simply expressed in differential form and the scattering amplitude is related to the asymptotic phase shift. Since the Sturmian scheme and the Faddeev formulation are equivalent, the theoretical results of the two approaches are shown to be so too. This proof is carried out in the zero range limit of the delta shell for s-state to s-state scattering.

In the following chapter, results of the numerical calculations are presented. All calculations are carried out for s-state to s-state scattering with vanishing core-core interaction. To test the integral equation program (i.e.p.) for energies below threshold it is first modified to incorporate the restriction enforced in the Sturmian approach. Good agreement is obtained with the results of the differential equation program (d.e.p.) that gives the solutions using the Sturmian scheme. For energies above threshold the full i.e.p. is compared with an iterative solution, using a suitably adjusted interaction strength.

The differential cross sections are presented for various centre of mass energies ranging between 1 and 50 MeV. The phase shifts are given in tabulated form and examples are shown of half-on-shell amplitudes.

In the final section of this chapter we test the restrictive assumptions in the Sturmian approach: the static and the adiabatic limits. By varying the mass ratio $m$ of the core and valence particles it is established that the static limit conditions set in for $m > 30$. No definite conclusion can be drawn for the range of the adiabatic region. In general the Sturmian approach shows limited agreement with the exact calculations. This discrepancy can be attributed to the long range behaviour of the form factors and half-on-shell amplitude in momentum space. This puts some doubt on the applicability of the Sturmian expansion (and for that matter, other schemes using the adiabatic limit) in approximate calculations for the case of local potentials.

In the final chapter the main achievements are summarised. An outline is sketched for further calculations which could give a direct answer to some of the questions raised earlier. Although the theory and calculations presented here have not been developed sufficiently to test the assumptions of the DWBA, it is hoped that further work, based on the present approach, will ultimately be of value in a comparison of theory and experiment.

# CHAPTER 2

## THE FADDEEV EQUATIONS FOR SEPARABLE POTENTIALS

The first section of this chapter contains a description of variables and some basic definitions. Following this the Faddeev equations are introduced. An important feature of the model is the choice of identical cores. The effects of this symmetry is studied in the next section. The final part deals with the core-core potential. A number of ways of incorporating this interaction in the model are discussed.

### 2.1 Variables and Basic Definitions

The heavy ion cores will be labelled 1 and 2, the valence particle has label 3 (see Fig. 2.1), with respective masses $m_i$ and momenta $k_i (i=1,2,3)$.

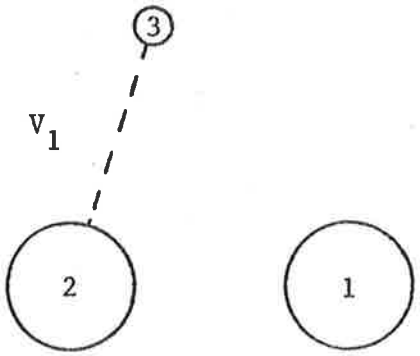


Fig. 2.1: Labelling of the particles and the two-body interaction

The free Hamiltonian (see f.i. 27) for the system is

$$H_o = \frac{p_i^2}{2\mu_i} + \frac{q_i^2}{2\bar{\mu}_i} , \tag{2.1}$$

where $\vec{p}_i$ and $\vec{q}_i$ are the usual momentum variables

$$\vec{p}_i = \frac{m_i(\vec{k}_j + \vec{k}_k) - (m_j + m_k)\vec{k}_i}{m_i + m_j + m_k} \qquad \vec{q}_i = \frac{m_k\vec{k}_j - m_j\vec{k}_k}{m_j + m_k} , \tag{2.2}$$

and the reduced masses are

$$\mu_i = \frac{m_i(m_j + m_k)}{m_i + m_j + m_k} , \quad \bar{\mu}_i = \frac{m_j m_k}{m_j + m_k} . \tag{2.3}$$

The momentum variables in the different channels are linearly dependent. The cyclic relations are

$$\vec{q}_i = \vec{p}_j + \frac{m_j}{m_j + m_k} \vec{p}_i \ , \tag{2.4}$$

and

$$\vec{q}_j = - \vec{p}_i - \frac{m_i}{m_i + m_k} \vec{p}_j \ . \tag{2.5}$$

In the model it is assumed that only two-body forces are acting. It has long been realized that representing the interactions by separable potentials has great advantages (20, 21). The interaction $V_i$ between the particles j and k may be written as

$$V_i = \sum_\alpha \lambda_{i\alpha} \int d^3p_i \ |f_{i,\alpha}, \vec{p}_i\rangle \langle \vec{p}_i, f_{i,\alpha}| \ . \tag{2.6}$$

The strength of the interaction is $\lambda_{i\alpha}$. In momentum space the form factor becomes

$$\langle \vec{p}_i, \vec{q}_i | f_{i,\alpha}, \vec{p}_i' \rangle = \delta(\vec{p}_i - \vec{p}_i') \ f_{i,\alpha}(\vec{q}_i) \ . \tag{2.7}$$

The two-body t-matrix acting in three-body space can now be expressed as

$$t_i(E) = \sum_\alpha \int d^3p_i \ |f_{i,\alpha}, \vec{p}_i\rangle \ \tau_{i\alpha}\left(E - \frac{p_i^2}{2\mu_i}\right) \langle \vec{p}_i, f_{i,\alpha}| \ . \tag{2.8}$$

To ease the notation the small positive imaginary part of the energy E is not denoted explicitly throughout. An exception is Chapter 4 on the numerical methods, where the imaginary part is used in the description of the treatment of the singular points. Before defining $\tau$, we introduce the two-body energy $\sigma$. In channel i this energy is

$$\sigma_i = E - \frac{p_i^2}{2\mu_i} \ , \tag{2.9}$$

and the free Green's operator in the two particle subsystem is defined by

$$g_o = \frac{1}{\sigma_i - q_i^2/2\bar{\mu}_i} \ . \tag{2.10}$$

The expression for the inverse of $\tau$ is the two-body equation[†]

$$\tau_{i\alpha}^{-1}(\sigma_i) = \lambda_{i\alpha}^{-1} - \langle f_{i,\alpha} | g_o(\sigma_i) | f_{i,\alpha} \rangle \quad . \tag{2.11}$$

It may be that there is a two-body bound state in channel $i,\alpha$ with the energy

$$\sigma_i = - \varepsilon_{i\alpha} \quad . \tag{2.12}$$

For this energy the $\tau$ will have a pole and, as can be seen from (2.11),

$$\lambda_{i\alpha}^{-1} = \langle f_{i,\alpha} | g_o(- \varepsilon_{i\alpha}) | f_{i,\alpha} \rangle \quad . \tag{2.13}$$

The corresponding bound state wave function is

$$|\phi_\alpha^{(i)}\rangle = G_o(E) | f_{i,\alpha}, \vec{p}_i \rangle \tag{2.14}$$

if the E is evaluated on the energy shell. The three-body free Green's operator is here defined as

$$G_o(E) = (E - H_o)^{-1} \quad . \tag{2.15}$$

It is assumed that the strength and the form factor are adjusted so that this state is normalised as follows:

$$\langle f_{i,\alpha}, \vec{p}_i' | G_o^2 \left( \frac{p_i^2}{2\mu_i} - \varepsilon_{i\alpha} \right) | f_{i,\alpha}, \vec{p}_i \rangle = \delta(\vec{p}_i - \vec{p}_i') \quad . \tag{2.16}$$

In the initial state assume particle 2 and 3 are bound. In the Faddeev formulation the eigenstate $\psi_{1\alpha}^+$ of the complete Hamiltonian is written as a sum of spectator wave functions,

---

[†]The two-body tau (2.11) and hence the two-body t-matrix (2.8) need not necessarily be diagonal in the form-factors. For simplicity this has been assumed here. As we shall show in the next chapter the label $\alpha(\beta)$ can, for the interaction of interest, be identified with the angular momentum quantum number. $V_i$ and $g_o$ both commute with the angular momentum operators $L^2$ and $L_3$ and the simplification is therefore allowed.

$$|\psi^{+}_{1\alpha}> = |\psi^{(1)}_{1\alpha}> + |\psi^{(2)}_{1\alpha}> + |\psi^{(3)}_{1\alpha}> \quad . \tag{2.17}$$

The Faddeev equations relate these wave functions (see 32, 33):

$$|\psi^{(i)}_{1\alpha}> = |\phi^{(i)}_{\alpha},\vec{p}_i> \delta_{i1}\delta_{\alpha\rho} + \sum_{j\neq i} G_o(E)\, t_i(E)\, |\psi^{(j)}_{1\alpha}> . \tag{2.18}$$

Let

$$X_{j\beta,i\alpha}(\vec{p}_j',\vec{p}_i) = \sum_{k\neq j} <\vec{p}_j, f_{j,\beta}\, |\psi^{(k)}_{i\alpha}> \quad , \tag{2.19}$$

then, following Lovelace (34),

$$X_{j\beta,i\alpha}(\vec{p}_j,\vec{p}_i) = Z_{j\beta,i\alpha}(\vec{p}_j,\vec{p}_i) + \sum_{k,\gamma} \int d^3p_k\, Z_{j\beta,k\gamma}(\vec{p}_j,\vec{p}_k)\, \tau_{k\gamma}(\sigma_k)\, X_{k\gamma,i\alpha}(\vec{p}_k,\vec{p}_i) \quad . \tag{2.20}$$

Note that (2.20) forms a set of coupled integral equations. The potential term Z is defined as

$$Z_{j\beta,i\alpha}(\vec{p}_j,\vec{p}_i) = (1 - \delta_{ij}) <\vec{p}_j, f_{j\beta}|\, G_o(E)\, |f_{i\alpha},\vec{p}_i> \quad . \tag{2.21}$$

These equations were derived independently by Amado applying field theoretical arguments (35). Lovelace shows that $X_{j\beta,i\alpha}$ on the energy shell is the physical scattering amplitude from channel $i\alpha$ to channel $j\beta$. In particular, the elastic scattering amplitude is given by

$$X_{1\beta,1\alpha}(\vec{p}',\vec{p}) = <\vec{p}', \phi^{(1)}_{\beta}|V^1|\psi^{+}_{1\alpha}> \quad , \tag{2.22}$$

and the amplitude for rearrangement scattering by

$$X_{2\beta,1\alpha}(\vec{p}',\vec{p}) = <\vec{p}', \phi^{(2)}_{\beta}|V^2|\psi^{+}_{1\alpha}> \quad , \tag{2.23}$$

where $V^i = \sum_{j\neq i} V_j$ is the interaction in the final channel.

## 2.2 Identical Particles

So far the theory has been general, in that all the particles were different. With the model, however, we wish to describe a scattering process with two identical particles. Spin is not taken into consideration, hence all particles are to be treated as bosons.

In the general case (36), with C a normalization constant and $S$ a symmetrization operator the scattering amplitude is

$$A^S = \frac{C_i C_f}{4} < S(\vec{p}',\phi_\beta) |T| S(\vec{p},\phi_\alpha)> \quad , \tag{2.24}$$

where the identical particles are identified as the two heavy ions. Writing $T$ ($V_f$ is the interaction in the final channel) as

$$T = \lim_{\xi \to o} V_f \frac{i\xi}{E - H + i\xi} \quad , \tag{2.25}$$

and symmetrizing the final state results in

$$A^S = \frac{C_i}{2\sqrt{2}} \{ < \vec{p}',\phi_\beta^{(1)} | \; V^1 \frac{i\xi}{E - H + i\xi} \; |S(\vec{p},\phi_\alpha)> \; + $$

$$< \vec{p}',\phi_\beta^{(2)} | \; V^2 \frac{i\xi}{E - H + i\xi} \; |S(\vec{p},\phi_\alpha)> \} \quad . \tag{2.26}$$

For the initial state we have

$$\frac{C_i}{2} \frac{i\xi}{E - H + i\xi} \; |S(\vec{p},\phi_\alpha)> \; = \frac{C_i}{2} \; |S\psi_{1\alpha}^+> \; =$$

$$\frac{1}{\sqrt{2}} \{ |\psi_{1\alpha}^+> \; + \; |\psi_{2\alpha}^+> \} \quad , \tag{2.27}$$

and therefore the symmetrized amplitude becomes

$$A^S = \tfrac{1}{2} \{ < \vec{p}',\phi_\beta^{(1)} |V^1| \psi_{1\alpha}^+> \; + < \vec{p}',\phi_\beta^{(2)} |V^2| \psi_{2\alpha}^+> \; +$$

$$< \vec{p}',\phi_\beta^{(1)} |V^1| \psi_{2\alpha}^+> \; + < \vec{p},\phi_\beta^{(2)} |V^2| \psi_{1\alpha}^+> \} \quad . \tag{2.28}$$

Not surprisingly this symmetrized form of the amplitude can partly be attributed to elastic scattering (first two terms), but the other part has the appearance of rearrangement elements. This confirms in a theoretical

manner, what has been clear from the outset, namely, that in the physical experiment it is impossible to distinguish between elastic and rearrangement scattering.

Dropping the energy, momentum and channel quantum label from the notation for the moment, there are two sets of integral equations that should be solved. One set where particle one is free in the initial state

$$\begin{aligned} X_{11} &= Z_{12}\,\tau_2\,X_{21} + Z_{13}\,\tau_3\,X_{31}\,, \\ X_{21} &= Z_{21} + Z_{21}\,\tau_1\,X_{11} + Z_{23}\,\tau_3\,X_{31}\,, \\ X_{31} &= Z_{31} + Z_{31}\,\tau_1\,X_{11} + Z_{32}\,\tau_2\,X_{21}\,, \end{aligned} \tag{2.29}$$

and one where particle two is free in the initial state

$$\begin{aligned} \bar{X}_{12} &= Z_{12} + Z_{12}\,\tau_2\,\bar{X}_{22} + Z_{13}\,\tau_3\,\bar{X}_{32}\,, \\ \bar{X}_{22} &= Z_{21}\,\tau_1\,\bar{X}_{12} + Z_{23}\,\tau_3\,\bar{X}_{32}\,, \\ \bar{X}_{32} &= Z_{32} + Z_{31}\,\tau_1\,\bar{X}_{12} + Z_{32}\,\tau_2\,\bar{X}_{22}\,. \end{aligned} \tag{2.30}$$

The scattering amplitude that is measured is given by

$$A^S = \tfrac{1}{2}\{X_{1\beta,1\alpha} + X_{2\beta,1\alpha} + \bar{X}_{1\beta,2\alpha} + \bar{X}_{2\beta,2\alpha}\}\,. \tag{2.31}$$

Identical cores, and hence identical interactions means also that some of the factors in (2.29) and (2.30) are related. With the following identities, that result directly from their definitions, we can reduce the number of integral equations to one

$$\tau_{1\alpha}\left(E - \frac{p^2}{2\mu_1}\right) = \tau_{2\alpha}\left(E - \frac{p^2}{2\mu_2}\right) = \tau_{\alpha}\left(E - \frac{p^2}{2\mu}\right)\,, \tag{2.32a}$$

$$Z_{1\alpha,2\beta}(\vec{p}\,',\vec{p}) = Z_{2\alpha,1\beta}(-\vec{p}\,',-\vec{p}) = (-)^{\alpha+\beta}\,Z_{2\alpha,1\beta}(\vec{p}\,',\vec{p})\,, \tag{2.32b}$$

$$Z_{3\alpha,1\beta}(\vec{p}\,',\vec{p}) = Z_{1\alpha,3\beta}(-\vec{p}\,',-\vec{p}) = (-)^{\alpha+\beta}\,Z_{3\alpha,2\beta}(\vec{p}\,',\vec{p})\,. \tag{2.32c}$$

Using the relations (2.32) one finds after some algebraic manipulations (Appendix A)

$$A^{S}_{\beta,\alpha}(\vec{p}',\vec{p}) = \tfrac{1}{2}[1 + (-)^{\alpha+\beta}]\, V_{\beta,\alpha}(\vec{p}',\vec{p})\delta_{\alpha\rho} + \sum_{\gamma}\int d^3p''\ (-)^{\beta+\gamma} V_{\beta,\gamma}(\vec{p}\,,\vec{p}'')\tau_{\gamma}\left(E - \frac{p''^2}{2\mu}\right) A^{S}_{\gamma,\alpha}(\vec{p}'',\vec{p}) \ , \qquad (2.33)$$

where the newly introduced function is

$$V_{\beta,\alpha}(\vec{p}',\vec{p}) = Z_{1\beta,2\alpha}(\vec{p}',\vec{p}) + 2\sum_{\gamma}\int d^3p''\ (-)^{\beta+\gamma} Z_{1\beta,3\gamma}(\vec{p}',\vec{p}'')\ \tau_{3\gamma}\left(E - \frac{p''^2}{2\mu}\right) Z_{3\gamma,1\alpha}(\vec{p}'',\vec{p}) \ . \qquad (2.34)$$

The integral part of V is a result of the elimination of the amplitude $X_{31}$ from the set of equations. This again reduces the number of coupled equations by one. Hence the original reduction, due to the symmetry in the cores, is the same as has been indicated by Lovelace (34) (from three to two coupled equations). The reason that we prefer the form given here instead of two coupled equations, is that it shows explicitly how the amplitude is affected when the core-core interaction is approximated. Some possibilities are discussed in the next section.

## 2.3 The Core-Core Interaction

In this section we shall indicate three possible levels at which the core-core interaction can be treated. The simplest way assumes a vanishing core-core potential. In the Faddeev formulation the minimum one needs in the theory to describe the desired process of elastic and rearrangement scattering is the interactions between the valence particle and each of the cores. This is a result of the multiple scattering character of the equations. It is in contrast with such theories as the DWBA, where the core-core interaction is essential, since it produces the distorted wave functions.

Before discussing the next level, it is advantageous to bring out the Lippmann-Schwinger character of (2.33). This is achieved by making the pole in the function $\tau$ explicit. Substituting (2.13) into (2.11) and applying the operator identity

$$A - B = A \left(\frac{1}{B} - \frac{1}{A}\right) B \tag{2.35}$$

on the Green's operators results in the new form for $\tau$:

$$\tau_{i\alpha}(\sigma_i) = \frac{1}{\sigma_i + \varepsilon_{i\alpha}} S^2_{i\alpha}(\sigma_i) \ , \tag{2.36}$$

where the new functions $S_{i\alpha}$ are defined by

$$S^{-2}_{i\alpha}(\sigma_i) = < f_{i\alpha} | g_o(\sigma_i) g_o(-\varepsilon_{i\alpha}) | f_{i\alpha} > \ . \tag{2.37}$$

From the normalization condition Eq. (2.16) on the bound state it follows directly, that the $S_{i\alpha}$ has the value unity on the energy shell. The explicit analytic properties of the scalar function $S_{i\alpha}$ depend on the choice of the form factors. In general one can say that it has a square root singularity at $\sigma = 0$. Eq. (2.33) is now "symmetrized" in the functions S through multiplication from the left by $S_{j\beta}(p')$ and from the right by $S_{i\alpha}(p)$, so

$$\begin{aligned} \tilde{A}^S_{\beta,\alpha}(\vec{p}',\vec{p}) &= \tfrac{1}{2} [\, 1 + (-)^{\beta+\alpha}] \ \tilde{V}_{\beta,\alpha}(\vec{p}',\vec{p}) \delta_{\alpha\rho} \ + \\ &\sum_\gamma \int d^3p'' \ (-)^{\beta+\gamma} \ \tilde{V}_{\beta,\gamma}(\vec{p}',\vec{p}'') \ \frac{1}{\sigma'' + \varepsilon_\gamma} \ \tilde{A}^S_{\gamma,\alpha}(\vec{p}'',\vec{p}) \ . \end{aligned} \tag{2.38}$$

The new wiggled functions are defined by the symbolic equation:

$$\tilde{B}_{j\beta,i\alpha}(\vec{p}',\vec{p}) = S_{j\beta}(p') \ B_{j\beta,i\alpha}(\vec{p}',\vec{p}) \ S_{i\alpha}(p) \ . \tag{2.39}$$

Note that because the S have the value of unity on the energy shell the $\tilde{A}^S$ will give the correct value for the scattering amplitude.

The intermediate level in the treatment of the core-core interaction is obtained if the effective potential $\tilde{V}$ can be written as

$$\tilde{V}_{\beta\alpha} = \tilde{V}^o_{\beta\alpha} + |\theta_\beta> \ c_{\beta\alpha} < \phi_\alpha| \ , \tag{2.40}$$

where the $\tilde{V}^o_{\beta\alpha}$ is the symmetrized form of the $Z_{\beta\alpha}$. If one denotes by $\tilde{A}^o$ the half-on-shell amplitude resulting from the integral equation containing only the $\tilde{V}^o$:

$$\tilde{A}^o = \tilde{V}^o + \tilde{V}^o \ g_o \ \tilde{A}^o \ , \tag{2.41}$$

and the complete integral equation by

$$\tilde{A}^S = \tilde{V} + \tilde{V}\, g_o\, \tilde{A}^S \ , \tag{2.42}$$

then it is shown in Appendix B that

$$\tilde{A}^S = \tilde{A}^o + (1 + A^o\, g_o)\ |\theta\rangle\ \Phi\ \langle\phi|\ (1 + g_o\, A^o) \ , \tag{2.43}$$

where the new operator is defined by

$$\Phi^{-1} = c^{-1} - \langle \phi|\ g_o(1 + A^o\, g_o)\,|\theta\rangle \ . \tag{2.44}$$

There are a number of remarks to be made about equation (2.43). First of all one notices that it properly reflects the fact that the total amplitude reduces to the amplitude $\tilde{A}^o$ when the core-core interaction becomes negligible. Secondly, it is observed that only matrix elements need to be calculated. No new integral equation needs to be solved to obtain the total amplitude at this level.

Equation (2.40) will only in a limited number of cases be a valid description for the interaction. In Appendix C we indicate how under certain conditions one can expect a separable form for the core induced part of the potential $\tilde{V}$.

The final level uses the form as it stands in Eq. (2.34). In actual calculations this means, that, after the equations have been digitalized, one has to calculate the integral part of the potential for preset combinations of $p'$ and $p$, tabulate these and store them. Depending on the choice of the form factors this integral will contain several kinds of moving singularities which makes that a considerable task. In this thesis we shall only present the results of calculations in the case of vanishing core-core interaction.

To summarize our achievements so far: in the first section the basic integral equations governing the scattering process have been set up. In the next section this set of coupled equations was reduced, using a symmetry

in the model: identical cores. Three levels of treating the core-core interaction were discussed in the final section. The interesting, intermediate level opens the possibility of testing, in a very simple manner, the influence on the scattering amplitude of different strength core-core interactions.

# CHAPTER 3

## THE DELTA SHELL INTERACTION AND THE PARTIAL WAVE EXPANSION OF THE INTEGRAL EQUATION

In order to develop the model further one has to decide on the specific form for the interaction between the particles. We choose a delta shell potential to describe the two-body interactions. This potential is local as well as separable.

Some of its special properties are that it has the same strength in each partial wave and a simple expression for the form factor in spherical harmonics. The form factor may be easily factorized when it depends on the sum of two momenta. This is worked out in the first section.

The next part deals with the partial wave expansion of the integral equation. This is facilitated by the factorization property of the form factor and allows the interaction in all angular momentum states to be parameterized simply.

### 3.1 The Delta Shell Potential

The locality property of the interaction shows clearly in configuration space:

$$\langle \vec{r}|V_i|\vec{r}'\rangle = \lambda_i \, \delta(\vec{r} - \vec{r}') \, \delta(r - r_o) \, , \tag{3.1}$$

where $\lambda_i$ is the strength of the interaction and $r_o$ the radius of the shell. The general expression for a separable potential using form factors has already been stated in (2.6). Leaving out the momentum of the third non-interacting particle (the potential is diagonal in this variable), we can write the interaction in momentum space as

$$\langle \vec{q}|V_i|\vec{q}'\rangle = \sum_\alpha \lambda_{i\alpha} \, f^*_{i\alpha}(\vec{q}) \, f_{i\alpha}(\vec{q}') \, . \tag{3.2}$$

A comparison of (3.1) and (3.2) can serve as a definition of the form factors as the two relations are connected via a Fourier transform. Inserting

complete sets of coordinate vectors before and after $V_i$ in (3.2), expanding the resulting plane waves in spherical harmonics and using (3.1) yields

$$f_{i,\ell_m}(\vec{q}) = \sqrt{\frac{2}{\pi}}\, r_o\, j_\ell(qr_o)\, Y_\ell^m(\hat{q})\, N_\ell \ . \tag{3.3}$$

The label $\alpha$ is then identified as the set of angular momentum quantum numbers $\ell$ and m. $N_\ell$ is a normalization constant. The notation does not show explicitly how the form factor discriminates between valence-core and core-core interactions (label i). This would be contained in the $r_o$, but is left out since no core-core interaction is considered here and with identical cores all form factors are similar to (3.3). Note that the form factors form an orthogonal set, due to the orthonormality of the $Y_\ell^m$. The two-body t-matrix will be diagonal in the form factors, since $G_o$ and $V_i$ commute with the angular momentum operators $L^2$ and $L_3$. This property was already exhibited by (2.11).

A useful expression for the form factor is also

$$f_{i,\ell_m}(\vec{q}) = \frac{N_\ell}{(2\pi)^{3/2}} \int e^{i\vec{q}\cdot\vec{r}}\, \frac{i^{-\ell}}{r}\, \delta(r - r_o)\, Y_\ell^m(\hat{r})\, d^3r \ . \tag{3.4}$$

Expansion of the plane wave reduces (3.4) almost immediately to (3.3). This relation facilitates the factorization of a form factor which depends on the vector sum $\vec{q}_1 + \vec{q}_2$ ,

$$f_{i,\ell_m}(\vec{q}_1 + \vec{q}_2) = \sum_{\ell_1 m_1, \ell_2 m_2} \frac{1}{r_o}\, \mathrm{cst}\, f^*_{i,\ell_1 m_1}(\vec{q}_1)\, f^*_{i,\ell_2 m_2}(\vec{q}_2) \ , \tag{3.5}$$

with the constant connecting the set of quantum numbers (using $\hat{\ell}=2\ell+1$)

$$\mathrm{cst} = \pi\sqrt{2}\, \frac{N_\ell}{N_{\ell_1} N_{\ell_2}}\, i^{\ell_1+\ell_2-\ell}\, [\hat{\ell}\ \hat{\ell}_1\ \hat{\ell}_2]^{\frac{1}{2}} \begin{pmatrix} \ell & \ell_1 & \ell_2 \\ 0 & 0 & 0 \end{pmatrix} \begin{pmatrix} \ell & \ell_1 & \ell_2 \\ -m & m_1 & m_2 \end{pmatrix} \ . \tag{3.6}$$

The derivation of (3.6) is straightforward. Apply definition (3.4) to the left hand side, and write the exponential as the product of two plane waves, which are then expanded in spherical harmonics. Integration over the

vector $\vec{r}$ yields the result, which is transformed to form factors with (3.3).

It is this factorization that simplifies the partial wave expansion of the integral equation for the amplitude. It makes it possible to incorporate high angular momentum states, expected to contribute significantly in heavy ion scattering above the Coulomb barrier.

An interesting observation that follows from the derivation of (3.3) is the identity

$$\lambda_{i\alpha} \equiv \lambda_i \ . \tag{3.7}$$

Hence the potential has the same strength in <u>each</u> partial wave. This in fact establishes that the delta shell potential is essentially a two parameter interaction. The relation between the strength $\lambda_i$, the range $r_o$ and the binding energy $\varepsilon_{i\ell}$ is determined from the condition that the two-body t-matrix has a single pole at the binding energy,

$$\lambda_i^{-1} = 2r_o^2 \, \bar{\mu}_i \, k_\ell \, j_\ell(ik_\ell \, r_o) \, h_\ell^{(1)} \, (ik_\ell \, r_o) \, N_{i\ell}^2 \ , \tag{3.8}$$

with

$$k_\ell^2 = 2\bar{\mu}_i \, \varepsilon_{i\ell} \ . \tag{3.9}$$

The $(\lambda_i \, N_{i\ell}^2)^{-1}$ is a monotone increasing function in $k_\ell$. The values for $k_\ell = 0$ are easily obtained using the MacLaurin expansion for the spherical Bessel and Hankel functions

$$(\lambda_i \, N_{i\ell}^2)^{-1} \, (0) = 2r_o \, \bar{\mu}_i \, \frac{(2\ell - 1)!!}{(2\ell + 1)!!} \ , \tag{3.10}$$

where

$$(2\ell + 1)!! = 1 \ . \ 3 \ . \ 5 \ \ldots \ (2\ell + 1) \ . \tag{3.11}$$

With the above properties it is clear that we can choose our parameters such that the potential supports none, one or more bound states. Figure 3.1 shows $(\lambda_i \, N_{i\ell}^2)^{-1}$ as a function of $k_\ell$.

It is also possible now to derive the explicit forms for the normalization constant of the bound state wave function (condition 2.16) and the

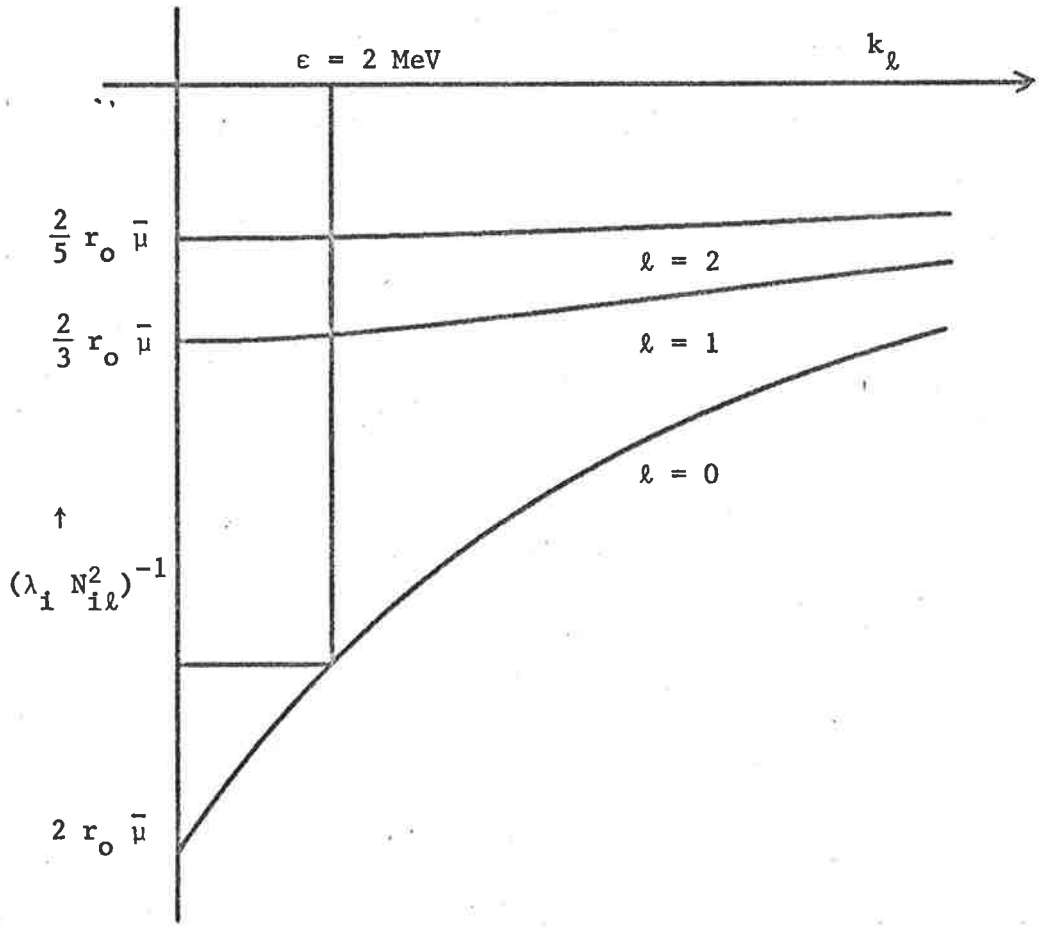


Fig. 3.1: $(\lambda_i\, N_{i\ell}^2)^{-1}$ as a function of $k_\ell$. The graph shows that with a mass ratio $M_o/m_o = 50$ only one bound state is supported with a binding energy of 2 MeV.

scalar S-function (2.37)

$$N_{i\ell}^{-2} = 4r_o^2\ \bar{\mu}_i^{\,2}\ \frac{F_\ell(k_\ell)}{k_\ell}\ , \tag{3.12}$$

with

$$F_\ell(k) = \frac{\partial}{\partial k}\ k\ j_\ell(ikr_o)\ h_\ell^{(1)}(ikr_o)\ , \tag{3.13}$$

and

$$S_{i\ell}^{-2}(\sigma_i) = \frac{2k_\ell}{F_\ell(k_\ell)}\ \frac{[k_i\ j_\ell(ik_ir_o)\ h_\ell^{(1)}(ik_ir_o) - k_\ell\ j_\ell(ik_\ell r_o)\ h_\ell^{(1)}(ik_\ell r_o)]}{(k_i^2 - k_\ell^2)}\ , \tag{3.14}$$

where

$$k_i^2 = -\ 2\bar{\mu}_i\ \sigma_i\ . \tag{3.15}$$

## 3.2 The Partial Wave Expansion

With the results of the previous section it is possible to make a partial wave expansion of the potential term that appears in the integral equation for the scattering amplitude. At the moment we will focus our attention on the case with a vanishing core-core interaction. This means that we are concerned with the integral equation

$$\tilde{A}^o_{\ell'm',\ell m}(\vec{p}',\vec{p}) = \tfrac{1}{2}[1 + (-)^{\ell'+\ell}]\ \tilde{V}^o_{\ell'm',\ell m}(\vec{p}',\vec{p}) +$$

$$\sum_{\ell''m''} \int d^3p''\ (-)^{\ell'+\ell''}\ \tilde{V}^o_{\ell'm',\ell''m''}(\vec{p}',\vec{p}'')\ \frac{1}{\sigma'' + \epsilon_{\ell''}}\ \tilde{A}^o_{\ell''m'',\ell m}(\vec{p}'',\vec{p})\ , \tag{3.16}$$

with the potential

$$\tilde{V}^o_{\ell'm',\ell m}(\vec{p}',\vec{p}) = S_{1\ell'}(p')\ Z_{1\ell'm',2\ell m}(\vec{p}',\vec{p})\ S_{2\ell}(p)\ . \tag{3.17}$$

Therefore the general form of the partial wave expansion for the amplitude in the relative momentum of the scatterers is needed,

$$\tilde{A}^o_{\ell'm',\ell m}(\vec{p}',\vec{p}) = \sum_{L'M',LM} \langle L'M',\ell'm'|A^o|LM,\ell m\rangle\ Y^{M'*}_{L'}(\hat{p}')\ Y^M_L(\hat{p})\ . \tag{3.18}$$

Here $\ell$ is the angular momentum of the initial bound state and L is the angular momentum of the initial free particle with respect to this bound state. The primed parameters have a similar meaning in the final state.

The angular momenta in the initial and final state couple to give the total angular momentum of the state,

$$\tilde{A}^{o}_{\ell'm',\ell m}(\vec{p}',\vec{p}) = \sum_{J'm_{J'},Jm_J,L'M',LM} < J'm_{J'}|L'M',\ell'm' >$$

$$< J'm_{J'},L'\ell'|\tilde{A}^{o}(p',p)|Jm_J,L\ell > < Jm_J|LM,\ell m > Y^{M'*}_{L'}(\hat{p}')\ Y^{M}_{L}(\hat{p}) \ . \qquad (3.19)$$

The notation and definition of the phase factors for the Clebsch Gordon coefficients and related 3-j Wigner symbols is as given by Rotenberg (37) and Messiah (38). The total angular momentum of the system is a conserved quantity and the matrix elements will have rotational symmetry, hence

$$< J'm_{J'},L'\ell'|\tilde{A}^{o}(p',p)|Jm_J,L\ell > = \delta_{JJ'}\ \delta_{m_J m_{J'}} < L'\ell'|A^{oJ}(p',p)|L\ell > \ . \qquad (3.20)$$

The other factor that needs expanding in partial waves is the potential. Using the definition for the Z-function (Eq. 2.21) it can be expressed in the form factors

$$\tilde{V}^{o}_{\ell'm',\ell m}(\vec{p}',\vec{p}) = S_{\ell'}(p')\ f^{*}_{\ell'm'}\left(\vec{p} + \frac{M_o}{m_o + M_o}\vec{p}'\right)$$

$$\frac{1}{E - \frac{p^2}{2\bar{\mu}} - \frac{p'^2}{2\bar{\mu}} - \frac{\vec{p}\cdot\vec{p}'}{m_o}}\ f_{\ell m}\left(-\vec{p}' - \frac{M_o}{m_o + M_o}\vec{p}\right)\ S_{\ell}(p) \ . \qquad (3.21)$$

No distinction needs to be made between the form factors to indicate which particle is free (see remark in 3.2 concerning the identity of the particles). The factorization of the formfactors and their expression in spherical harmonics was discussed in the previous section. For the expansion of the Green's function the following relation between Legendre functions of the first ($P_n$) and second kind ($Q_n$) proves useful

$$Q_n(u) = \tfrac{1}{2}\int \frac{P_n(t)}{u - t}\,dt \ . \qquad (3.22)$$

Multiplying both sides by $\hat{n}\ P_n(s)$, summing over n, and using the closure relation for the $P_n$ yields

$$\frac{1}{u - s} = \sum_n \hat{n}\ P_n(s)\ Q_n(t) \ . \qquad (3.23)$$

Hence the Green's function can be expanded as

$$\frac{1}{E - \frac{p^2}{2\bar{\mu}} - \frac{p'^2}{2\bar{\mu}} - \frac{\vec{p}\cdot\vec{p}'}{m_o}} =$$

$$\frac{m_o}{p'p} 4\pi \sum_{nm_n} Y_n^{m_n *}(\hat{p}') \, Y_n^{m_n}(\hat{p}) \left[ Q_n \frac{1}{2p'p} \left\{ 2m_o E - \frac{m_o + M_o}{M_o} (p^2 + p'^2) \right\} \right] . \tag{3.24}$$

After this the simplification of the expression for the potential is a matter of some tedious algebra. The spherical harmonics are pairwise coupled, resulting in a string of vector coupling coefficients. The integration over the angles of $p''$ is trivial as all angular dependence is concentrated in the spherical harmonics. The last step consists of collecting the coupling coefficients into a number of 6-j symbols through the summation over all the magnetic quantum numbers. A general treatment, including spin can be found in (39). After our manipulations one still has to solve

$$\tilde{A}^{oJ}_{L'\ell',L\ell}(p',p) = \tfrac{1}{2} \left[ 1 + (-)^{\ell'+\ell} \right] c_J \, \tilde{V}^{oJ}_{L'\ell',L\ell}(p',p) +$$

$$\sum_{L''\ell''} \int d\,p'' \; p''^2 \, c_{L''} \, \tilde{V}^{oJ}_{L'\ell',L''\ell''}(p',p'') \frac{1}{E + \epsilon_{\ell''} - \frac{p''^2}{2\mu}} \tilde{A}^{oJ}_{L''\ell'',L\ell}(p'',p) \; , \tag{3.25}$$

where

$$c_\alpha = \frac{2}{\pi} m_o r_o^2 \, \hat{\alpha} \; , \tag{3.26}$$

and

$$\tilde{V}^{oJ}_{L'\ell',L\ell}(p',p) = \sum_{\ell_1\ell_2\ell_1'\ell_2'n} \frac{\tilde{c}_{L'\ell'L\ell}}{p'p} S_{\ell'}(p') \, S_\ell(p) \, N_{\ell'} \, N_\ell$$

$$j_{\ell_1}(p'r_o) j_{\ell_2}\left( \frac{M_o}{m_o + M_o} pr_o \right) j_{\ell_1'} \left( \frac{M_o}{m_o + M_o} p'r_o \right) j_{\ell_2'}(pr_o)$$

$$Q_n \left[ \frac{1}{2p'p} \left\{ 2m_o E - \frac{m_o + M_o}{M_o} (p^2 + p'^2) \right\} \right] , \tag{3.27}$$

with the constant $\tilde{c}$ also dependent on the summation variables $\ell_1\ell_2\ell_1'\ell_2'$ and n (not denoted implicitly in the symbol)

$$\tilde{c}_{L'\ell',L\ell} = \sum_{kk'} \hat{\ell}_1\ \hat{\ell}_2\ \hat{\ell}_1'\ \hat{\ell}_2'\ \hat{n}\ \hat{k}\ \hat{k}'\ [\hat{\ell}\ \hat{\ell}']^{\frac{1}{2}}\ (-)^{\ell'+L'+L}$$

$$i^{\ell-\ell_1-\ell_2-\ell'+\ell_1'+\ell_2'} \begin{pmatrix} \ell & \ell_1 & \ell_2 \\ 0 & 0 & 0 \end{pmatrix} \begin{pmatrix} \ell' & \ell_1' & \ell_2' \\ 0 & 0 & 0 \end{pmatrix} \begin{pmatrix} L & \ell_2 & k \\ 0 & 0 & 0 \end{pmatrix} \begin{pmatrix} k & \ell_2' & n \\ 0 & 0 & 0 \end{pmatrix} \begin{pmatrix} L' & \ell_1 & k' \\ 0 & 0 & 0 \end{pmatrix} \begin{pmatrix} k' & \ell_2' & n \\ 0 & 0 & 0 \end{pmatrix}$$

$$\begin{Bmatrix} J & \ell_1 & k \\ \ell_2 & L & \ell \end{Bmatrix} \begin{Bmatrix} J & \ell_2' & k' \\ \ell_1' & L' & \ell' \end{Bmatrix} \begin{Bmatrix} J & \ell_1 & k \\ n & \ell_2' & k' \end{Bmatrix} . \qquad (3.28)$$

In experiments the quantity measured is the cross section, rather than the scattering amplitude. To establish the relation between the two, the amplitude is expressed in Legendre polynomials

$$\tilde{A}^{o}_{\ell'\ell}(\vec{p}',\vec{p}) = \sum_{L,m'm} C^{L}_{\ell'm',\ell m}(p',p)\ P_L(\cos\theta) , \qquad (3.29)$$

where $\theta$ is the angle between the two momentum vectors $\vec{p}'$ and $\vec{p}$. The cross section is then

$$\frac{d}{d\Omega}\sigma_{\ell'\ell}(E,\theta) = (2\pi)^4\ \mu^2 \left|\tilde{A}^{o}_{\ell',\ell}(\theta)\right|^2 . \qquad (3.30)$$

The cross section given in (3.30) corresponds to the physical situation where the angular momenta of the initial and final bound states ($\ell$ and $\ell'$ resp.) are fixed and one measures the angle of the scattered ions, at a fixed total energy in the process. Combining (3.18), (3.19) and (3.25) with (3.29) gives an expression for the $C^L$

$$C^{L}_{\ell'm',\ell m}(p',p) = \sum_{\substack{Jm_J,LM \\ m'm\ M}} \frac{1}{4\pi}\ (-)^{\ell'+\ell+M+M}\ [\hat{L}\ \hat{L}]^{\frac{1}{2}}$$

$$\begin{pmatrix} J & \ell' & L \\ m_J & m' & -M \end{pmatrix} \begin{pmatrix} J & \ell & L \\ m_J & m & -M \end{pmatrix} \tilde{A}^{oJ}_{L\ell';L\ell}(p',p) . \qquad (3.31)$$

A sum over the conserved total angular momentum J is contained in (3.31). Experimentally one cannot prepare a process with a certain total angular momentum. An approximate upper limit to the relative angular momentum of the scattering particles (L) is determined by the total energy in the system and the impact parameter. The values of the total angular momentum contributing to the cross section are then restricted by the Clebsch-Gordon coefficients.

It might be useful to recapitulate the more important results obtained in this chapter. The delta shell potential has shown itself extremely useful for the partial wave expansion of the integral equation for the scattering amplitude. The reason for this is the simple form for the form factor when expressed in spherical harmonics and the way it factorizes if its argument is a vector sum. Because the potential has the same strength for each partial wave, high angular momentum states are effortlessly incorporated in the model. The number of bound states supported by the delta shell is regulated by the choice of two parameters: the strength and the radius of the interaction. This is of importance in the numerical calculation.

In the next chapter we shall see that the usual approach to the solution of the integral equation breaks down for this interaction. This may be the reason that, despite its many theoretical advantages, the delta shell has been used so sparingly in the past to describe three-body scattering processes.

# CHAPTER 4

## NUMERICAL METHODS

In the previous chapter we have derived the set of integral equations for $\tilde{A}^o$ (see 3.25). The general form of the integral equation can be classified as Fredholm type of the second kind. Leaving out angular momentum labels, and using x, y, and z for the momentum variables, the equation (3.25) may be written as

$$\tilde{A}^o(x,y) = \tilde{V}^o(x,y) + \int_o^\infty dz\ K(x,z)\ \tilde{A}^o(z,y)\ , \qquad (4.1)$$

with the kernel

$$K(x,z) = z^2\ \tilde{V}^o(x,z)\ \frac{1}{E + \varepsilon - z^2/2\mu}\ .$$

The main building blocks of the potential consist of

1. spherical Bessel-functions,
2. Legendre functions of the second kind,
3. the S-function defined by (2.37).

The spherical Bessel-functions are analytic for finite arguments. The Legendre-functions, however, have a logarithmic singularity for argument values ± 1. The S-function arising from separation of the pole from the two-body propagator $\tau$, contains a square root singularity. Symmetrizing the equations with respect to S has made it part of the potential. The kernel includes also the propagator term, which has a simple pole.

In the first section of the chapter each of the singularities in the kernel is studied in general and its location in the x-z plane is determined. Then it is possible to decide which numerical technique is best suited for the problem at hand. The next section is used to explain in general terms the construction of the standard mesh. In the final section some essential details in the treatment of the different types of singularities are discussed.

## 4.1 The Location of the Singularities in the Kernel

### 4.1.1 The Logarithmic Singularity

The form of the Legendre function in the kernel is

$$Q_n \left[ \frac{1}{2xz} \{2m_o E + i\xi - \frac{m_o + M_o}{M_o} (x^2 + z^2)\} \right] . \qquad (4.2)$$

The small imaginary parts of the energy is denoted explicitly. Its mathematical implication shall come forward in the final section, for the moment it can be ignored. The Legendre-function arises from the inner product of the two momentum vectors in the momentum representation of the free Green's operator in three-body space (3.24). In the x-z plane the singularities lie on the two ellipses

$$x^2 + z^2 \pm \frac{2M_o}{m_o + M_o} xz - \frac{2m_o M_o}{m_o + M_o} E = 0 . \qquad (4.3)$$

Only the (physical) first quadrant of the x-z plane is of interest (see Fig. 4.1). The logarithmic structure of the singularities is exposed in the relation between the Legendre-function of the first kind ($P_n$) and of the second kind ($Q_n$) (40)

$$Q_n(u) = \tfrac{1}{2} P_n(u) \ln\left|\frac{1 + u}{1 - u}\right| - W_{n-1}(u) , \qquad (4.4)$$

where

$$W_{n-1}(u) = \sum_{k=1}^{n} \frac{1}{k} P_{k-1}(u) P_{n-k}(u) , \qquad (4.5)$$

and

$$u = \frac{1}{2xz} \{2m_o E - \frac{m_o + M_o}{M_o} (x^2 + z^2)\} . \qquad (4.6)$$

### 4.1.2 The Square Root Singularity

As stated above the S-functions appeared when the pole term in the two-body propagator $\tau$ was made explicit. Their form, for a delta-shell interaction, was given in (3.14). They are functions of

$$k_i = (-2\bar{\mu}_i \sigma_i)^{\frac{1}{2}} = [-2\bar{\mu}_i (E + i\xi) + \frac{\bar{\mu}}{\mu} z^2]^{\frac{1}{2}} . \qquad (4.7)$$

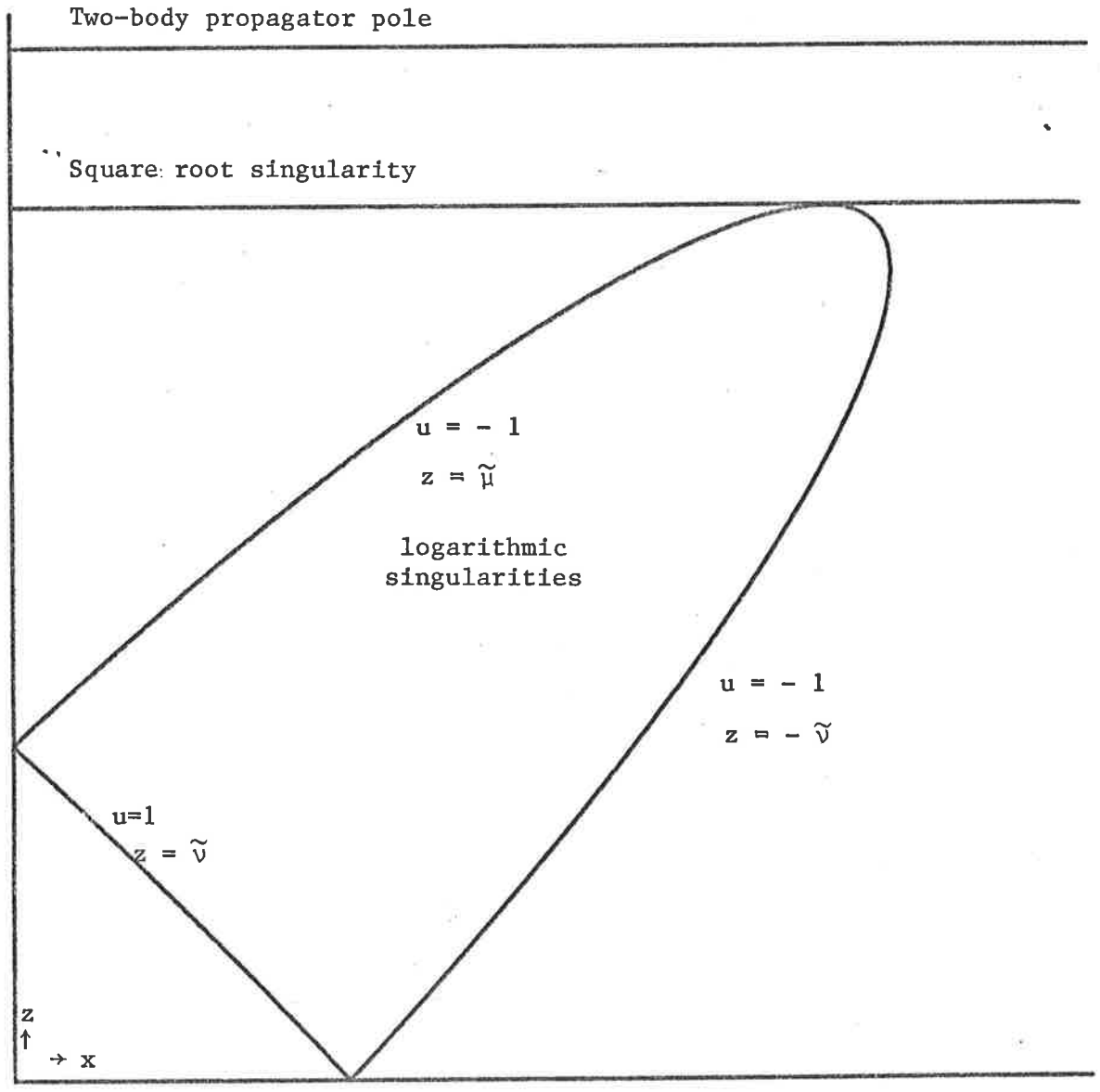


Fig. 4.1: Location of the Singularities in the x-z Plane

There is a square root cut in the complex z-plane. The square root branch point, independent of x, is reached for a z-value which corresponds to the line that grazes the ellipse of the logarithmic singularity (see Fig. 4.1). The small complex part of the energy tells how to construct the $k_i$ so as to ensure that the function is evaluated on the physical sheet (see Fig. 4.2). A reference point for this procedure is the condition that the on-shell

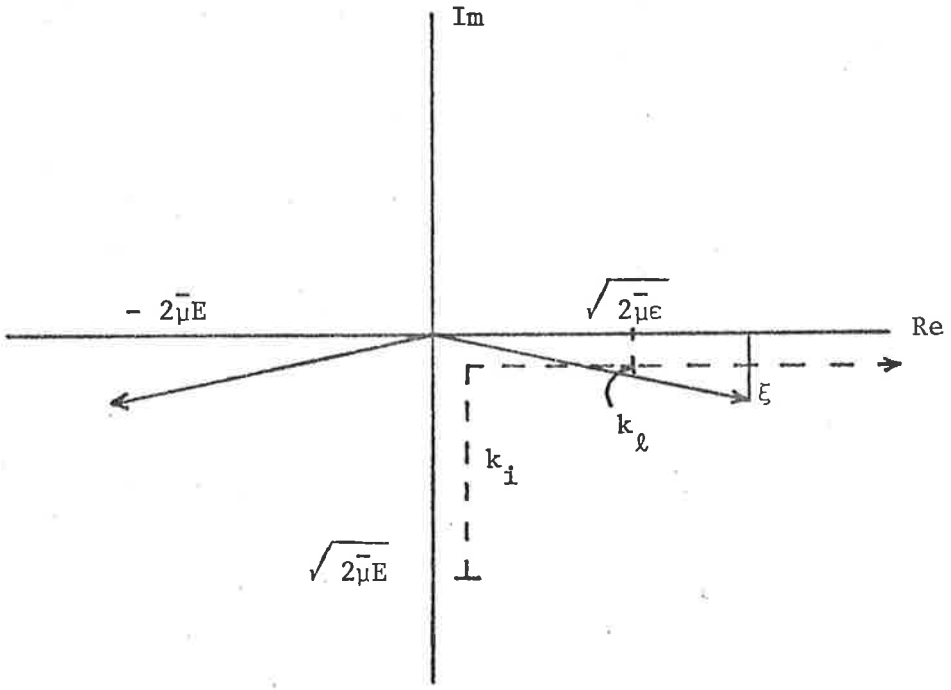


Fig. 4.2: The dotted line indicates the path followed by the $k_i$ in the complex value for increasing z (see 4.7). $k_\ell$ is the on-shell value for $k_i$. The solid arrows give the position of $k_i^2$ for z=0 and corresponding to the square root singularity ($z^2 = 2\mu \{E + \epsilon\}$).

function value of unity reached for

$$k_i = k_\ell > 0 \ . \tag{4.8}$$

In the physical limit ($\xi \to 0$) the S-function will be continuous at the branch point, but not differentiable. This property is carried over to the half-on-shell amplitude, which has become proportional to the S-function when the equations were symmetrized with respect to S. The analytic

properties of the S-function at the branch point will be of importance in the construction of the integration procedure near this point.

4.1.3 The Two-Body Propagator Pole

The form of this singularity, a simple pole, can be read immediately from (4.1) and is reached for

$$E + \epsilon - z^2/2\mu = 0 \ . \tag{4.9}$$

Independent of x, it is a straight line in the x-z plane, parallel to the location of the square root singularity, shifted by the constant

$$c = \sqrt{2\mu\epsilon} \ , \tag{4.10}$$

(see Fig. 4.1).

This completes the description of the location of the singularities in the x-z plane.

4.2 The Choice of the Numerical Approach

In the past the usual approach has been a rotation of the integration path into the complex plane in order to weaken the effects of the singularities (41 - 45). Although the analytic form of the form factors is known in our case this simple procedure cannot be used. The potential contains spherical Bessel functions and the analytic continuation off the real axis at infinity becomes singular. A way of circumventing this problem is to deform the integration path into the complex plane and return to the real line (46). Recently, integration along the real axis to infinity, by treating carefully each singularity as it is met, has been shown to be feasible (47, 48, 13). Integration along the real line was favoured here over contour deformation on the grounds that it would be more direct, the treatment of the singular structure more transparent and it seemed simpler to program. For the most part we follow the method of Larson and Hetherington (31). However, some changes to their approach are given below as the treatment of each of the singularity types is discussed.

## 4.3 The Construction of the Standard Mesh

The first step is to break up the integration path into a number of finite intervals. The infinite set of intervals is truncated at a point $z_{max}$ such that no significant contribution to the integral is expected for values of $z > z_{max}$. In the numerical calculation this is checked by extending the upper limit of the integration region. So

$$\tilde{A}^o(x,y) = \tilde{V}^o(x,y) + \sum_{j=1}^{N} \int_{C_j}^{C_{j+1}} dz\, K(x,z)\, \tilde{A}^o(z,y) \,, \tag{4.11}$$

with

$$c_1 = 0 \quad ; \quad c_{N+1} = z_{max} \,.$$

On each interval the unknown function $\tilde{A}^o$ is represented by another function whose form is known, with the condition that the approximating function has the same values as the original at a fixed number of mesh points $\{z_k\}$, $k=1,\ldots,n$. One could use a spline function for this purpose (49). We choose to use a Lagrange interpolation polynomial, because it has a simple analytic structure

$$\tilde{A}^o(z,y) = \sum_{k \,\varepsilon\, s_j} \prod_{\ell(\varepsilon\, s_j)\neq k} \frac{z - z_\ell}{z_k - z_\ell}\, \tilde{A}^o(z_k,y) \cdot z_j < z < z_{j+1} \,. \tag{4.12}$$

The union of the index subsets $s_j$ is the set of integers 1 to n. The subsets $s_j$ are not necessarily disjoint. In other words a meshpoint can be a member of more than one subset (see Fig. 4.3).

Another flexible feature lies in the choice of the location of the boundary points $c_j$ of the integration regions. They need not correspond with the mesh positions. There is also no restriction on the location of the $c_j$'s in that they can lie inside as well as outside the range spanned by the values of $z_\ell$ in the subset $s_j$.

Evaluating the integral equation for values of x and y from the sets $\{x_k\}$ and $\{y_k\}$, identical to the set $\{z_k\}$ yields the matrix equation

$$\tilde{A}^o(x_i,y_k) = \tilde{V}^o(x_i,y_k) + \sum_{j=1}^{N} \Omega(x_i,z_j)\, \tilde{A}^o(z_j,y_k) \,. \tag{4.13}$$

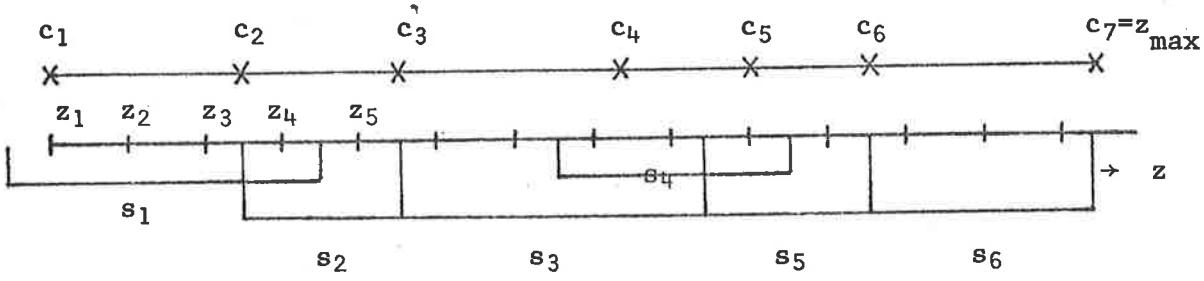


Fig. 4.3: Schematic illustration of the location of the meshpoints (z), the subsets $s_j$ containing the interpolation points, and the boundary points $c_j$ of the integration regions.

The matrix elements $\Omega$ are obtained from the finite integrals

$$\Omega(x_i,z_j) = \sum_{\ell\varepsilon t_j} \sum_{m\varepsilon s_\ell} \int_{C_\ell}^{C_{\ell+1}} dz\, K(x_i,z) \prod_{m\neq\ell} \frac{z - z_m}{z_\ell - z_m} . \qquad (4.14)$$

Notice that the integrand of (4.14) consists solely of known functions. The index subset $t_j$ contains the label of the index subsets $s_\ell$ that have $z_j$ as a member.

As an example, $z_4$ in Fig. 4.3 is part of the index subsets $s_1$ and $s_2$, ($t_4 = \{1,2\}$). The function value at $z_4$ is used for approximation in the integration regions $c_1 - c_2$ and $c_2 - c_3$. Contributions to $\Omega(x_i,z_4)$ come therefore from integrations spanning both these regions.

The mesh $\{y_k\}$ has to be chosen in such a manner that a close fit with the amplitude is obtained. The mesh used in the calculations is tested by doubling the number of mesh points.

We have used a three point Lagrange interpolation throughout. The boundary points $c_j$ of the integration regions are in general taken half way between the mesh points. A few exceptions are mentioned later.

## 4.4 Treatment of the Singular Points in the Numerical Integration

### 4.4.1 The Logarithmic Singularity

In order to single out the specific singularity under study the integral in (4.14) is rewritten. This defines a new function $F_1(x_i,z)$ which is analytic in the integration interval, but its precise form is not of importance here

$$\int_{C_\ell}^{C_{\ell+1}} dz\, K(x_i,z) \prod_{m\neq\ell} \frac{z - z_m}{z_\ell - z_m}$$

$$\int_{C_\ell}^{C_{\ell+1}} F_1(x_i,z) \frac{z}{x_i} Q_n \left[\frac{1}{2x_i z}\{2m_o E + i\xi - \frac{m_o + M_o}{M_o}(x_i^2 + z^2)\}\right] dz . \qquad (4.15)$$

The Legendre function does not facilitate the taking of the physical limit. More suited is relation (3.22) which expresses the Legendre function as an integral over the Legendre polynomial (40)

$$Q_n(v) = \tfrac{1}{2} \int_{-1}^{+1} \frac{P_n(t)}{v - t}\, dt \quad . \tag{4.16}$$

In the limit $\xi$ to zero the integral in (4.15) splits in a principle part and a delta function contribution:

$$\int_{C_\ell}^{C_{\ell+1}} F_1(x_i,z)\, \frac{z}{x_i}\, Q_n\left[u_i + \frac{i\xi}{2x_i z}\right] dz = P \int_{C_\ell}^{C_{\ell+1}} F_1(x_i,z)\, \frac{z}{x_i}\, Q_n[u_i]\, dz$$
$$- \pi i \int_{C_\ell}^{C_{\ell+1}} dz\, F_1(x_i,z)\, \frac{y}{x_i}\, \tfrac{1}{2} \int_{-1}^{+1} dt\, P_n(t)\, \delta(u_i - t) \quad . \tag{4.17}$$

where $u_i$ is the previously defined u (4.6) for $x = x_i$. On integrating over t the delta function restricts the range of the z integration to the interval on the line $x = x_i$ for which $|u_i| \leqslant 1$. The set of boundary points to these intervals consists of the part of the ellipses (4.3) in the physical-first quadrant.

Turning to the principle part integral, the relation (4.4) is used for the Legendre function. The argument of the logarithm in (4.4) is factorized

$$\ell n \left| \frac{1 + u_i}{1 - u_i} \right| = \ell n \left| \frac{(z - \tilde{\mu})(z + \tilde{\nu})}{(z + \tilde{\mu})(z - \tilde{\nu})} \right| \quad , \tag{4.18}$$

with

$$\tilde{\mu} = \frac{2M_o}{m_o + M_o}\, x_i + \tilde{\nu} \tag{4.19}$$

$$\tilde{\nu} = -\frac{M_o}{m_o + M_o}\, x_i + \sqrt{\frac{2m_o M_o}{m_o + M_o}\, E - \frac{2m_o M_o + m_o^2}{(m_o + M_o)^2}\, x_i^2} \quad . \tag{4.20}$$

The logarithmic singularities are reached for $z = \tilde{\mu}$ and $z = \pm \tilde{\nu}$ (see Fig. 4.1).

If an integration interval contains a point with a logarithmic singularity it is split in two on the singular point. As an example we show the explicit treatment of one case ($z = \tilde{\nu}$), all the others are similar. The integrand is separated into a singular and a non-singular part in the following way:

$$\int_a^{\tilde{\nu}} F_1(x_i,z)\ \frac{z}{x_i}\ Q_n[u_i]\ dz =$$

$$\int_a^{\tilde{\nu}} F_1(x_i,z)\ \frac{z}{x_i}\left[\tfrac{1}{2}\ P_n(u_i)\ \ln\left|\frac{(z+\tilde{\nu})(z-\tilde{\mu})}{(a-\tilde{\nu})(z+\tilde{\mu})}\right| - W_{n-1}(u_i)\right] dz$$

$$+\ \tfrac{1}{2}\int_a^{\tilde{\nu}} F_1(x_i,z)\ \frac{z}{x_i}\ P_n(u_i)\ \ln\frac{a-\tilde{\nu}}{z-\tilde{\nu}}\ dz\ . \qquad (4.21)$$

The linear transformation

$$z - \tilde{\nu} = (a - \tilde{\nu})\ v \qquad (4.22)$$

puts the second integral into a form where one can use a Gaussian quadrature scheme for functions with a logarithmic singularity

$$\int_0^1 F(v)\ \ln\frac{1}{v}\ dv = \sum_i A_i\ F(v_i)\ . \qquad (4.23)$$

The quadrature points and weights have been calculated by Krylov (50). We use a five point quadrature scheme, which gives the exact result for F(v) being a polynomial up to order 9. The place where the singular regions $z = \tilde{\mu}$ and $z = -\tilde{\nu}$ meet is treated in the same fashion (inclusion of a factor 2 in the singular integral). As can be seen from (4.18) the point $z = \tilde{\nu} = -\tilde{\nu}$ is non-singular.

The limit where $x_i$ goes to zero has to be handled slightly different since there is a factor $x_i$ in the denominator in (4.15). We use again the expression (4.16). The limiting case yields

$$\lim_{x_i\to o}\frac{z}{x_i}\ Q_n[u_i] = \lim_{x_i\to o}\int_{-1}^{+1}\frac{z^2\ P_n(t)}{2m_oE - \frac{m_o+M_o}{M_o}(x_i^2+z^2) - 2x_i\ zt}\ dt$$

$$= \frac{2\delta_n\ z^2}{2m_oE - \frac{m_o+M_o}{M_o}\ z^2}\ . \qquad (4.24)$$

Hence for $x_i = 0$ the logarithmic singularity becomes a simple pole which is treated in a similar manner as the simple pole of the propagator, to be discussed in the last subsection.

4.4.2 The Square Root Singularity

The S-function in the complex z-plane contains a square root

branch cut . In the physical limit $\xi \to 0$ only the branch point shows up in the amplitude and the kernel. At the branch point the function is continuous. This means no special extra arrangements are necessary. The property of being non-differentiable, carried over to the amplitude does, however, affect the interpolation procedure. No close fit can be obtained if the amplitude is approximated by a polynomial across the branch point. This is avoided by placing a mesh point on the lower edge of the branch point and also locating the end point of an integration region there. In the first region above the branch point backward extrapolation is used to determine the desired function values.

4.4.3 The Pole in the Two-Body Propagator

Again the integral (4.14) is rewritten, defining another function $F_2(x_i,z)$

$$\int_{c_\ell}^{c_{\ell+1}} dz\, K(x_i,z) \prod_{m\neq\ell} \frac{z - z_m}{z_\ell - z_m} = \int_{c_\ell}^{c_{\ell+1}} dz\, F_2(x_i,z) \frac{1}{z_o^2 - z^2 + i\xi} \prod_{m\neq\ell} \frac{z - z_m}{z_\ell - z_m} , \tag{4.25}$$

$z_o$ is the on-shell value of the momentum

$$z_o^2 = 2\mu(E + \varepsilon) \qquad c_\ell < z_o < c_{\ell+1} . \tag{4.26}$$

Taking $z_o$ as one of the mesh points ($z_k$) saves the necessity of an extra calculation of the on-shell amplitude via the integral equation. In the physical limit ($\xi \to o$) the integral again splits into a principle part plus a term proportional to $\pi i\delta(z - z_o)$. The singularity in the principle part integral is handled by the substraction technique. Some extra advantages are obtained by positioning the simple pole in the middle of the integration interval (see footnote*)

---

* $\int_{-1}^{+1} \frac{dx}{x} = 0$, hence $\int_{-1}^{+1} \frac{g(y)}{y}\, dy = \int_{-1}^{+1} \frac{g(y) - g(o)}{y}\, dy = \int_a^b \frac{g(x) - g(c)}{x - c}\, dx$ ,

with $a - c = c - b$ .

$$\int_{c_\ell}^{c_{\ell+1}} F_2(x_i,z)\,\frac{1}{z_o^2 - z^2 + i\xi}\prod_{m\neq\ell}\frac{z - z_m}{z_\ell - z_m}\,dz = -\pi i\,\frac{F_2(x_i,z_o)}{2z_o}\,\delta_{\ell k}$$

$$- P\int_{c_\ell}^{c_{\ell+1}} \frac{F_2(x_i,z)\prod_{m\neq\ell}\dfrac{z - z_m}{z_\ell - z_m} - F_2(x_i,z_o)\delta_{\ell k}}{z + z_o}\,\frac{1}{z - z_o}\,dz\ . \qquad (4.27)$$

This shows another advantage of having a mesh point corresponding to the on-shell value.The interpolation polynomial becomes a delta function, which reduces the number of times the special calculation has to be carried out.

There is one other point that needs special mention. It is $c_1 = 0$, where a mesh point is taken to coincide with a boundary point. The first integration interval stretches from $z = 0$ to half way between the first two mesh points.

This means that there are three mesh points which have a fixed location from the outset: the origin, the square root branch point and the two-body scattering pole. The other mesh points are arbitrary. We have chosen a fairly even distribution, guided by the form of the resulting amplitude that we want to approximate. An example for 15 mesh points is shown in Fig. 4.4.

Similarly there is a great freedom in the location of the boundary points of the integration regions. Only $c_1$ and the square root branch point are forced. Our choice has been stated in Section 4.3.

For the integrations, in which we now only encounter regular functions, we have used a 6 point Gaussian quadrature scheme. The accuracy of this is easily tested by going to a higher order quadrature scheme.

Our treatment differs from and extends the approach of Larson and Hetherington at a number of places. Firstly: we never use the mesh points for dual purposes; that is, for describing the scattering amplitude and simultaneous as quadrature point. The decoupling means that we are freer to choose our mesh points in order to get a good approximation of the amplitude. This comes at the cost of a little extra computer time in the integration, traded off against a smaller total number of mesh points. Secondly, we have

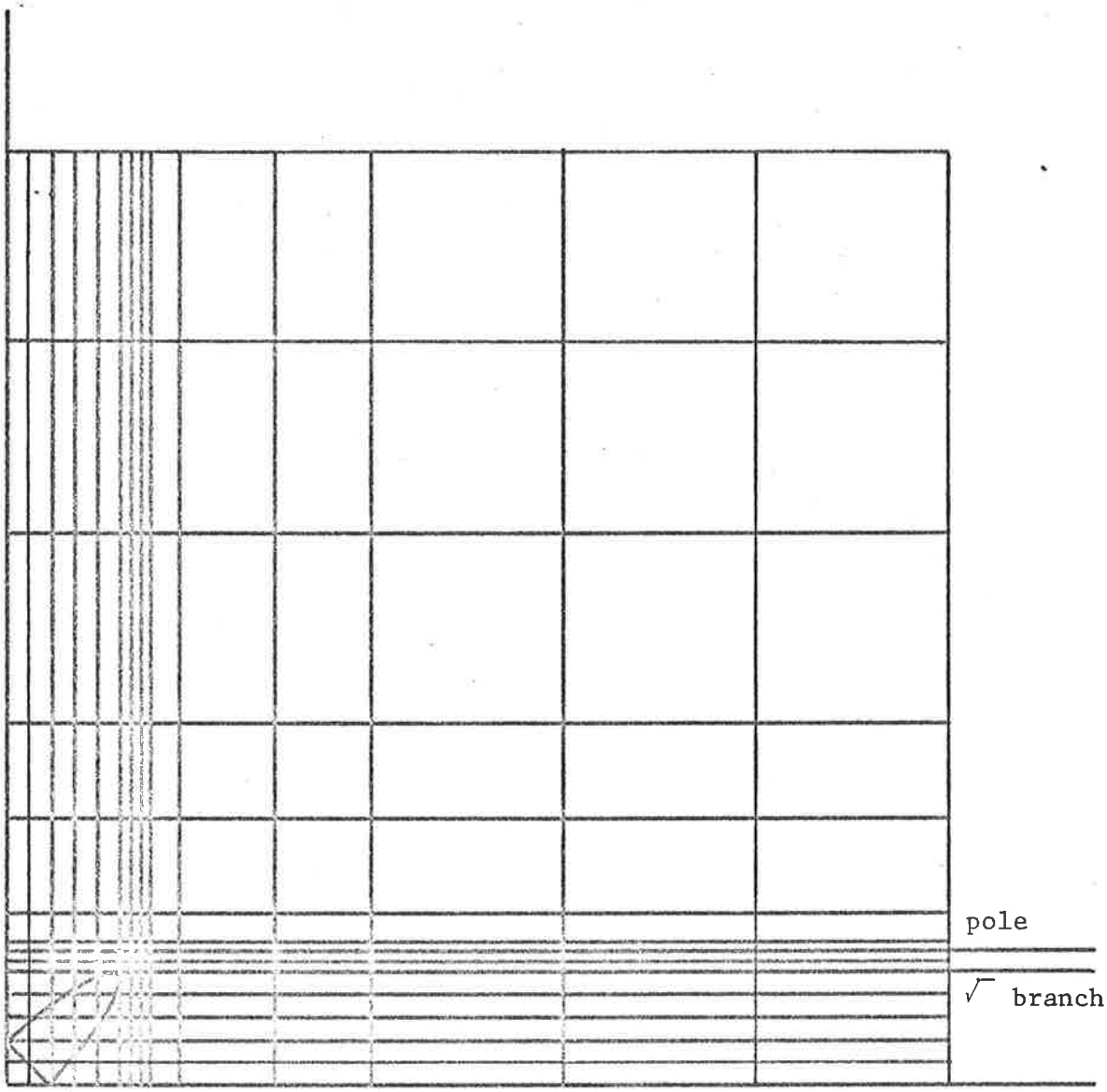


Fig. 4.4: Example of the location of 15 mesh points. Note the even distribution below the square root singularity and around the propagator pole.

given a complete mathematical description of the treatment for the logarithmic singularity, especially the approach to the physical limit. And we have shown how, for $x = 0$ the singularity reduces to a simple pole. Thirdly, from the properties of the amplitude at the branch point (continuous, but not differentiable), we have emphasized the necessity of avoiding interpolation by means of polynomials across the branch point. Finally, our freer choice of mesh points means that it is not necessary to consider a large number of special cases in the treatment of the logarithmic singularity.

# CHAPTER 5

## THE STURMIAN EXPANSION

Usually the quality of a model is measured by its predictive merits. The calculated results are compared with a physical experiment. The delta shell potential, however, does not correspond closely to a real interaction. This means that we cannot test our calculated scattering amplitude in this fashion.

Another test is to derive the same quantity in a different manner. Quite often this is made feasible by restricting the parameters of the model to a range where a direct comparison can be made. In our case there are a number of parameters that can be used to define suitable limiting cases: the total energy of the process, the mass ratio of the valence particle and the heavy ion core, the strength and the radius of the delta shell. We shall explore how the first two of these can be used to our advantage in the first section on the close coupling scheme. The spectator wave functions (see Eq. 2.17) are expanded in terms which describe the two particle subsystem. If this expansion is truncated to contain only the bound states, a simple set of coupled Lippmann-Schwinger type equations results. This is not very satisfactory, since the, then excluded, continuum states are part of the Faddeev formulation for three-body scattering. The next section deals with the completely discrete Sturmian expansion. Using this expansion a new set of equations is derived, equivalent to the Faddeev equations. The expansion may, however, have an infinite number of terms. In Section 3 the scattering amplitude is derived using the Sturmian scheme. The special conditions in the model: identical cores and no core-core interactions are enforced in the calculations. In the final section a link is established between the close coupling and Sturmian schemes. In the adiabatic limit the effective potentials, that appear in the scattering

amplitudes are compared. This suggests that corrections on close coupling calculations can be obtained by considering terms in the perturbation expansion of the calculation based on the Sturmian scheme.

5.1 The Close Coupling Scheme

It is well known that for "slow" processes a significant simplification is obtained from an expansion of the wave function in molecular states (17, 51 - 53). A slow process implies that the time in which colliding particles are close together and can interact is long compared with the interaction time. This is realized if the kinetic energy available for the relative movement of the particles is small. In this case we show that the off-shell effects in the two-body energy $\sigma = E - p^2/2\mu$ may be treated as a perturbation. For a given kinetic energy the velocity of the scatterers is reduced if the mass of the ion core is made very large. ($m = M_o/m_o >> 1$, and hence $\mu = (m_o + M_o)M_o/(m_o + 2M_o) \approx M_o/2$).

In coordinate space it is then reasonable to expand the wave function in terms which describe the composite particle at a fixed distance from the other scatterer. The functions which appear as expansion coefficients depict the relative motion of the cores.

Let $\phi_\alpha^i$ be a complete set of states for the two-body subsystem of particle j and k. The spectator wave function (2.17) decomposes as

$$|\psi^{(i)}> = \sum_\alpha |\phi_\alpha^{(i)}> \; |\psi_\alpha^{(i)}> \quad . \tag{5.1}$$

One should be aware that this complete set in general will consist of discrete and continuum elements. The discrete elements correspond to the bound state wave functions, of which there can be an infinite number, depending on the interaction. We shall call (5.1) the close coupling expansion. The relation between the coefficients is determined by the Faddeev equations (2.18)

$$|\psi_\alpha^{(i)}\rangle = |\vec{p}\rangle \delta_{i1}\,\delta_{\alpha\rho} + \sum_{\substack{j\neq i \\ \beta}} \langle \phi_\alpha^{(i)}|G_o\, t_i|\phi_\beta^{(j)}\rangle\ |\psi_\beta^{(j)}\rangle \quad . \tag{5.2}$$

For the bound states in the expansion there is a considerable simplification because

$$\begin{aligned}\langle \phi_\alpha^{(i)}|G_o\, t_i|\phi_\beta^{(j)}\rangle &= \langle \phi_\alpha^{(i)}|\ (E - H_i)^{-1}\ V_i\ |\phi_\beta^{(j)}\rangle \\ &= g_o^{(i)}\ (E + \varepsilon_{i\alpha})\ \underline{V}_{\alpha\beta}^{(ij)} \quad , \end{aligned} \tag{5.3}$$

where $g_o^{(i)}$ is the free Green's operator in the j - k subsystem, which depends on the relative motion of particle i. The potential $\underline{V}_{\alpha\beta}^{(ij)}$ only involves the two particles in the bound system

$$\underline{V}_{\alpha\beta}^{(ij)} = \langle \phi_\alpha^{(i)}|V_i|\phi_\beta^{(j)}\rangle \quad , \tag{5.4}$$

and the problem is reduced to a set of two-body Lippmann-Schwinger equations

$$|\psi_\alpha^{(i)}\rangle = |\vec{p}\rangle \delta_{i1}\,\delta_{\alpha\rho} + \sum_{\substack{j\neq i \\ \beta}} g_o^{(i)}\ (E + \varepsilon_{i\alpha})\ \underline{V}_{\alpha\beta}^{(ij)}\ |\psi_\beta^{(j)}\rangle \quad . \tag{5.5}$$

This means that we have a very well behaved set of equations if the continuum states are omitted from the expansion (5.1). But the continuum states are part of the Faddeev formulation of the three-body scattering and cannot be ignored.

## 5.2 The Sturmian Scheme

The two aspects of the close coupling scheme that combined to produce the well behaved set of equations (5.5) are: the expansion of the spectator wave function in terms describing the two-body system and the use of the discrete terms in this expansion. This suggests that one should use a similar, but completely discrete system to describe the subsystem.

It is known that for a wide class of potentials (54 - 56) the kernel of the two-body Lippmann-Schwinger equation can be symmetrized, and becomes compact, implying that it has a point spectrum only. The eigenvectors and

and eigenvalues are given by

$$V_i \, g_o(\sigma_i) \, |\chi_\alpha^{(i)}(\sigma_i)> = \Gamma_{i\alpha}(\sigma_i) \, |\chi_\alpha^{(i)}(\sigma_i)> \quad . \tag{5.6}$$

The $\chi_\alpha^{(i)}$, for negative $\sigma_i$, obey the orthonormality relations

$$< \chi_\alpha^{(i)}(\sigma_i) | g_o(\sigma_i) | \chi_\beta^{(i)}(\sigma_i) > = - \delta_{\alpha\beta} \quad . \tag{5.7}$$

Note that the eigenvalues $\Gamma_{i\alpha}$ and the states $\chi_\alpha^{(i)}$ are a function of the pair subenergy $\sigma_i$. The two-body t-matrix required in the Faddeev equations is easily deduced from (5.6) and (5.7)

$$t_i = - \sum_\alpha |\chi_\alpha^{(i)}(\sigma_i)> \frac{\Gamma_{i\alpha}(\sigma_i)}{1 - \Gamma_{i\alpha}(\sigma_i)} < \chi_\alpha^{(i)}(\sigma_i)| \quad . \tag{5.8}$$

The other object that needs to be expressed in the eigenvectors is the bound state wave function. Using its definition

$$|\phi_\rho^{(i)}> = g_o(-\varepsilon_{i\rho}) \, V_i \, |\phi_\rho^{(i)}> \quad , \tag{5.9}$$

and the fact that the two-body t-matrix has a pole for $\sigma_i = -\varepsilon_{i\rho}$ and hence $\Gamma_{i\rho}(-\varepsilon_{i\rho}) = 1$ it is seen that it is consistent to take for the bound state

$$|\phi_\rho^{(i)}> = - \tilde{N}_\rho^{(i)} \, g_o(-\varepsilon_{i\rho}) \, |\chi_\rho^{(i)}(-\varepsilon_{i\rho})> \quad . \tag{5.10}$$

$\tilde{N}_\rho^{(i)}$ is determined by the normalization condition on the bound state. Differentiating (5.6) one finds that

$$\tilde{N}_\alpha^{(i)\,-2} = \left[\frac{\partial \, \Gamma_{i\alpha}}{\partial \, \sigma_i}\right]_{\sigma_i = -\varepsilon_{i\alpha}} \quad . \tag{5.11}$$

An extension of the orthonormality relation (5.7) shows that the identity operator in three-body space is

$$I = - \sum_\alpha \int d^3p \, g_o(\sigma_i) \, |\chi_\alpha^{(i)}(\sigma_i)> |p>< p| < \chi_\alpha^i(\sigma_i)| \tag{5.12}$$

This and the form of the bound state wave function suggests that the expansion (5.1) should be replaced by

$$|\psi^{(i)}> = - \sum_\alpha \tilde{N}_\alpha^{(i)} \, g_o(\sigma_i) \, |\chi_\alpha^{(i)}> \, |\psi_\alpha^{(i)}> \quad . \tag{5.13}$$

For eigenstates which do not correspond to bound states the constants $\tilde{N}_\alpha^{(i)}$ may be taken as unity. The coefficients $|\psi_\alpha^{(i)}>$ are again determined by the Faddeev equations. Substituting (5.13) in (2.18) and using the orthonormality relation (5.7) results in

$$|\psi_\alpha^{(i)}> = |\vec{p}>\delta_{il}\,\delta_{\alpha\rho} - \sum_{\substack{j\neq i\\ \beta}} \frac{\Gamma_{i\alpha}}{1-\Gamma_{i\alpha}}\,\tilde{N}_\alpha^{(i)\,-2}\,V_{\alpha\beta}^{(ij)}\,|\psi_\beta^{(j)}> \quad , \tag{5.14}$$

with

$$V_{\alpha\beta}^{(ij)} = \tilde{N}_\alpha^{(i)} < \chi_\alpha^{(i)}|G_o|\chi_\beta^{(j)}>\,\tilde{N}_\beta^{(j)} \quad . \tag{5.15}$$

The Lippmann-Schwinger character of (5.14) can be brought to the foreground in a similar fashion as in Chapter 2. Define $\tilde{S}_\alpha^{(i)}$ by

$$-\frac{\Gamma_{i\alpha}(\sigma_i)}{1-\Gamma_{i\alpha}(\sigma_i)}\,\tilde{N}_\alpha^{(i)\,-2} = \frac{1}{\sigma_i+\varepsilon_{i\alpha}}\,\tilde{S}_\alpha^{(i)\,2}\,(\sigma_i) \quad . \tag{5.16}$$

The function $\tilde{S}$ and S (see 2.36) differ at the most by a constant factor, as the left hand side of (5.16) is proportional to the two-body propagator $\tau$. Using L'Hospital's rule and (5.11) it is easily established that the on-shell values of $\tilde{S}$ and S are the same, hence the functions are identical everywhere. Therefore, the equation can be symmetrized with respect to S. The on-shell value of the new wave function is not changed if

$$|\tilde{\psi}_\alpha^{(i)}> = S_\alpha^{(i)}\,|\psi_\alpha^{(i)}> \quad , \tag{5.17}$$

and

$$|\tilde{\psi}_\alpha^{(i)}> = |\vec{p}>\,\delta_{il}\,\delta_{\alpha\rho} + \sum_{\substack{j\neq i\\ \beta}} g_o(E+\varepsilon_{i\alpha})\,\tilde{V}_{\alpha\beta}^{(ij)}\,|\tilde{\psi}_\beta^{(j)}> \quad , \tag{5.18}$$

with the symmetric effective potential

$$\tilde{V}_{\alpha\beta}^{(ij)} = \tilde{N}_\alpha^{(i)}\,S_\alpha^{(i)} < \chi_\alpha^{(i)}|G_o|\chi_\beta^{(j)}>\,S_\beta^{(j)}\,\tilde{N}_\beta^{(j)} \quad . \tag{5.19}$$

It should be noted that (5.18) form a discrete set of coupled equations that rigorously follows from the Faddeed equations. The number of equations, however, is determined by the number of eigenvalues which are not identically

zero (c.f. 5.14), and hence depends on the choice of the potential.

Our interest of course centres on the separable interactions. These are in the class for which the Sturmian expansion can be made. Suppose the potential has a finite number of terms

$$V_i = \sum_{\gamma=1}^{n} |\theta_\gamma^{(i)}> \; \nu_\gamma^{(i)} \; < \theta_\gamma^{(i)}| \; , \tag{5.20}$$

where $\theta_\gamma$ are a set of n orthonormal vectors spanning a subspace R of the two particle space. Substitution of (5.20) in (5.6) means that one can construct n eigenvectors with non-zero eigenvalue. The other eigenvectors in the set are not of interest here since they do not contribute to $t_i$ (Eq. 5.8) and hence do not appear in (5.18).

## 5.3 The Scattering Amplitude

Ultimately we seek the scattering amplitude which still needs to be expressed in Sturmian states. If particle 1 is free in the initial state then the elastic scattering amplitude is

$$A_{\beta\rho}^{(11)} = < \phi_\beta^{(1)}, \vec{p}' | V_2 + V_3 | \psi^+ > \; . \tag{5.21}$$

The eigenvalue equation gives the general form for the potential

$$V_i = - \sum_{\alpha} |\chi_\alpha^{(i)}> \; \Gamma_{i\alpha} \; < \chi_\alpha^{(i)}| \; . \tag{5.22}$$

In the evaluation of (5.21) the projection of the Sturmian state on the scattering state is required

$$< \chi_\alpha^{(i)} | \psi^+ > = \tilde{N}_\alpha^{(i)} \; |\psi_\alpha^{(i)} > - \sum_{\substack{j \neq i \\ \beta}} < \chi_\alpha^{(i)} | g_o | \chi_\beta^{(j)} > \; |\psi_\beta^{(j)} > \; . \tag{5.23}$$

This can be rewritten, applying the relation (5.14). In the elastic scattering amplitude there will be no contribution from the Born term, but in general

$$< \chi_\alpha^{(i)} | \psi^+ > = \frac{\tilde{N}_\alpha^{(i)}}{\Gamma_{i\alpha}} \; |\psi_\alpha^{(i)} > - \frac{1 - \Gamma_{i\alpha}}{\Gamma_{i\alpha}} \tilde{N}_\alpha^{(i)} \; |\vec{p} > \delta_{il} \; \delta_{\alpha\rho} \; . \tag{5.24}$$

Substitution of (5.9), (5.22) and (5.24) in (5.21) results in

$$A^{(11)}_{\beta\rho} = \sum_{\alpha} \{ < \vec{p}' | V^{(12)}_{\beta\alpha} | \psi^{(2)}_{\alpha} > + < \vec{p}' | V^{(13)}_{\beta\alpha} | \psi^{(3)}_{\alpha} > \} \quad . \tag{5.25}$$

Similar to the previous section the potentials can be symmetrized with respect to the function S. The on-shell value of the amplitude and hence the cross section are not changed by this process,

$$\tilde{A}^{(11)}_{\beta\rho} = \sum_{\alpha} \{ < \vec{p}' | \tilde{V}^{(12)}_{\beta\alpha} | \tilde{\psi}^{(2)}_{\alpha} > + < \vec{p}' | \tilde{V}^{(13)}_{\beta\alpha} | \tilde{\psi}^{(3)}_{\alpha} > \} \quad . \tag{5.26}$$

For the rearrangement amplitude, where in the final state particle 2 is free, it seems as if there would appear an extra term

$$< \vec{p}' | \tilde{V}^{(21)}_{\beta\alpha} \ (1 - \Gamma_{1\alpha}) \ | \vec{p} > \delta_{\alpha\rho} \ , \tag{5.27}$$

originating in the Born term of the Lippmann-Schwinger form (5.14). However, the eigenvalue $\Gamma_{1\alpha}$ is equal to unity on-shell and this term therefore vanishes, giving rise to the rearrangement amplitude

$$\tilde{A}^{(21)}_{\beta\rho} = \sum_{\alpha} \{ < \vec{p}' | \tilde{V}^{(21)}_{\beta\alpha} | \tilde{\psi}^{(1)}_{\alpha} > + < \vec{p}' | \tilde{V}^{(23)}_{\beta\alpha} | \tilde{\psi}^{(3)}_{\alpha} > \} \quad . \tag{5.28}$$

The model for the heavy ion scattering features two assumptions that will simplify the amplitude. These are identical cores and a vanishing core-core interaction. The second assumption is easily incorporated in the amplitudes by dropping the terms dependent on $\tilde{\psi}^{(3)}$. The assumption of identical cores implies that physically the elastic and rearrangement amplitudes are indistinguishable and the measured amplitude is a mixture of the two. Since all particles are treated as bosons the total amplitude is

$$\tilde{A}_{\beta\rho} = \sum_{\alpha} \{ < \vec{p}' | \tilde{V}^{(21)}_{\beta\alpha} | \tilde{\psi}^{(1)}_{\alpha} > + < \vec{p}' | \tilde{V}^{(12)}_{\beta\alpha} | \tilde{\psi}^{(2)}_{\alpha} > \} \quad . \tag{5.29}$$

Without the core-core interaction the set (5.18) reduces to

$$\begin{aligned} | \tilde{\psi}^{(1)}_{\alpha} > &= | \vec{p} > \delta_{\alpha\rho} + \sum_{\beta} g_o(E + \varepsilon_{1\alpha}) \ \tilde{V}^{(12)}_{\alpha\beta} | \ \psi^{(2)}_{\beta} > \ , \\ | \tilde{\psi}^{(2)}_{\alpha} > &= \sum_{\beta} g_o(E + \varepsilon_{2\alpha}) \ \tilde{V}^{(21)}_{\alpha\beta} | \ \psi^{(1)}_{\beta} > \ . \end{aligned} \tag{5.30}$$

The fact that the cores are identical means that the interaction between the valence particles and each of the cores is the same,

$$\tilde{V}^{(12)}_{\alpha\beta} = \tilde{V}^{(21)}_{\alpha\beta} = \tilde{V}_{\alpha\beta} \ , \tag{5.32a}$$

and also

$$\varepsilon_{1\alpha} = \varepsilon_{2\alpha} = \varepsilon_{\alpha}. \tag{5.32b}$$

With the definition

$$|\tilde{\psi}_{\alpha}> = |\tilde{\psi}^{(1)}_{\alpha}> + |\tilde{\psi}^{(2)}_{\alpha}> \ , \tag{5.33}$$

and incorporating (5.33) the equation (5.29) becomes

$$\tilde{A}_{\beta\rho} = \sum_{\alpha} < \vec{p}^{\,-}|\tilde{V}_{\alpha\beta}|\tilde{\psi}_{\beta}> \ , \tag{5.34}$$

where

$$|\tilde{\psi}_{\alpha}> = |\vec{p}> \delta_{\alpha\rho} + \sum_{\beta} g_o(E + \varepsilon_{\alpha}) \ \tilde{V}_{\alpha\beta} \ |\tilde{\psi}_{\beta}> \ . \tag{5.35}$$

Although (5.35) exhibits a straightforward Lippmann-Schwinger form there are difficulties hidden by the fact that the effective potential is energy dependent, in general non-local and, non-Hermitian. The intention has been to obtain a discrete and possibly finite expansion for the scattering state. In the next section the effective potentials in the close coupling approach and in the Sturmian basis are related to define the domain in which the theory can be most effectively applied in our case.

## 5.4 The Adiabatic Approximation

The term "adiabatic limit" is used to denote the type of slow process as described at the start of Section 5.1. In a low energy process it seems reasonable to approximate the amplitude by one in which only scattering between states with the valence particle bound in the ground state takes place. Excited states are not very likely to be occupied with this energy restriction.

With identical cores and no core-core interaction the amplitude using the close coupling scheme simplifies to give

$$A_{\rho\rho} = \langle \vec{p}' | V_{\rho\rho} | \psi_\rho \rangle \quad , \tag{5.36}$$

where

$$|\psi_\rho\rangle = |\vec{p}\,\rangle + g_o(E + \varepsilon_\rho)\, V_{\rho\rho}\, |\psi_\rho\rangle \quad . \tag{5.37}$$

The form of the amplitude is similar to the one in the Sturmian expansion (5.34). This suggests that the correspondence between the close coupling scheme and the Sturmian approach may be established by comparing the respective effective potentials in the amplitudes

$$V_{\rho\rho} = \langle \phi_\rho^{(1)} | V | \phi_\rho^{(2)} \rangle \quad , \tag{5.38}$$

and

$$\tilde{V}_{\rho\rho} = \tilde{N}_\rho^{(1)}\, S^{(1)}(\sigma_1) \langle \chi_\rho^{(1)}(\sigma_1) | g_o(\sigma_2) | \chi_\rho^{(2)}(\sigma_2) \rangle\, S_\rho^{(2)}(\sigma_2)\, \tilde{N}_\rho^{(2)} \quad . \tag{5.39}$$

Using the eigenvalue equation (5.6) this is rewritten as

$$\tilde{V}_{\rho\rho} = \tilde{N}_\rho^{(1)}\, S_\rho^{(1)}(\sigma_1)\, \frac{1}{\Gamma_{1\rho}(\sigma_1)} \langle \chi_\rho^{(1)}(\sigma_1) | g_o(\sigma_1) V\, g_o(\sigma_2) | \chi_\rho^{(2)}(\sigma_2) \rangle\, S_\rho^{(2)}(\sigma_2)\, \tilde{N}_\rho^{(2)} \tag{5.40}$$

The energy dependent functions in (5.40) are expressed in Taylor series around the on-shell value of the two-body energy. With $\delta = \sigma + \varepsilon$ one easily obtains

$$\Gamma_\alpha(\sigma) = 1 - \delta\, \Gamma_\alpha^{(1)}(-\varepsilon_\alpha) + \delta^2\, \Gamma_\alpha^{(2)}(-\varepsilon_\alpha) + O(\delta^3) \quad , \tag{5.41}$$

where

$$\Gamma_\alpha^{(1)}(-\varepsilon_\alpha) = \langle \chi_\alpha | g_o{}^2 | \chi_\alpha \rangle \Big|_{\sigma=-\varepsilon_\alpha} \quad ,$$

$$\Gamma_\alpha^{(2)}(-\varepsilon_\alpha) = \left[ \langle \chi_\alpha | g_o{}^3 | \chi_\alpha \rangle + \sum_{\beta\,\alpha} \frac{\Gamma_\beta}{1 - \Gamma_\beta} \langle \chi_\alpha | g_o{}^2 | \chi_\beta \rangle^2 \right]_{\sigma=-\varepsilon_\alpha} \quad ,$$

$$S_\alpha^2(\sigma) = 1 - \delta \left[ \Gamma_\alpha^{(1)}(-\varepsilon_\alpha) + \frac{\Gamma_\alpha^{(2)}(-\varepsilon_\alpha)}{\Gamma_\alpha^{(1)}(-\varepsilon_\alpha)} \right] + O(\delta^2) \quad , \tag{5.42}$$

and

$$\tilde{N}_\alpha\, g_o(\sigma)\, |\chi_\alpha(\sigma)\rangle = |\phi_\alpha\rangle + \tfrac{1}{2}\delta\, \Gamma_\alpha^{(1)}(-\varepsilon_\alpha)\, |\phi_\alpha\rangle + O(\delta^2) \quad . \tag{5.43}$$

Substitution of (5.41) - (5.43) into (5.40) shows that

$$\langle \vec{p}' | \tilde{V}_{\rho\rho} | \vec{p}\,\rangle = \langle \vec{p}' | V_{\rho\rho} | \vec{p}\,\rangle + O(\delta') + O(\delta) \quad . \tag{5.44}$$

Hence the close-coupling scheme and the Sturmian approach give rise to the same effective interaction and therefore the same cross section, if the off-shell terms are neglected. But this is allowed under the conditions of the adiabatic approximation.

There are two conclusions to be drawn from the comparison in (5.44). In the first place: the Sturmian scheme in the adiabatic limit will indeed provide the test we are looking for. The scattering amplitude is obtained in a simple manner different from the one described in Chapter 3. In the second place, it shows how calculations based on the close coupling scheme can be improved through the inclusion of terms from the perturbation expansion of the effective "Sturmian" potential.

The general theory and some examples are reported in a paper by L. R. Dodd and K. J. Nieukerke (57). The next chapter will deal with the specific case when the interaction between valence particle and core is described by a delta shell potential.

# CHAPTER 6

## THE STURMIAN EXPANSION FOR THE DELTA SHELL

This chapter breaks into two parts in a natural way. In the first half the theory of the Sturmian expansion is worked out for the special choice of delta shell interactions. The scattering amplitude will be related to the phase shift of the radial part of the wave function, which is determined by a differential equation.

The second half is concerned with a theoretical check on the manipulations performed in the first section. The usual general theory, described in Chapters 2 and 3, and the Sturmian scheme are equivalent. In order to obtain a simply manageable form, the Sturmian scheme has been applied with a number of restrictions in force. These are: the adiabatic limit and the large mass ratio of the cores and the valence particle. It is shown that in the case of s-state to s-state scattering the differential equation in the Sturmian scheme and the integral equation (3.25) are still equivalent. The proof is given in the zero range limit for the potential. In the next chpater, dealing with the numerical results, a comparison is also made when this extra restriction is not in force.

### 6.1 The Delta-Shell in the Sturmian Expansion

The first task is to construct the eigenvectors and eigenvalues of (5.6). Using expression (2.6) for the potential, with the form factors given by (3.3), the eigenvalue is

$$\Gamma_{i\alpha}(\sigma_i) = \lambda_i \langle f_{i\alpha} | g_o(\sigma_i) | f_{i\alpha} \rangle \quad , \tag{6.1}$$

and explicitly in momentum space

$$\Gamma_{i,\ell m}(k_i) = 2\bar{\mu}_i \, r_o^{\,2} \, \lambda_i \, k_i \, j_\ell(ik_i \, r_o) \, h_\ell^{(1)}(ik_i \, r_o) \, N_{i\ell}^2 \quad . \tag{6.2}$$

Here the label has been replaced by the angular momentum quantum number $\ell$ and its projection m. The $k_i$ has been previously defined in (3.15). The

property of $\Gamma_{i,\ell m}(-\varepsilon_\ell) = 1$ is easily shown by substitution of the explicit form for $\lambda_i$ (3.8) into (6.2). The corresponding Sturmian vector is parallel to the form factor

$$|\psi^{(i)}_{\ell m}> = a_\ell(\sigma_i)\ |f_{i,\ell m}> , \tag{6.3}$$

$a_\ell$ is an energy dependent constant that can be determined from the orthonormality relation

$$a_\ell^{-2}(\sigma_i) = -\ 2\bar{\mu}_i\ r_o^{\,2}\ k_i\ j_\ell(ik_i\ r_o)\ h^{(1)}_\ell(ik_i\ r_o) . \tag{6.4}$$

As shown in Section 5.2 the S functions are unchanged, but the normalization constants of the bound states are related through a factor $a_\ell(-\varepsilon_\ell)$

$$\tilde{N}^{(i)\,-2}_\alpha = N^{-2}_{i,\ell}\ a^2_\ell(-\varepsilon_\ell) = 4\bar{\mu}_i^{\,2}\ r_o^{\,2}\ \frac{F_\ell(k_\ell)}{k_\ell}\ a^2_\ell(-\varepsilon_\ell) . \tag{6.5}$$

To obtain the amplitude given by Eq. (5.34) the solution of the wave equation

$$\tilde{\psi}_\alpha(\vec{p}\,') = \delta(\vec{p}\,' - \vec{p})\ \delta_{\alpha\rho} + \sum_\beta \int d^3p''\ \frac{1}{E + \varepsilon_\alpha - \frac{p''^{\,2}}{2\mu}}\ \tilde{W}_{\alpha\beta}(\vec{p}\,',\vec{p}\,'')\ \tilde{\psi}_\beta(\vec{p}\,'') , \tag{6.6}$$

is required, where the effective potential

$$\tilde{W}_{\alpha\beta}(\vec{p}\,',\vec{p}\,'') = \tilde{N}_\alpha\ S_\alpha(\sigma')\ <\vec{p}\,',\chi_\alpha|G_o(E)|\vec{p}\,'',\chi_\beta>\ S_\beta(\sigma'')\ \tilde{N}_\beta , \tag{6.7}$$

has been renamed W to indicate that it relates specifically to the Sturmian set of the delta shell interaction. The potential (6.7) may be simplified by considering the two restrictions on the parameter set for which the Sturmian expansion is expected to be useful. In Section 5.4 the S function has already been expanded around the on-shell two-body energy. Now also the Taylor expansion of the $a_\ell(\sigma)$ is needed. With the function $F_\ell$, defined by (3.13), the series is

$$a_\ell^{-2}(\sigma) = a_\ell^{-2}(-\varepsilon) + \delta\ F_\ell(-\varepsilon) + O(\delta^2) . \tag{6.8}$$

If the off-shell terms in the $S_{\alpha(\beta)}$ and the $a_\ell$ are neglected and the Sturmian states written in form factors, the effective potential reduces to

$$\tilde{W}_{\alpha\beta}(\vec{p}',\vec{p}'') = N_{\ell_\alpha} \langle \vec{p}', f_{\ell_\alpha m_\alpha} \left| G_o(E) \right| f_{\ell_\beta m_\beta}, \vec{p}'' \rangle \; N_{\ell_\beta}$$

$$= N_{\ell_\alpha} f^*_{\ell_\alpha m_\alpha} \left( \frac{M_o}{m_o + M_o} \vec{p}' + \vec{p}'' \right) \frac{2m_o}{2m_o E - 2\vec{p}',\vec{p}'' - \frac{m_o + M_o}{M_o}(p'^2 + p''^2)} \cdots$$

$$f_{\ell_\beta m_\beta} \left( - \vec{p}' - \frac{M_o}{m_o + M_o} \vec{p}'' \right) N_{\ell_\beta} \; . \tag{6.9}$$

The other restriction in force is the static limit, where $M_o/m_o >> 1$. With the on-shell momentum

$$\bar{k}_\alpha^{\,2} = 2\mu(E + \varepsilon_\alpha) \; , \tag{6.10}$$

one can make the off-shell contributions in the Green's function in momentum space explicit

$$2m_o E - 2\vec{p}',\vec{p}'' - \frac{m_o + M_o}{M_o}(p'^2 + p''^2) = - 2m_o \varepsilon_\alpha - (\vec{p}' + \vec{p}'')^2$$

$$+ \frac{m_o}{M_o}(2\bar{k}_\alpha^{\,2} - p'^2 - p''^2) + \frac{m_o}{M_o} \cdot \frac{m_o}{m_o + M_o} \bar{k}_\alpha^{\,2} \; . \tag{6.11}$$

The third term in the denominator is first order in the mass ratio as well as first order in the off-shell expansion, while the fourth term is a second order term in the mass ratio. In the static limit the potential then only depends on the vector sum of the two momentum variables. Changing the sign of the integration variable gives the potential the usual form of a local interaction. This suggests a change to configuration space. After a Fourier transform we have

$$\tilde{\psi}_\alpha(\vec{r}) = \frac{1}{(2\pi)^{3/2}} e^{i\vec{r},\vec{p}} \, \delta_{\alpha\rho} +$$

$$\sum_\beta 2\mu(2\pi)^{3/2} \int d^3r' \; G_o(\vec{r},\vec{r}',\bar{k}_\alpha^{\,2}) \; \tilde{W}_{\alpha\beta}(\vec{r}') \; \tilde{\psi}_\beta(-\vec{r}') \; . \tag{6.12}$$

Since there are advanced computer routines available for its solution, it is useful to consider the corresponding differential equation with the appropriate boundary conditions,

$$[\nabla^2_{\vec{r}} + \bar{k}_\alpha^{\,2}] \; \tilde{\psi}_\alpha(r) = \sum_\beta 2\mu(2\pi)^{3/2} \; \tilde{W}_{\alpha\beta}(\vec{r}) \; \tilde{\psi}_\beta(-\vec{r}) \; . \tag{6.13}$$

A partial wave expansion is now called for. Using (3.3) and (3.4) and combining the result (6.11) we find that

$$2\mu(2\pi)^{3/2}\, W_{\ell_\alpha m_\alpha,\ell_\beta m_\beta}(\vec{r}) = \sum_{\ell m} C_{\ell m,\ell_\alpha m_\alpha \ell_\beta m_\beta}\, \omega_{\ell\ell_\alpha\ell_\beta}(r)\, Y_\ell^m(\hat{r}) \ , \qquad (6.14)$$

with the constant

$$C_{\ell m,\ell_\alpha m_\alpha \ell_\beta m_\beta} = 32\mu\, m_o\, r_o^2\, N_{\ell_\alpha}\, N_{\ell_\beta}\, i^\ell\, (-)^{\ell_\beta+m_\beta}$$

$$\left(\frac{\hat{\ell}\,\hat{\ell}_\alpha\,\hat{\ell}_\beta}{4\pi}\right)^{\frac{1}{2}} \begin{pmatrix} \ell & \ell_\alpha & \ell_\beta \\ 0 & 0 & 0 \end{pmatrix} \begin{pmatrix} \ell & \ell_\alpha & \ell_\beta \\ m & m_\alpha & -m_\beta \end{pmatrix} . \qquad (6.15)$$

The radial part is given by

$$\omega_{\ell\ell_\alpha\ell_\beta}(r) = \int_o^\infty \frac{q^2}{-2m_o\varepsilon - q^2}\, j_\ell(qr)\, j_{\ell_\alpha}(qr_o)\, j_{\ell_\beta}(qr_o)\, dq \ . \qquad (6.16)$$

For the most general form of the partial wave expansion of the function $\tilde{\psi}(\vec{r})$ one has to remember that the vector $\vec{r}$ connects the centres of mass of the two scatterers. The partial wave numbers therefore correspond to the relative angular momentum of these particles. This can be coupled with the angular momentum of the bound state to give the total angular momentum J of the system

$$\tilde{\psi}_{\ell_\alpha m_\alpha}(\vec{r}) = \sum_{Jm_J,LM} \langle Jm_J | LM,\ell_\alpha m_\alpha\rangle\ Y_L^M(\hat{r})\ \bar{\psi}_{L\ell}^J(r)$$

$$= \sum_{Jm_J,LM} \sqrt{\frac{2}{\pi}}\, i^{\ell_\alpha}\, (-)^{\ell_\alpha - L + m_J}\, \hat{J}^{\frac{1}{2}} \begin{pmatrix} \ell_\alpha & L & J \\ m_\alpha & M & -m_J \end{pmatrix} Y_L^M(\hat{r})\ \psi_{L\ell}^J(r) \ . \qquad (6.17)$$

The constants in the expansion are chosen to correspond to the ones in the expansion of the plane wave into a spherical Bessel function. After substitution of (6.14 - 17) into (6.13) an integration over the angle of $\vec{r}$ may be carried out. The various 3 - j symbols are collected in a 6 - j symbol through summation over all the magnetic quantum numbers,

$$\left[\nabla_r^2 + \bar{k}_\alpha^2 - \frac{L(L+1)}{r^2}\right]\psi^J_{L\ell_\alpha}(r)$$

$$= \sum_{L'\ell_\beta\ell} \text{cst}\; i^{\ell+\ell_\alpha+\ell_\beta}\,(-)^J \begin{Bmatrix} J & \ell_\alpha & L \\ \ell & L' & \ell_\beta \end{Bmatrix} \omega_{\ell\ell_\alpha\ell_\beta}(r)\; \psi^J_{L'\ell_\beta}(r)\;, \qquad (6.18)$$

with

$$\text{cst} = \frac{8}{\pi}\,\mu m_o\, r_o^2\, N_{\ell_\alpha}\, N_{\ell_\beta}\, \hat{\ell}[\hat{\ell}_\alpha\, \hat{\ell}_\beta\, \hat{L}'\hat{L}]^{\frac{1}{2}} \begin{pmatrix} \ell & \ell_\alpha & \ell_\beta \\ 0 & 0 & 0 \end{pmatrix} \begin{pmatrix} \ell & L & L' \\ 0 & 0 & 0 \end{pmatrix}. \qquad (6.19)$$

It is interesting to read from the 6 - j symbol in (6.18) that "$\ell$" corresponds to the transferred angular momentum in the process. The scattering amplitude is related to the phase shift of the wave function,

$$\tilde{A}_{\beta\rho} = \sum_\alpha \langle \vec{p}' | \tilde{W}_{\beta\rho} | \tilde{\psi}_\alpha \rangle = -\frac{1}{2\pi^2}\, f/2\mu\;, \qquad (6.20)$$

with

$$f = \frac{1}{2i\bar{k}_\alpha} \sum_L (2L+1)\,[\exp(2i\delta_L) - 1]\, P_L(\cos\theta)\;. \qquad (6.21)$$

The phase shift $\delta_L$ is determined by the asymptotic logarithmic derivative of the radial part of the wave function.

## 6.2 Comparison with the General Calculation

With the set of equations (6.18) we have achieved our aim, stated at the start of Chapter 5. The scattering amplitude can be calculated in two different ways. Before the computer routines are put to the test, it is worthwhile to check theoretically that the same quantity is still obtained. The proof is straightforward if a very small value is used for the radius of the delta shell. Some care has to be excercised when this limit is applied. The kernel becomes non-compact if the adiabatic limit is not first taken. We will return to this point in the next chapter.

The arguments of the spherical Bessel functions in the potential of (3.25) are proportional to the radius $r_o$. The vector coupling coefficients simplify and the summations are reduced dramatically in the zero range limit, since

$$\lim_{x\to o} \; j_\ell(x) = \delta_{\ell,o} \; . \tag{6.22}$$

As a direct result of this reduction one finds that the reaction is restricted to s-state to s-state scattering. Similarly this limit reduces the coupled set (6.18) to one differential equation only.

One has to remember that the delta shell interaction is basically a two parameter potential. In the process of limiting the radius the other free parameter, the binding energy for a certain angular momentum state, is kept fixed (we have used throughout a 2 MeV s-state binding energy). This condition means that together with a shrinking radius also a stronger reaction is being considered.

The normalization constant and the S function also depend parametrically on the radius $r_o$. It is easy to show for s-states (where $k_o \equiv k_{\ell=o}$) that

$$\lim_{r_o\to o} \; F_o(k_o) = 1 \; , \tag{6.23}$$

and hence

$$(N_{io}\, r_o)^{-2}_{r_o\to o} = \frac{4\bar{\mu}_i^{\,2}}{k_o} \; , \tag{6.24}$$

and

$$S^2_{io}(\sigma_i) = \frac{k_o}{k_o - ik_i} = 1 + O(\delta) \; . \tag{6.25}$$

Under these constraints the integral equation (3.25) reduces to

$$\tilde{A}^J_{Jo,Jo}(p',p) = \frac{C}{p'p}\, Q_J\left[\frac{1}{2p'p}\left\{2m_oE - \frac{m_o + M_o}{M_o}\,(p'^2 + p^2)\right\}\right] +$$

$$C\int dp''\; \frac{p''}{p}\; \frac{1}{E + \varepsilon - \frac{p''^2}{2\mu}}\; Q_J\left[\frac{1}{2p'p''}\left\{2m_oE - \frac{m_o + M_o}{M_o}\,(p'^2 + p''^2)\right\}\right] \tilde{A}^J_{Jo,Jo}(p'',p) \; , \tag{6.26}$$

with

$$C = \frac{1}{\pi}\,\frac{m_o}{\bar{\mu}}\,\sqrt{\frac{\varepsilon}{2\bar{\mu}}} \; . \tag{6.27}$$

The off-shell effects in the S-function have been ignored. This is justified as a restriction on the energy is already in force in the derivation of (6.18).

In the zero range limit the integration in (6.16) is easily carried out and the radial part of the potential is then

$$\omega_{ooo}(r)_{r_o \to o} = -\frac{\pi}{2} \frac{e^{-k_o r}}{r} . \tag{6.28}$$

Not surprisingly the potential in this limit takes the form of a Yukawa interaction, with space exchange, depending only on the binding energy. Using (6.28) and simplifying the constants for the s-s state case (6.18) is then written

$$\left[\nabla_r^2 + \bar{k}_o^2 - \frac{L(L+1)}{r^2}\right] \tilde{\psi}^L_{L,o}(r) = U(r)\, \tilde{\psi}^L_{L,o}(r) , \tag{6.29}$$

where

$$U(r) = C_1 \frac{e^{-k_o r}}{r} , \tag{6.30}$$

and

$$C_1 = (-)^{L+1} \frac{2\mu\, m_o}{\bar{\mu}} \sqrt{\frac{\varepsilon}{2\bar{\mu}}} . \tag{6.31}$$

For the corresponding integral equation in momentum space the t-matrix elements are introduced. The factor $1/2\mu$ is needed for dimensional reasons

$$T(\vec{p}', \vec{p}) = \frac{1}{2\mu} < \vec{p}' | U | \tilde{\psi} > . \tag{6.32}$$

They obey the equation

$$T(\vec{p}', \vec{p}) = \frac{1}{2\mu} U(\vec{p}', \vec{p}) + \int d^3p'\, U(\vec{p}', \vec{p}'') \frac{1}{\bar{k}_o^2 - p''^2} T(\vec{p}'', \vec{p}) . \tag{6.33}$$

The potential in momentum space is the Fourier transform of (6.30)

$$U(\vec{p}', \vec{p}) = \frac{C_1}{2\pi^2} \frac{1}{k_o^2 + |\vec{p}' - \vec{p}|^2} . \tag{6.34}$$

Invoking the expected radial symmetry on the t-matrix

$$T(\vec{p}',\vec{p}) = \sum_J \frac{\hat{J}}{4\pi} P_J(\cos\theta)\, T^J(p',p) \ . \qquad (6.35)$$

J is in our case the total angular momentum of the system and $\theta$ the angle between $\vec{p}'$ and $\vec{p}$. Multiplying (6.33) by $P_L(\cos\theta)$ and integrating over $\hat{p}$ gives

$$T^J(p',p) = \frac{C}{p'p} Q_J\left[\frac{1}{2p'p}\{-2m_o\varepsilon - (p'^2 + p^2)\}\right] +$$

$$2\mu C \int dp'' \frac{p''}{p} \frac{1}{\bar{k}_o^2 - p''^2} Q_J\left[\frac{1}{2p'p''}\{-2m_o\varepsilon - (p'^2 + p''^2)\}\right] T^J(p'',p) \ . \qquad (6.36)$$

For the Born term use has been made of (4.16), Comparison of (6.36) and (6.26) shows that the amplitude and the t-matrix satisfy the same integral equation if in the argument of the Legendre function the off-shell effects are neglected and the static limit is taken. It should be pointed out that (6.35) is a s- to s-state reduction of the general partial wave expansion of the amplitude given by (3.29).

# CHAPTER 7

## NUMERICAL RESULTS

We have developed two computer programs. An integral equation program (i.e.p.) to solve equation (3.25), and a differential equation program (d.e.p.) for equation (6.18).

The i.e.p. follows the methods described in Chapter 4 for the treatment of the singular structure of the kernel. The program puts no restriction on the choice of the parameter set. In the input section of the program one has to specify the value of:

the radius of the delta shell,

the s-state binding energy ($E_\phi$) ,

the three-body centre of mass energy,

the mass ratio of core and valence particle ($m$),

the cut-off value in the momentum variable.

The standard mesh is set to contain 20 points. By changing the dimension statements this is readily changed to any other number. One has to distribute explicitly these points over the square root region, the bound state pole area, and the asymptotic area. As stated in Chapter 4 the points can be evenly spread over the regions. The square root and logarithmic singularities in the kernel are not reached for positive values of the momentum variable if the energy is below the break-up threshold. The mesh points are then distributed only over the other regions.

The program is designed to calulate the matrix elements for s-state to s-state scattering, to invert the matrix equation and to calculate the phase shift. The constant $\tilde{C}_{L'\ell',L\ell}$ (Eq. 3.28), containing the vector coupling coefficients is calculated and stored separately.

Extension of the program to incorporate scattering from s-state to p-state or higher angular momentum would be fairly straightforward. The

kernel contains a summation over the angular momentum of the intermediate bound state. This gives rise to an increase in the number of basic blocks that constitute, the matrix representing the kernel (one block for s-state, nine for s- to p-state scattering, etc.). In order to keep the amount of core taken up by the program under 100 k(octal) - presently 77k - one would have to store the matrix elements and perform the inversion separately.

The radius of the delta shell is a determining factor in the number of angular momentum states that contribute in the factorization of the form factor Eq. (3.5 - 6). This is best illustrated by an example. For s- to s-state scattering, let the maximum value taken into account for the $\ell_1$, $\ell_2$, $\ell_1'$ and $\ell_2'$ be three. Then approximately thirty combinations of the set $\{\ell_1, \ell_2, \ell_1', \ell_2', n\}$ contribute in the summations of Eq. (3.27) for the potential. For a mesh with 40 points, necessary for accurate results in some cases when J = 0, the computer time becomes approximately 1000 sec. This is the type of combination that will occur for a radius of .1 fm. A larger radius requires a larger span for the $\ell_1$, etc. An increase here of one leads to approximately double the number of combinations contributing and a tripling of the computer time. This is why we have, for most of our calculations restricted the radius $r_o$ to values $r_o \leq .1$ fm. Depending on the energy considered, it often suffices to use only zero and first order Bessel functions in (3.27) for J = 0 and zero order only for J > 0, resulting in average computer times of approximately 60 sec.

The d.e.p. solves (6.18) for

$$\ell = \ell_\alpha = \ell_\beta = 0 \ . \tag{7.1}$$

The condition (7.1) reduces the number of coupled equations in (6.18) to one. The $\ell_\alpha$ and $\ell_\beta$ are the order of spherical Bessel functions with arguments proportional to the radius $r_o$ (c.f. 6.16). This restriction is therefore strictly speaking only valid in the limit of zero range interactions.

Practice has shown, however, that in the static limit good results are obtained for values of $r_o$ up to .1 fm.

The d.e.p. uses Hamming's predictor corrector method. The software was taken from the S.S.P. (58). The calculation of the wave function usually requires about 20 sec. The program was tested using a weak square well potential, and also by solving the Schrödinger equation for a Yukawa interaction for a range of parameters.

7.1 Comparison of the d.e.p. and the i.e.p.

In Section 6.2 we have shown that the solution to the differential equation (6.18) and the integral equation (3.25) lead to the same scattering amplitude. The equivalence of the equations was explicitly shown in the zero range limit. This is easily simulated in both programs by taking a radius $r_o = 10^{-8}$ fm. Two other restrictions were also enforced - the adiabatic limit and the static limit. Both of these are already absorbed in the explicit formulation of (6.18). In the adiabatic limit the S-function becomes equal to unity. The static limit resulted in a local effective potential (c.f. 6.9 and 6.11). These limits were incorporated in the i.e.p. by altering the routines calculating the S-function and the Legendre function, whose argument was set equal to the expression shown in (6.36). Phase shifts obtained by the d.e.p. and the modified integral equation program (m.i.e.p.) are compiled in Table 7.1. The parameters used for the energy and mass ratio were

$$E_{\phi} = 2. \quad \text{MeV}$$

$$E = -1.99 \text{ MeV}$$

$$M_o = 50\, m_o$$

with $m_o$ corresponding to the mass of the neutron

$$2m_o = .0481 \text{ MeV}^{-1} \text{ fm}^{-2} .$$

| | $r_o = 10^{-8}$ | | $r_o = .01$ | | $r_o = .1$ | |
|---|---|---|---|---|---|---|
| | d.e.p. | m.i.e.p. | d.e.p. | m.i.e.p. | d.e.p. | m.i.e.p. |
| $\delta_0$ | .8493 | .8314 | .8411 | .8252 | .4530 | .4522 |
| $\delta_1$ | - .2393 | - .2393 | - .2393 | - .2393 | - .2394 | - .2393 |
| $\delta_2$ | .05739 | .05735 | .05739 | .05733 | .05746 | .05526 |
| $\delta_3$ | - .003609 | - .003639 | - .003607 | - .003639 | - .003607 | - .003639 |
| $\delta_4$ | $.34310^{-3}$ | $.35510^{-3}$ | $.34310^{-3}$ | $.35510^{-3}$ | $.34310^{-3}$ | $.35510^{-3}$ |
| $\delta_5$ | $-.2010^{-4}$ | $-.2010^{-4}$ | $-.2010^{-4}$ | $-.2010^{-4}$ | $-.2010^{-4}$ | $-.2010^{-4}$ |

Table 7.1

Phase shifts as calculated by the d.e.p. and m.i.e.p. using the parameters given in Section 7.1, and the values $10^{-8}$, .01 and .1 fm for the radius of the delta shell.

The mesh in the m.i.e.p. was made up of forty points. The cut-off depended on the value of the total angular momentum considered. For J = 0 it was put at three hundred times the on-shell momentum. The range of the half on-shell amplitude became much smaller for higher angular momentum states (approximately twenty times the on-shell momentum for J > 0). This change can be attributed to the quicker fall-off for the higher order Legendre functions of the second kind.

Testing is not restricted to the zero range limit only. In the d.e.p. this means that one should consider the full coupled set of equations. However, as mentioned in the introduction of the chapter, we have enforced the restriction (7.1) throughout.

The calculations have been carried out for $r_o = .01$ and $r_o = .1$ (Table 7.1). For $r_o$ non-zero spherical Bessel functions of higher order then zero may need to be considered in the integral equation. Tests show that only if J = 0 Bessel functions of order one for $r_o = .01$ and of order one and two if $r_o = .1$ have to be incorporated.

## 7.2 Solution by Iteration and Inversion

The i.e.p. has been especially designed for calculations of scattering processes with energies above the break-up threshold. The comparison between m.i.e.p. and the d.e.p. left an important part of the i.e.p. untouched, namely the square root and logarithmic singularities of the kernel. One way of testing the program for positive three-body energy is a comparison of the half-on-shell amplitude as determined by the i.e.p. and a Born series. In this test we want to use a parameter set corresponding to the process of interest. We choose

$$E_{\phi} = 2 \text{ MeV}$$

$$E = 5 \text{ MeV}$$

$$M_o = 12\, m_o \quad .$$

For practical reasons we select a delta shell radius of $r_o = .1$ fm. This ensures that only the lower order spherical Bessel functions (zero and one) have to be included in the calculations.

The Born series can only converge if the largest eigenvalue of the kernel is less than one. The convergence is not apparent after two iterations with the given parameter set, although the absolute value of the largest eigenvalue is only .4284.

The structure of the kernel is unaffected if the constant $c_\alpha$ (Eq. 3.26) is divided by a constant greater than one, but the eigenvalues are reduced by the same factor. Division by three or more allows a favourable test on the kernel. It should be noted that a different reaction is considered by altering the $c_\alpha$, but that is not the main point of interest here. The results are presented in Fig. 7.1 and Table 7.2.

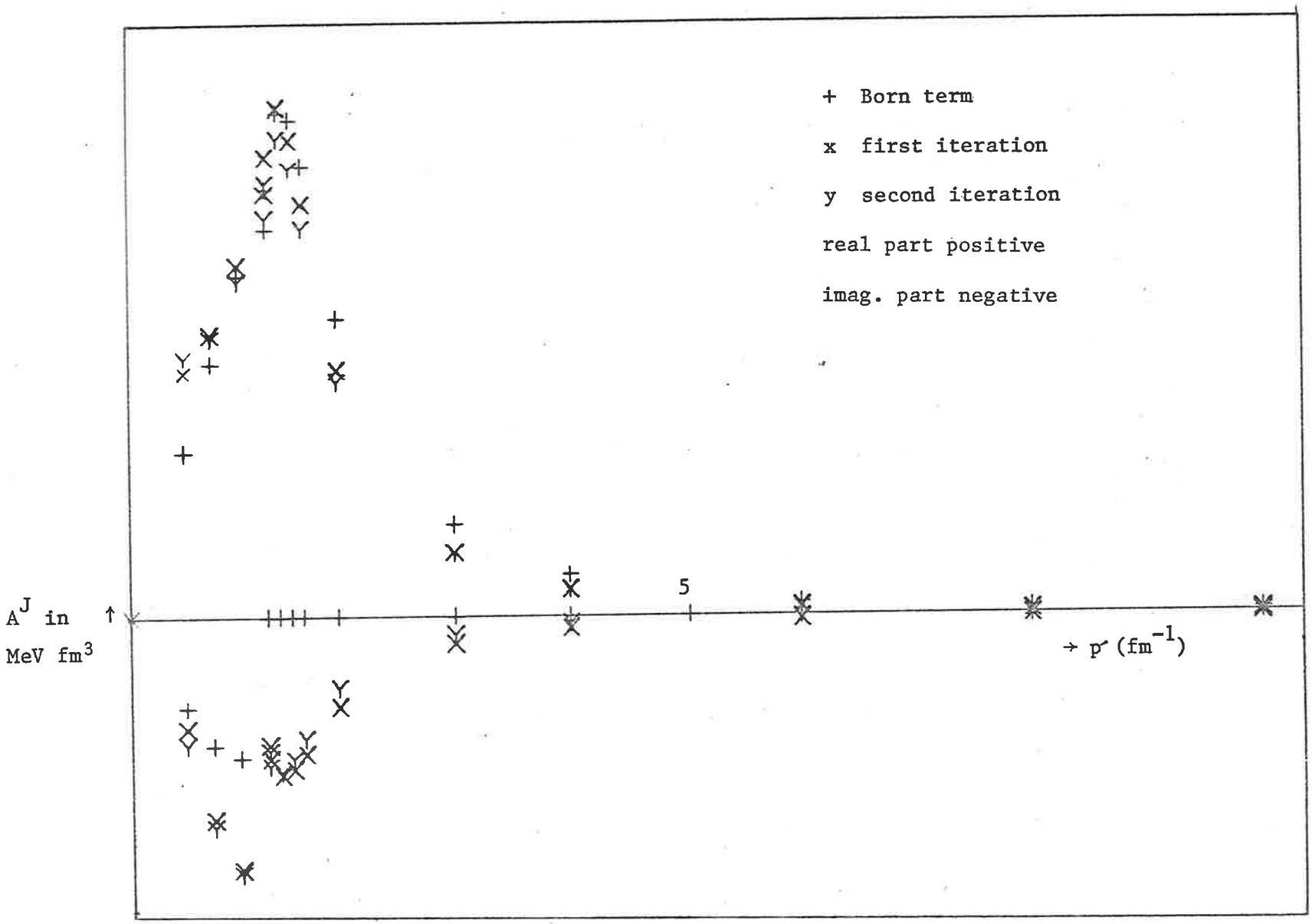


Fig. 7.1: Comparison of real and imaginary parts of Born term (+), first-(x) and second-(y) iterative half-on-shell amplitude. See also Table 7.2.

| p′ | $\tilde{V}$ | | first iteration | | second iteration | | exact | |
|---|---|---|---|---|---|---|---|---|
| | real | imag. | real | imag. | real | imag. | real | imag. |
| 0.000 | 0. | 0. | 0. | 0. | 0. | 0. | 0. | 0. |
| .490 | .139E+00 | -.754E-01 | .205E+00 | -.927E-01 | .217E+00 | -.105E+00 | .215E+00 | -.108E+00 |
| .735 | .212E+00 | -.106E+00 | .237E+00 | -.168E+00 | .233E+00 | -.175E+00 | .232E+00 | -.176E+00 |
| .981 | .286E+00 | -.117E+00 | .295E+00 | -.210E+00 | .281E+00 | -.215E+00 | .281E+00 | -.214E+00 |
| 1.226 | .325E+00 | -.439E-07 | .355E+00 | -.106E+00 | .334E+00 | -.112E+00 | .334E+00 | -.109E+00 |
| 1.236 | .359E+00 | 0. | .387E+00 | -.118E+00 | .364E+00 | -.124E+00 | .363E+00 | -.121E+00 |
| 1.343 | .424E+00 | 0. | .428E+00 | -.132E+00 | .402E+00 | -.130E+00 | .403E+00 | -.126E+00 |
| 1.450 | .418E+00 | 0. | .400E+00 | -.127E+00 | .376E+00 | -.119E+00 | .378E+00 | -.116E+00 |
| 1.557 | .378E+00 | 0. | .346E+00 | -.114E+00 | .325E+00 | -.101E+00 | .328E+00 | -.998E-01 |
| 1.865 | .249E+00 | 0. | .206E+00 | -.749E-01 | .196E+00 | -.593E-01 | .199E+00 | -.599E-01 |
| 2.901 | .764E-01 | 0. | .530E-01 | -.229E-01 | .525E-01 | -.152E-01 | .534E-01 | -.161E-01 |
| 3.936 | .339E-01 | 0. | .213E-01 | -.102E-01 | .219E-01 | -.603E-02 | .222E-01 | -.668E-02 |
| 6.008 | .109E-01 | 0. | .607E-02 | -.327E-02 | .660E-02 | -.172E-02 | .667E-02 | -.200E-02 |
| 8.080 | .477E-02 | 0. | .247E-02 | -.143E-02 | .279E-02 | -.697E-03 | .281E-02 | -.843E-03 |
| 10.152 | .242E-02 | 0. | .119E-02 | -.726E-03 | .138E-02 | -.335E-03 | .139E-02 | -.417E-03 |
| 13.923 | .831E-03 | 0. | .392E-03 | -.249E-03 | .466E-03 | -.110E-03 | .466E-03 | -.140E-03 |
| 17.693 | .303E-03 | 0. | .140E-03 | -.909E-04 | .169E-03 | -.393E-04 | .168E-03 | -.507E-04 |
| 21.464 | .103E-03 | 0. | .474E-04 | -.310E-04 | .574E-04 | -.133E-04 | .572E-04 | -.172E-04 |
| 25.235 | .282E-04 | 0. | .129E-04 | -.846E-05 | .156E-04 | -.361E-05 | .156E-04 | -.469E-05 |
| 29.006 | .395E-05 | 0. | .181E-05 | -.119E-05 | .219E-05 | -.506E-06 | .219E-05 | -.657E-06 |

Table 7.2

Comparison of Born term, first and second iterative and exact solutions

of the i.e.p. E = 5 MeV, J = 1, $r_o$ = .1 fm.

## 7.3 Energies Above the Three-Body Break-up Threshold

The previous stages have all been leading up to the calculations concerning the process (1.1)

$$C^{12} + C^{13} \rightarrow C^{12} + C^{13}$$

at energies above the break-up threshold.

The range of the delta shell was taken as $r_o$ = .1 fm. The phase shift for varying total angular momentum has been obtained for the centre of mass energies 1, 5, 10 and 50 MeV. The mesh contained 20 points, except for J = 0, when 40 points were used. The other parameters were

$$E_\phi = 2 \text{ MeV}$$

$$M_o = 12\ m_o \ .$$

Only in the case of total angular momentum zero was it necessary to include first order spherical Bessel functions in the calculations. Everywhere else it sufficed to use zero order only. Some typical results are listed in Table 7.3. The corresponding differential cross sections are plotted in Figs. 7.2 - 7.5. They all exhibit the same basic structure. There are two peaks, located at forward and backward scattering angles. The width of the forward peak is energy dependent and decreases from $40^o$ at E = 1 MeV to $17^o$ at E = 50 MeV. The backward peak has almost constantly a width of $20^o$ reducing slightly at higher energies. The height ratio between backward and forward scattering is approximately 6.7. The total cross section reduces from 900 mb at E = 1 MeV to 33 mb at 50 MeV. These results indicate that the two competing processes take place without causing much deflection. From the ratio of the area under the peaks one then concludes that in the majority of the scattering processes, exchange of the valence particle takes place. Not surprisingly, there is a reduction in the cross section for higher energies, as the particles have less time to "see" each other.

| | E = 1 MeV<br>σ = 904 mb | E = 5 MeV<br>σ = 398 mb | E = 10 MeV<br>σ = 258 mb | E = 50 MeV<br>σ = 33 mb |
|---|---|---|---|---|
| $\delta_0$ | .808 + i.009 | .302 + i.016 | - .005 + i.003 | - .430 + i.028 |
| $\delta_1$ | - .975 + i.007 | - .904 + i.101 | - .879 + i.144 | - .338 + i.248 |
| $\delta_2$ | .652 + i.000 | .652 + i.010 | .629 + i.046 | .427 + i.098 |
| $\delta_3$ | - .385 | - .448 + i.012 | - .467 + i.017 | - .283 + i.106 |
| $\delta_4$ | .249 | .306 + i.002 | .318 + i.014 | .244 + i.037 |
| $\delta_5$ | - .161 | - .209 + i.002 | - .270 + i.001 | - .204 + i.049 |
| $\delta_6$ | .105 | .145 + i.000 | .181 + i.002 | .162 + i.020 |
| $\delta_7$ | - .070 | - .108 | - .158 + i.002 | - .148 + i.025 |
| $\delta_8$ | .047 | .071 | .112 + i.001 | .114 + i.011 |
| $\delta_9$ | - .032 | - .057 | - .098 + i.001 | - .106 + i.013 |
| $\delta_{10}$ | .021 | .041 | .072 + i.000 | .083 + i.006 |
| $\delta_{11}$ | - .015 | - .030 | - .062 | - .077 + i.007 |
| $\delta_{12}$ | .010 | .022 | .046 | .061 + i.004 |

Table 7.3

Phase shifts and total cross section
obtained by the i.e.p. with $r_o = .1$ .

The general shape of the half-on-shell amplitude for various energy and total angular momentum is shown in Fig. 7.6 - 7.9. It is long ranged and has a broad peak for J = 0. For all other values of J it becomes short ranged and the imaginary and real part have opposite sign. It is interesting to note that most half-on-shell amplitudes exhibit a discontinuous first derivative at the square root singularity. As can be seen in Figs. 7.6 - 7.9 this effect becomes more pronounced for larger centre-of-mass energy. This justifies our precaution of not interpolating the function across this singular point.

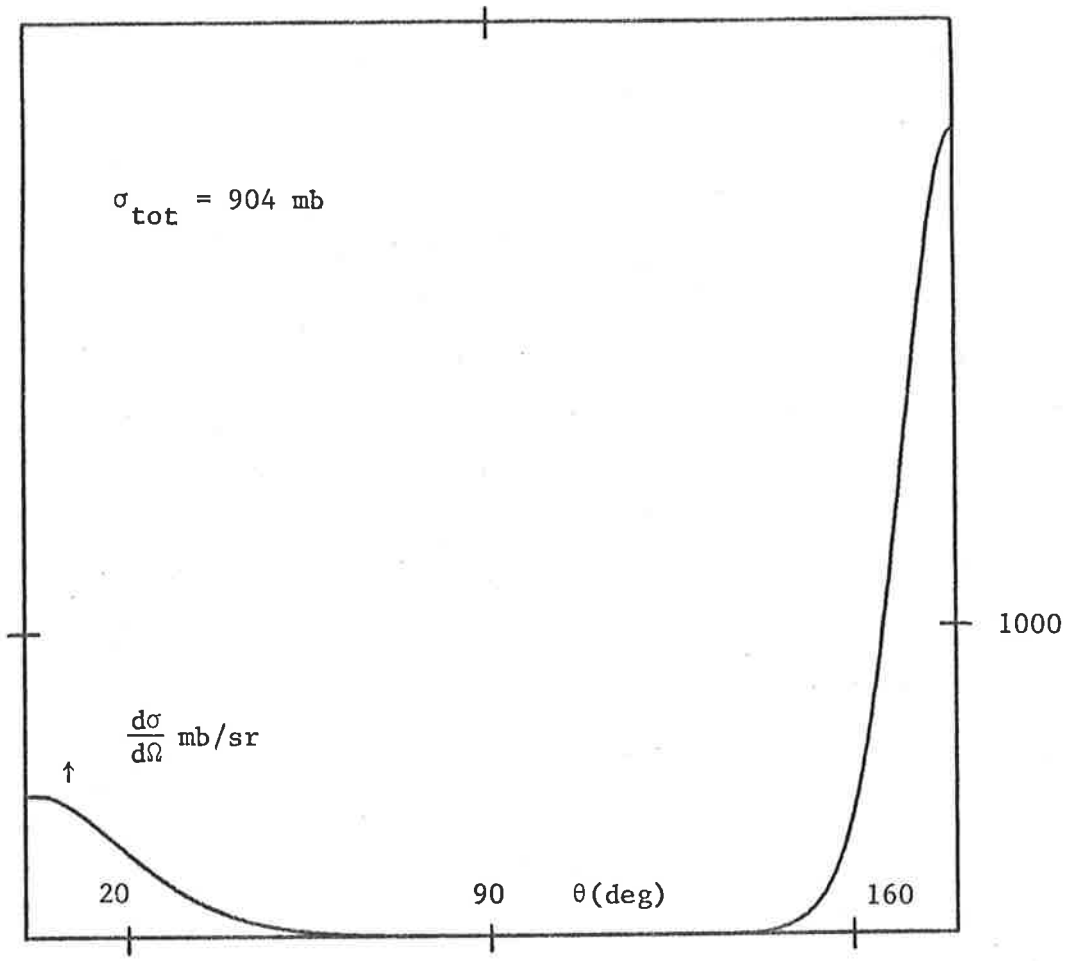


Fig. 7.2: dif. cross section, E = 1 MeV

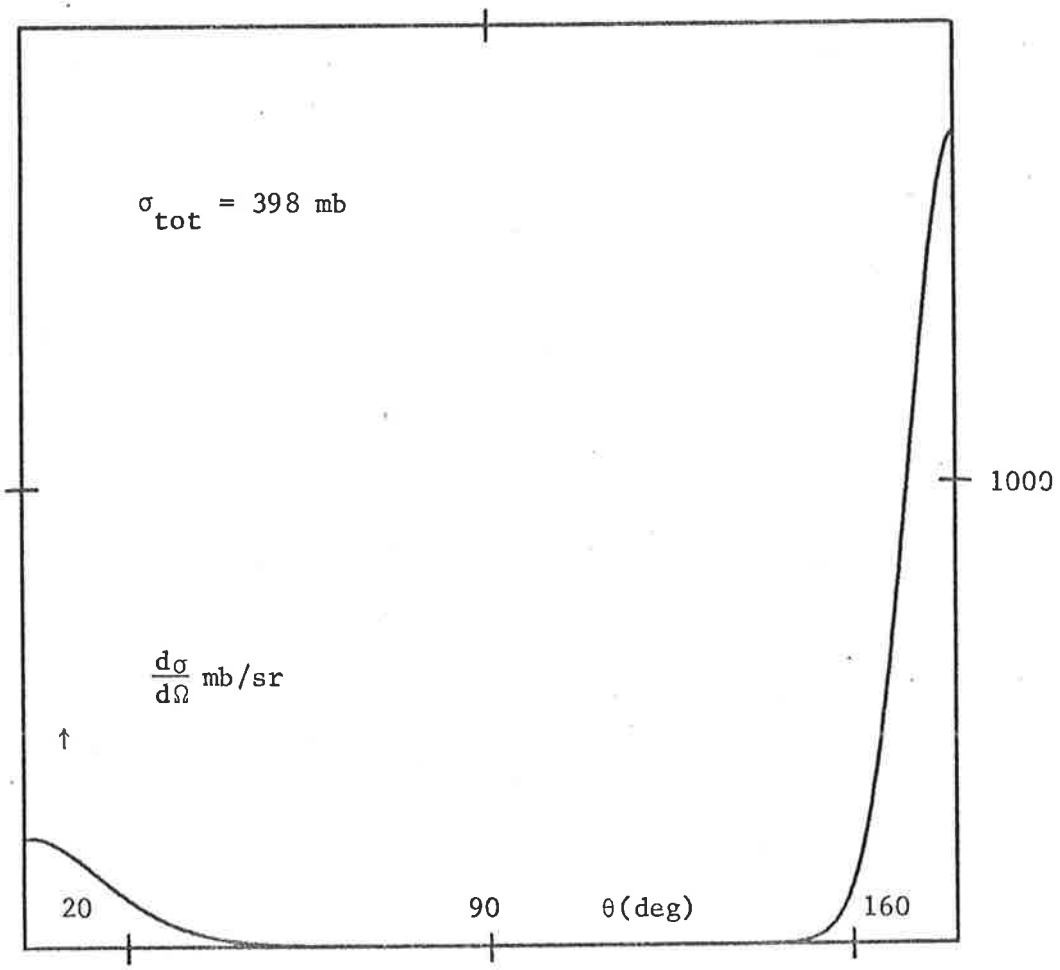


Fig. 7.3: dif. cross section, E = 5 MeV

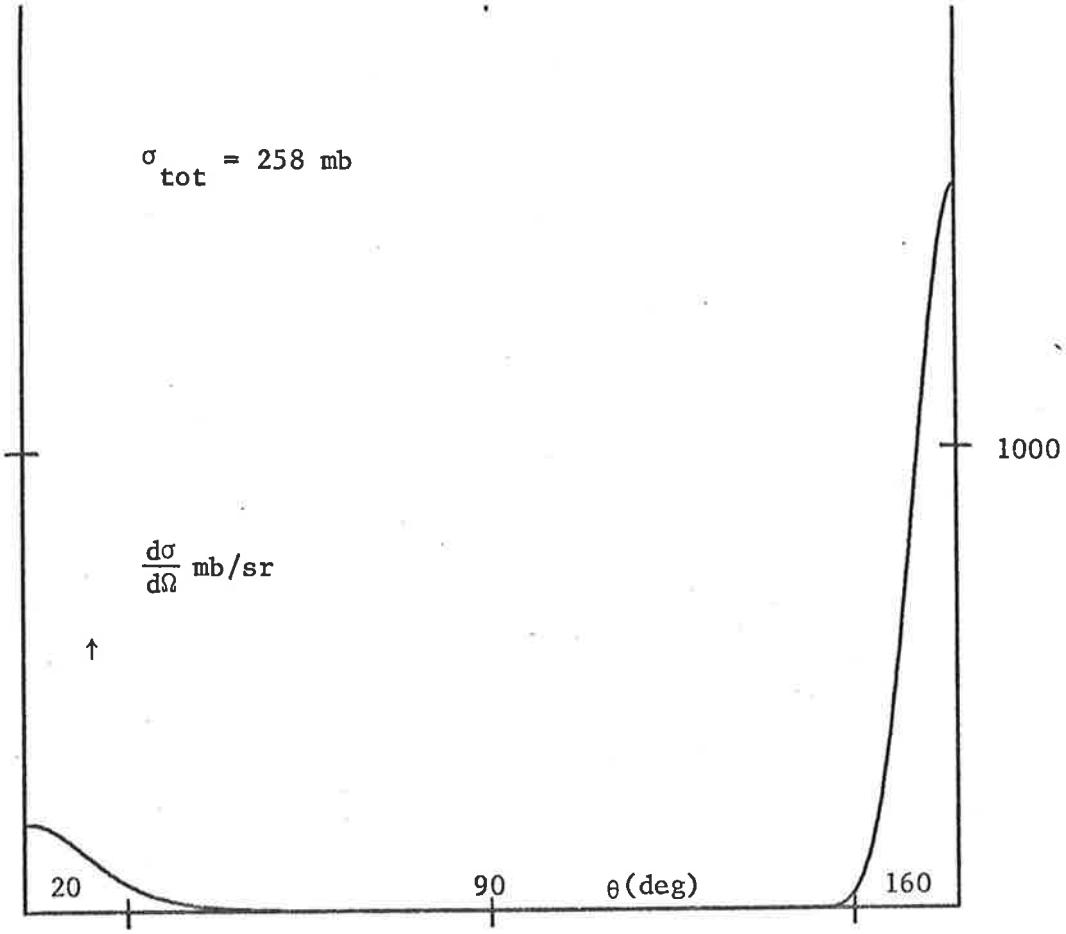


Fig. 7.4: dif. cross section, E = 10 MeV

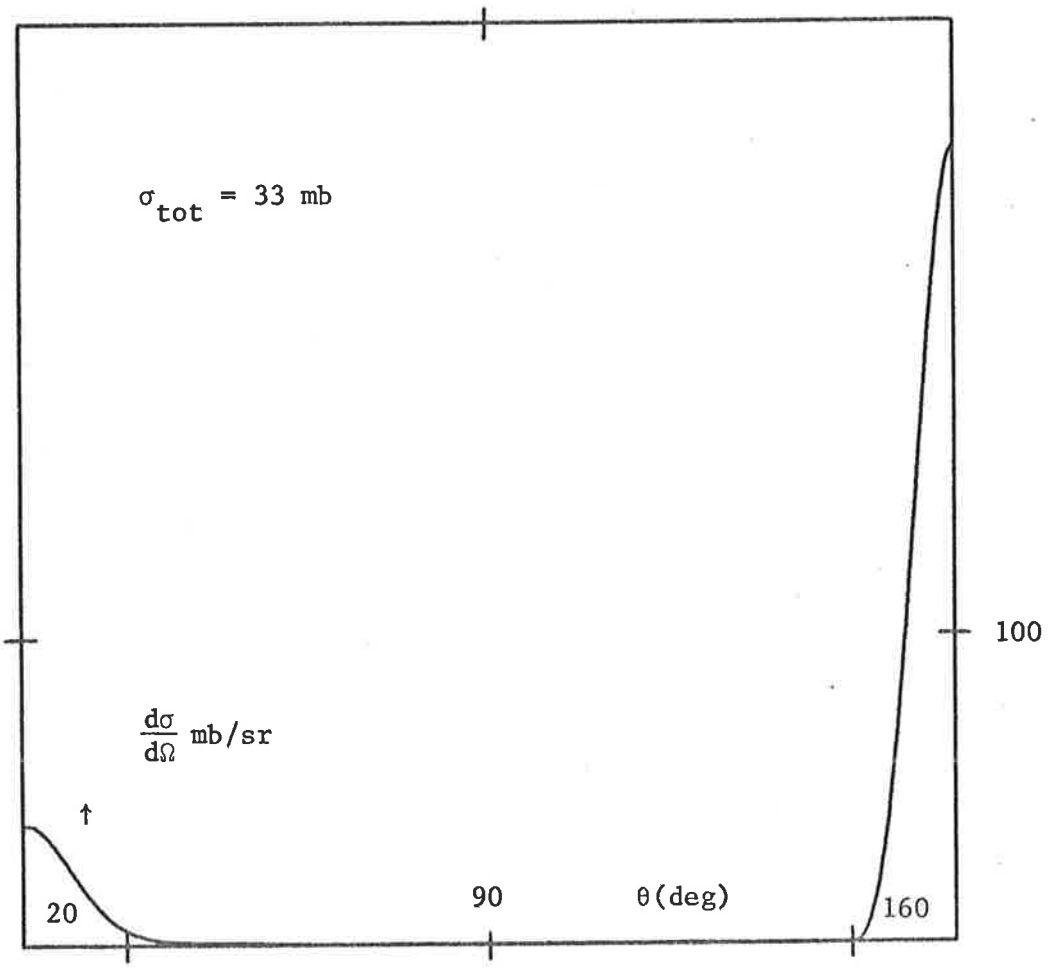


Fig. 7.5: dif. cross section, E = 50 MeV

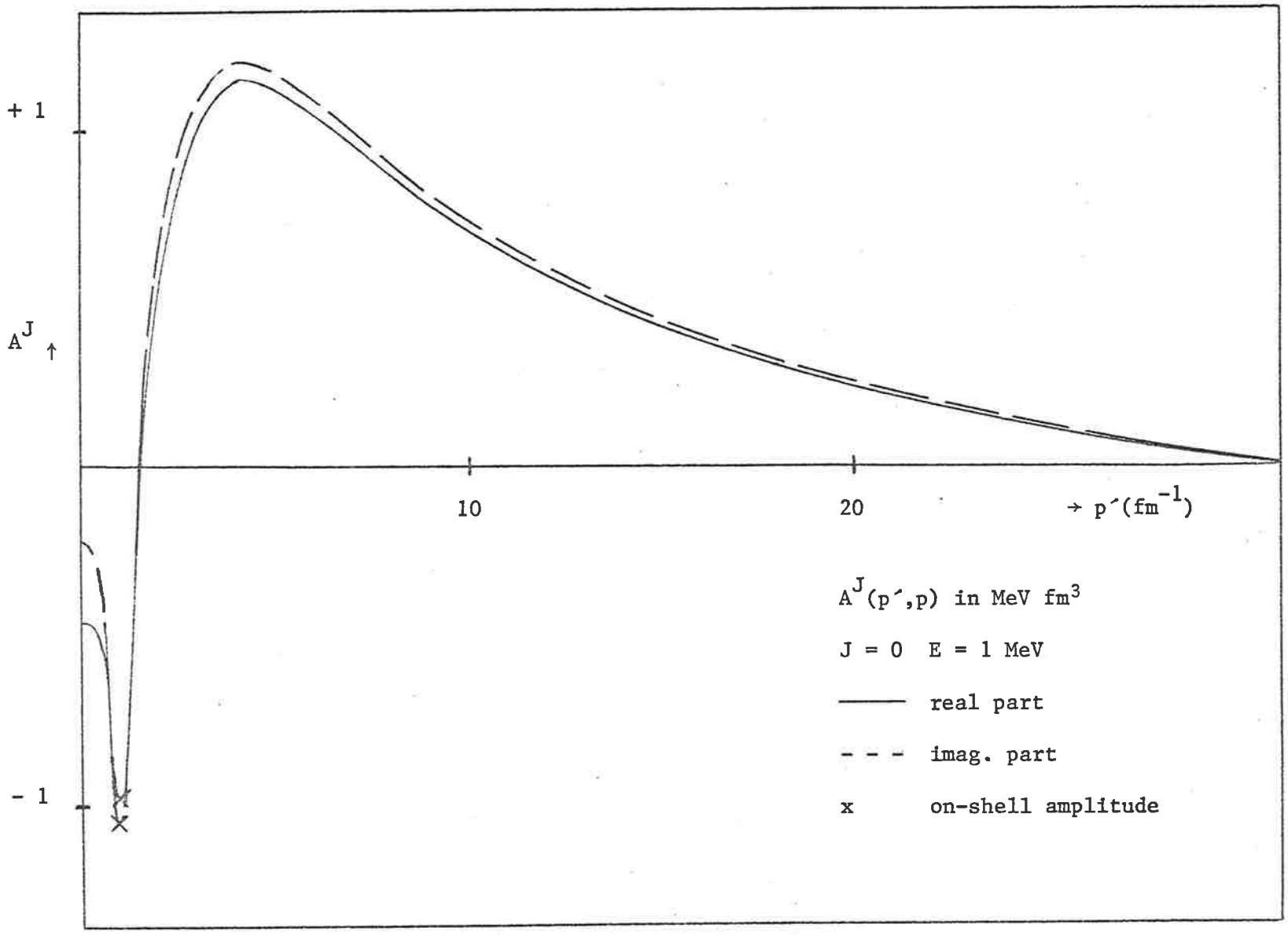


Fig. 7.6: Half-on-shell amplitude $A^J(p',p)$

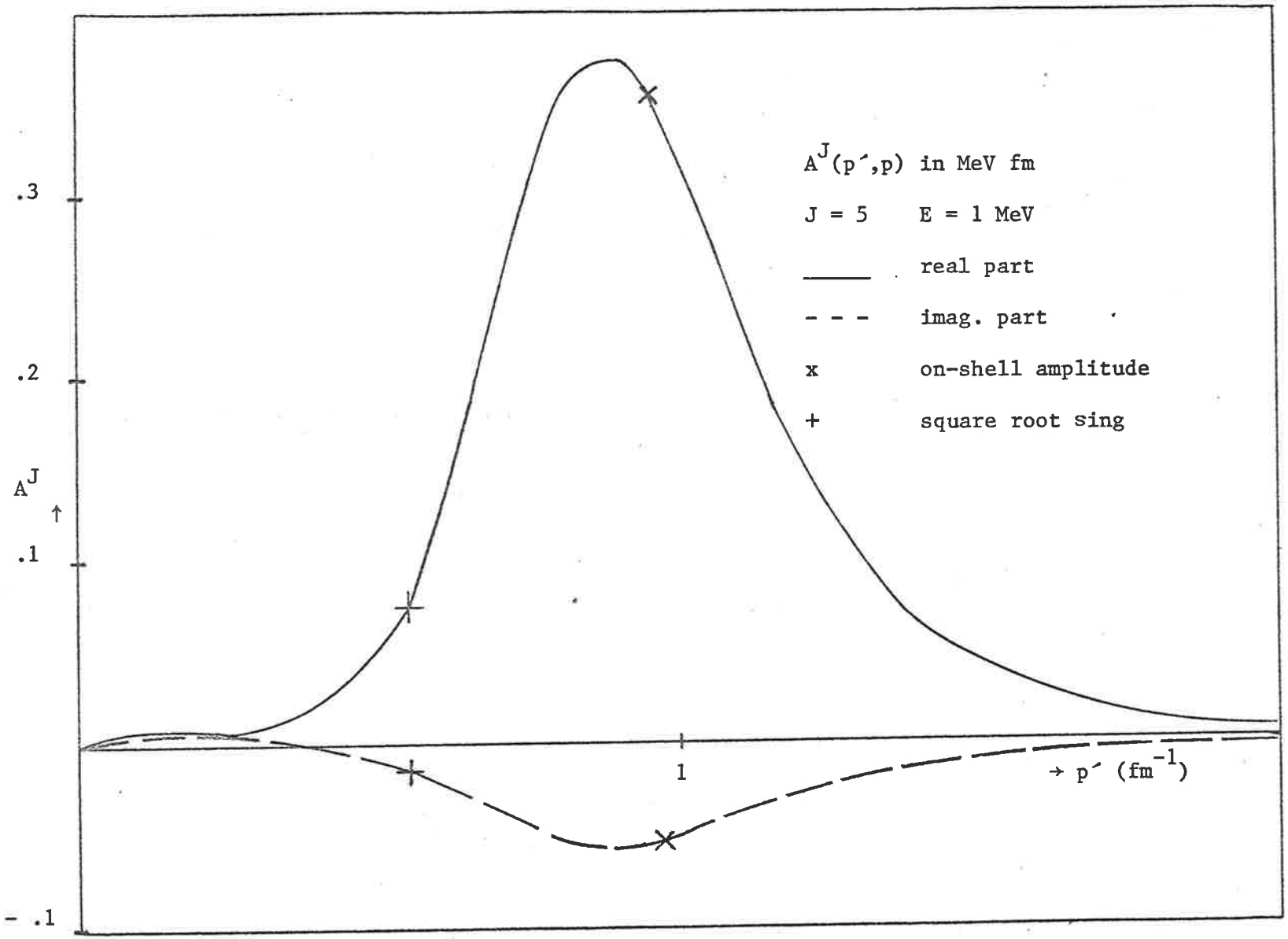


Fig. 7.7: Half-on-shell amplitude $A^J(p',p)$

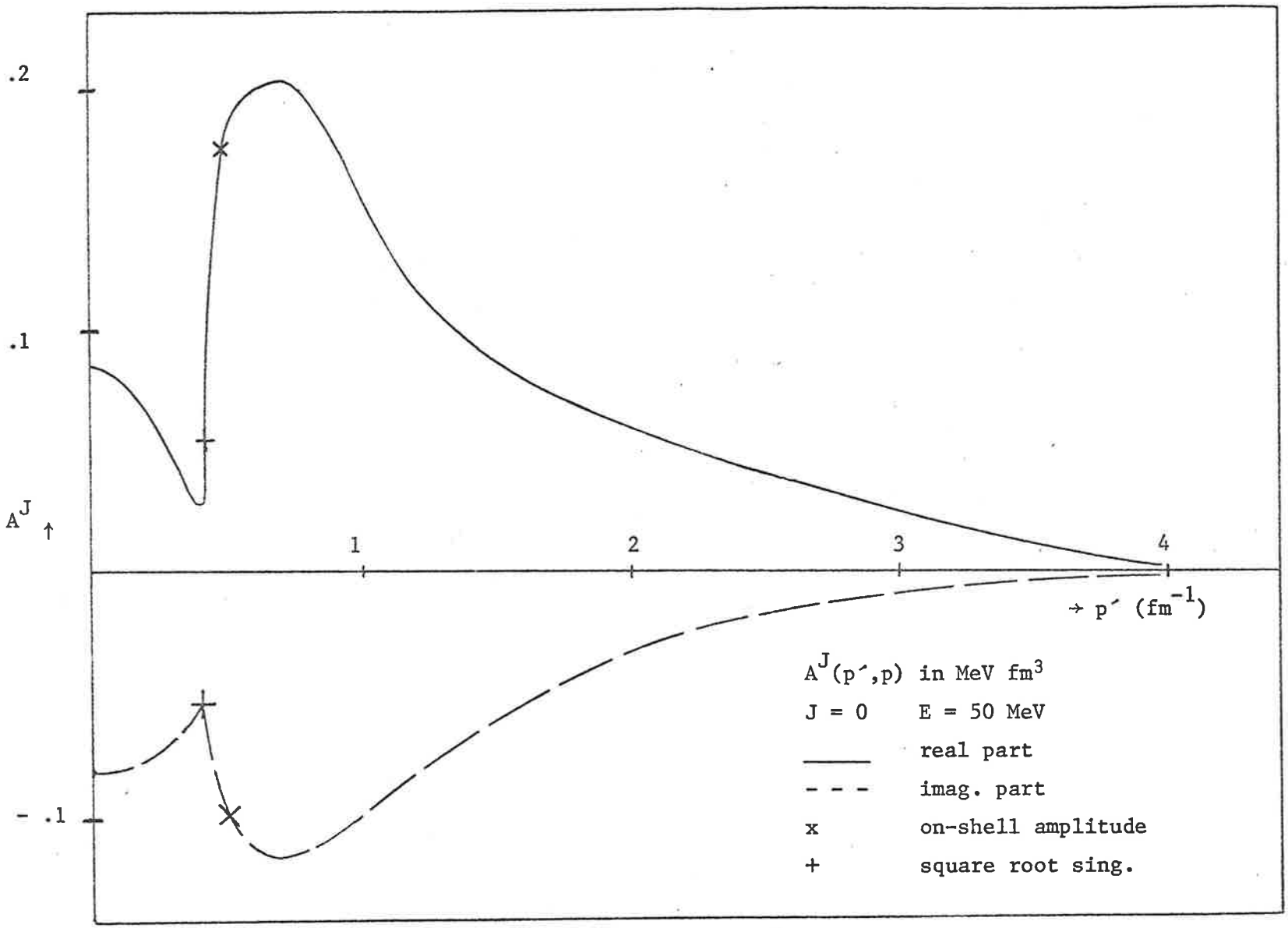


Fig. 7.8: Half-on-shell amplitude $A^J(p',p)$

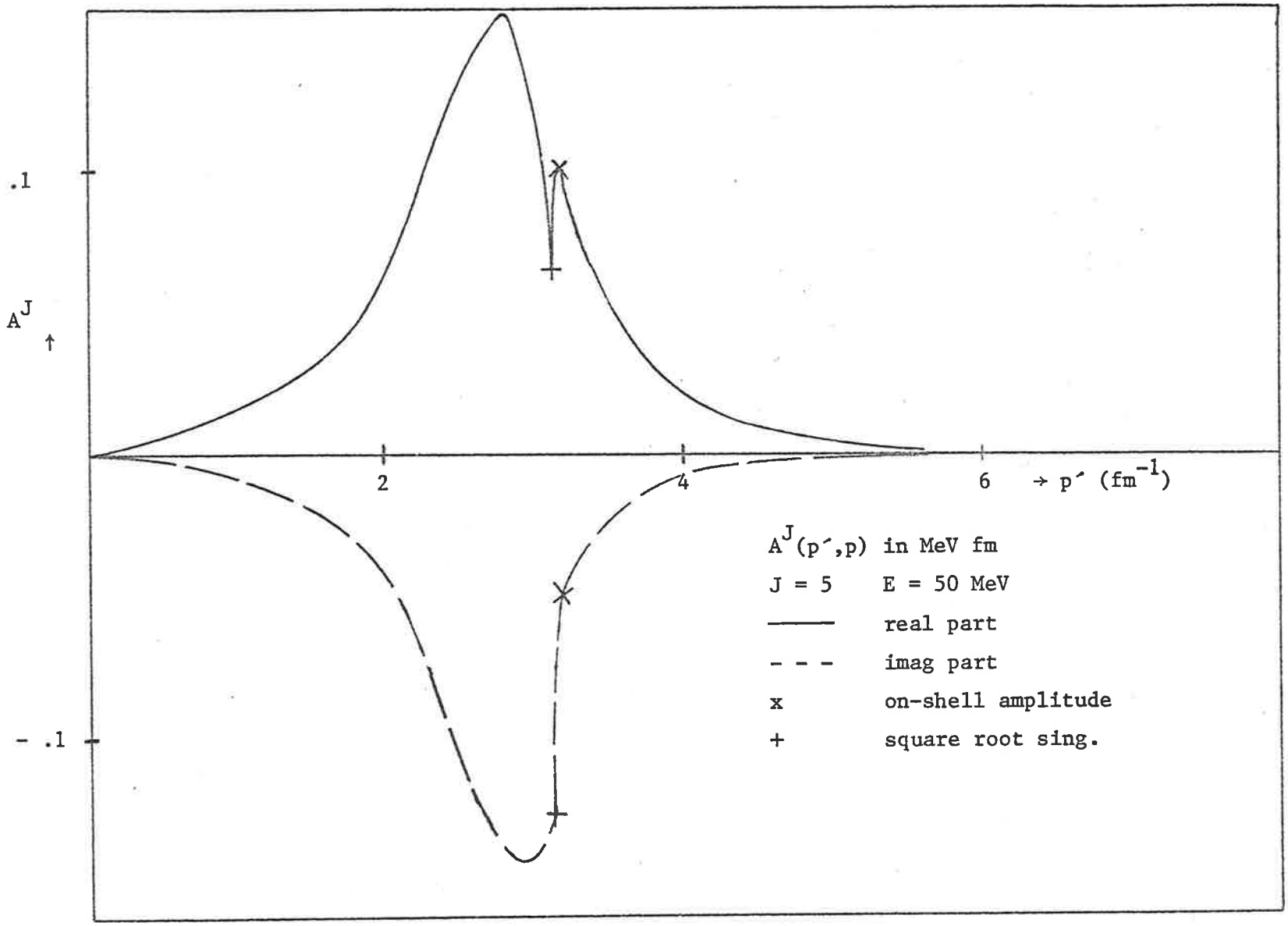


Fig. 7.9: Half-on-shell amplitude $A^J(p´,p)$

## 7.4 Calculations Testing the Validity of the Static and Adiabatic Limit

In a recent study by Fonseca and Shanley (59) the three-body bound state energy spectrum and the three-body bound state wave function have been calculated. The three particles are made up of two identical heavy ions and a light valence particle. The valence-core potential is also the only interaction taken into account. The exact solution is compared with the Born-Oppenheimer approximation for varying mass ratio. They obtain very good agreement for $m > 30$. But even for smaller values up to the equal mass case their agreement was surprisingly good. By varying the mass ratio $m$ in the d.e.p. and the i.e.p. a test is created for a similar configuration of interacting particles, but now engaged in a scattering process.

The Sturmian expansion relies on two limiting processes: the static limit and the adiabatic limit. The static limit is essential in the reduction of the problem to a differential equation. The effective interaction takes the form of a local potential when the limit is applied. We have compared the phase shift for varying mass ratio as calculated by the d.e.p., the m.i.e.p. and the i.e.p. In the i.e.p. the adiabatic limit was enforced by putting the S-function equal to unity. The following parameter set was used

$$r_o = .1 \text{ fm} ,$$

$$E_\phi = 2 \text{ MeV} ,$$

$$E = -1.90 \text{ MeV} ,$$

$$1 < m = M_o/m_o < 100 .$$

The d.e.p. and m.i.e.p. gave identical answers, confirming once more that the restriction (7.1) was still justified. The results of the d.e.p. are well understood. Recalling the essential form of the d.e. (c.f. 6.29 - 30 for L = 0)

$$[\nabla_r^2 + \bar{k}_o^2]\ u_\ell(r) = U_\ell(r)\ u_\ell(r)\ , \tag{7.2}$$

$$U_\ell(r) = C_1 \frac{e^{-k_o r}}{r}\ . \tag{7.3}$$

with $\bar{k}_o$, $k_o$ and $C_1$ defined by resp. Eq.(6.20),(3.9) and (6.31). In the case of equal masses the wave number $\bar{k}_o$ becomes so small, that the potential $U_\ell$ dies out before there is a noticeable change in the radial part of the wave function. The $k_o(m)$ and $C_1(m)$ increase for increasing value of $m$, resulting in a deeper but shorter potential. For small $m$ the effect on $k_o$ and $C_1$ balance out ($1 < m < 5$). For $5 < m < 30$ the change in the $C_1(m)$ dominates over the variation in $k_o(m)$, which has almost become constant and an increase in the $\delta_o$ results. Where $M_o > 30\ m_o$ the true static limit sets in. The $C_1(m)$ is now proportional to $M_o$ and the phase shift increases linearly. The i.e.p., (with $S \equiv 1$) shows a similar dependence, but the phase is shifted back by approximately $\pi/4$. Another difference is for the very low values of $m$, when the phase shift keeps decreasing. It appears that a mass ratio of thirty is indeed sufficient for the static limit condition to be satisfied. A result which agrees with the findings of Fonseca and Shanley.

The other limiting process to be tested is the adiabatic limit. For this we ran four different programs: the d.e.p. (1), the i.e.p. with the "static" changes to the Legendre-function (2), the i.e.p. with $S \equiv 1$ (3), and the full i.e.p. (4). The parameter set used was

$$r_o = .1 \text{ fm}$$

$$E_\phi = 2 \text{ MeV}$$

$$M_o = 50\ m_o$$

and the centre of mass energy varied between -1.999 MeV and - 1.70 MeV. The four programs compare then the situation when the adiabatic plus static limit (1), the adiabatic limit on its own (2), the static limit on its own (3) and no limit is enforced.

The behaviour of the d.e.p. again is predictable. The only parameter in (7.2-3) that depends on the energy E is the wave number $\bar{k}_o$. An increase in E causes an increase in the $\bar{k}_o$ and a decrease in the phase shift.

Results of the three comparison programs all show a similar variation in the phase shift over the energy domain studied. However, the magnitude of the phase shift varies, depending on which limit is applied. The effect of not enforcing the static limit causes a phase shift of $-\pi/4$. The amount corresponds to the previous test as we use a mass ratio of fifty, well into the "static" area. Dropping the adiabatic restrictions results in an even larger, though uniform shift of $-\pi/3$, while the exact calculations give a phase shift situated between the adiabatic and the adiabatic plus static solutions. A graphical comparison is given in Figs. 7.10 - 11.

The discrepancy between the Sturmian expansion and the comparison calculation can in both tests be traced back to the long range behaviour of the half-on-shell amplitude. In the static limit we made the change

$$\frac{1}{p'p} Q_o\left[\frac{1}{2p'p}\left\{2m_oE - \frac{m_o + M_o}{M_o}(p'^2 + p^2)\right\}\right] \to \frac{1}{p'p} Q_o\left[\frac{1}{2p'p}\left\{-2m_oE_\phi - p'^2 - p^2\right\}\right].$$

This does not alter the asymptotic behaviour of the function off the line $p' = p$. However, close to this line the function values are changed sufficiently to influence the half-on-shell amplitude and the phase shift.

The differences in the adiabatic limit are more apparent. One easily derives the asymptotic momentum behaviour of the constituent factors to the kernel (see Appendix D for 7.4)

$$S_o^2(p) = -(2m)^{3/2} r_o^2 \frac{p^2}{k_o}, \tag{7.4}$$

$$\frac{1}{p'p} Q_o\left[\frac{1}{2p'p}\left\{-2m_oE_\phi - p'^2 - p^2\right\}\right] \sim \frac{1}{-2m_oE_\phi - p'^2 - p^2}, \tag{7.5}$$

$$j_o(pr_o) = \frac{\sin(pr_o)}{pr_o}. \tag{7.6}$$

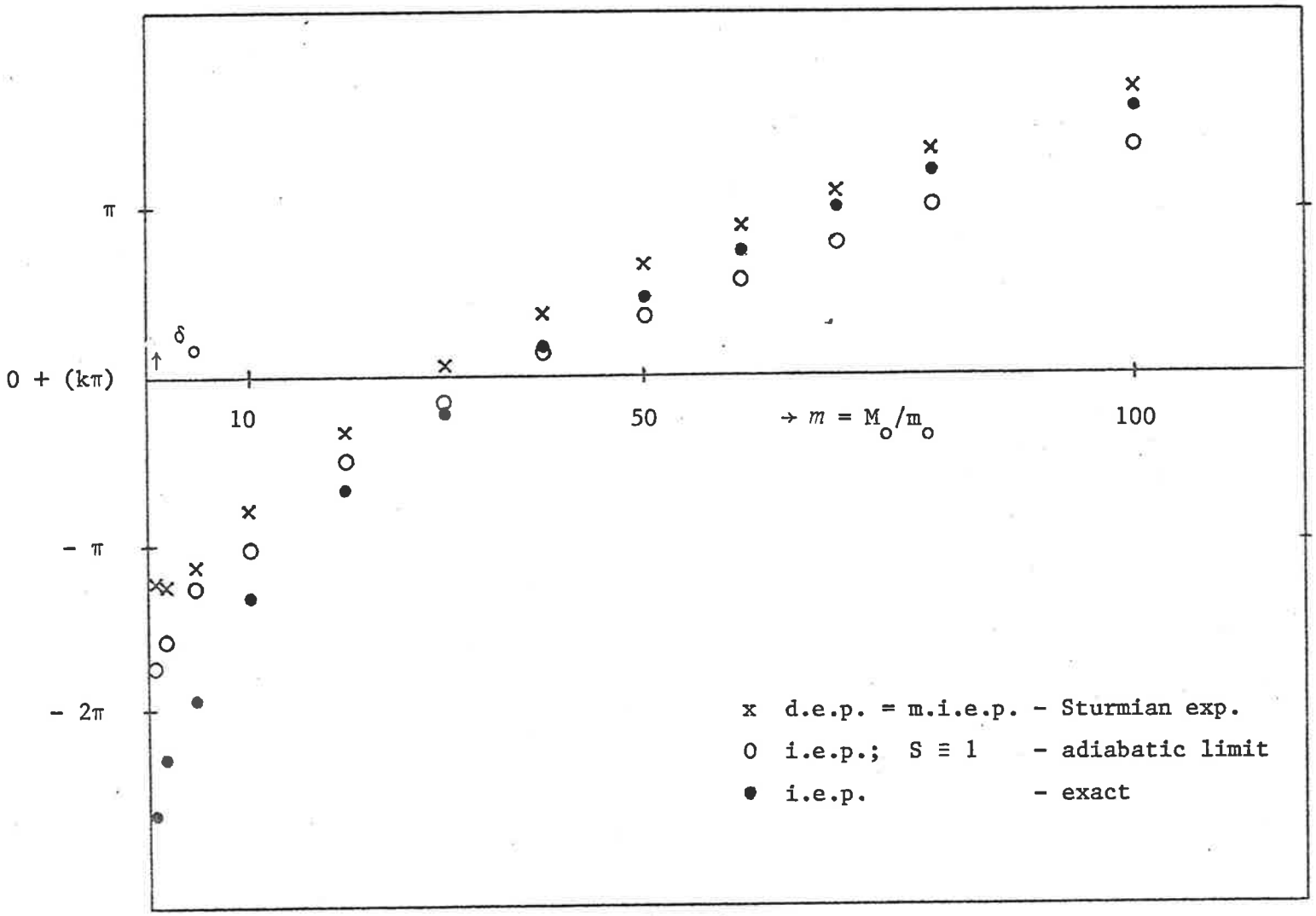


Fig. 7.10: The phase-shift as a function of the mass ratio $m$. Comparison of calculation using the Sturmian expansion (x), the exact formulation with enforced adiabatic condition (O) and the exact formulation (• ).

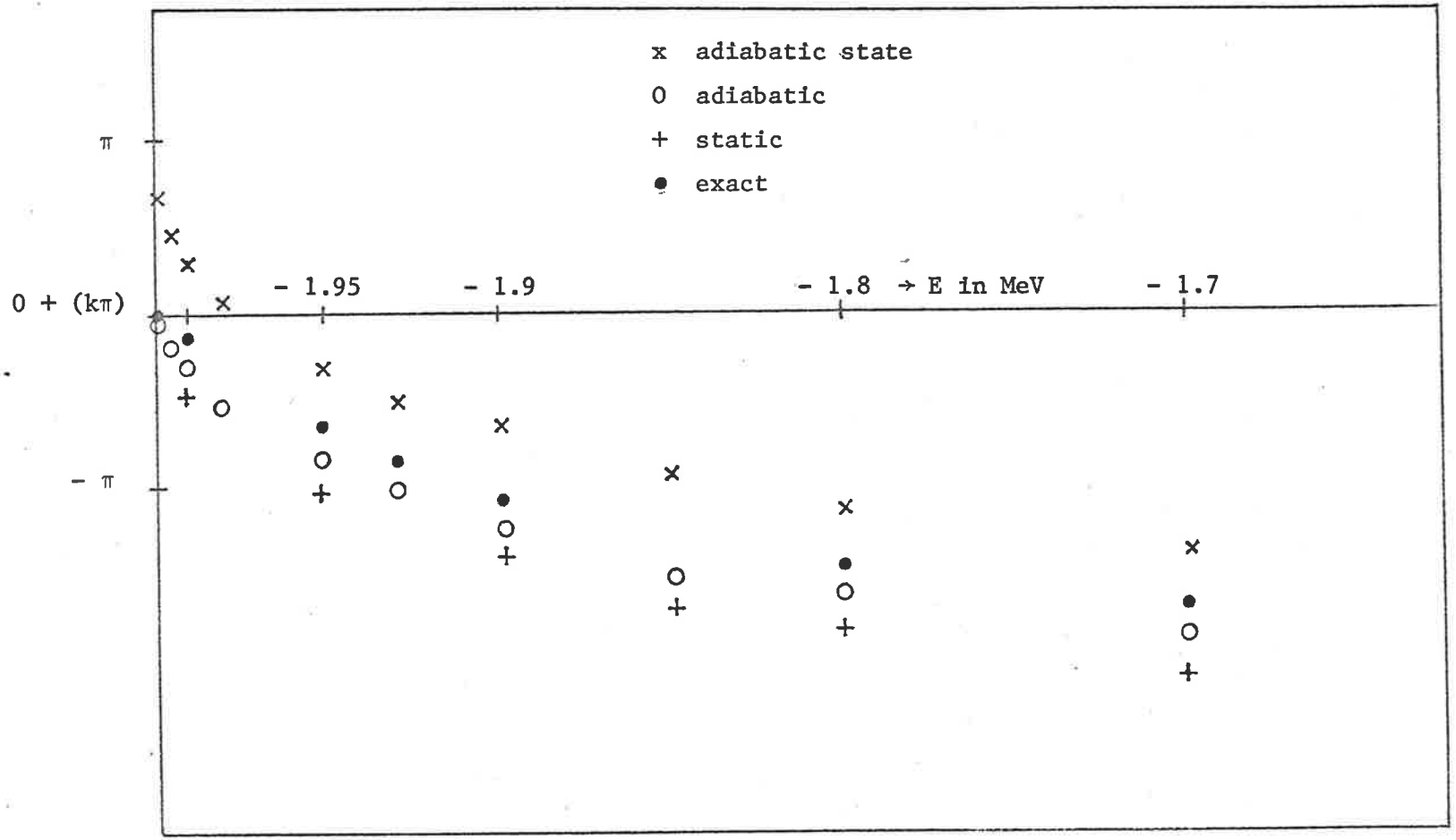


Fig. 7.11: Comparison of the phase shift calculated by the i.e.p. with the various limits enforced and for varying three-body centre-of-mass energy. Binding energy is 2 MeV, hence zero kinetic energy for E = - 2 MeV.

And the kernel therefore behaves as

$$2\mu C \frac{p''^2}{\bar{k}_o^2 - p''^2} \frac{1}{p'p''} Q_o\left[\frac{-2m_o E_\phi - p'^2 - p''^2}{2p'p''}\right] \{S_o(p') S_o(p'') j_o^2(p'r_o) j_o^2(p''r_o)\}$$

$$\sim \frac{2\mu C}{k_o} \frac{p''^2}{\bar{k}_o^2 - p''^2} \frac{1}{k_o^2 + p'^2 + p''^2} \{(p'p'')^{3/2} \frac{\sin^2(p'r_o) \sin^2 p''r_o)}{p'^2 p''^2 r_o^2}\} . \quad (7.7)$$

The discrepancy between the adiabatic limit calculation and the exact results can be attributed to the long range behaviour of the kernel and the half-on-shell amplitude. As is clear from (7.7) a significant contribution to the kernel is expected from the region where (7.4) is valid. An interesting observation is that the kernel even becomes non-compact if first the zero range limit is applied to the left hand side of Eq. (7.7). The Bessel functions become identical to the unit value and hence their converging power is lost.

In both tests a better agreement of the exact result and the Sturmian expansion could then be expected if the range of the amplitude is reduced. This would occur in the case of more rapidly converging form factors. In their bound state calculations Fonseca and Shanley use

$$f = \frac{1}{(p^2 + \beta^2)^3} ,$$

which may be a contributing factor in the excellent agreement of the adiabatic and three-body bound state energies. The present calculations raise the question of whether this agreement would be preserved in the case of local interactions especially in the scattering domain.

# CHAPTER 8

## DISCUSSION

Our aim has been to present a calculable model for a heavy ion rearrangement scattering process using delta shell interactions. In Chapter 2 we derived the integral equation for the half-on-shell scattering amplitude, using the Faddeev equations. It was realized that there are three levels at which the core-core interaction can be incorporated in the model.

The form factors for the delta shell interaction in momentum space are proportional to spherical Bessel functions. These are entire functions which become singular at infinity off the real axis. This prevented the use of contour rotations, the standard method for solving this type of integral equation. We have used an integral path that stretches along the real line, a scheme described by Larson and Hetherington. This scheme was augmented at a number of places. A greater freedom in distributing the mesh points resulted from using them solely as interpolation points and not as integration points as well. As a result, fewer special situations needed to be considered. A complete mathematical description was given of the logarithmic singularity. We showed explicitly that this singularity reduced to a simple pole for the off-shell momentum equal to zero. We also have emphasized the necessity of avoiding interpolation by polynomials across the square root branch point. This was supported by the examples of calculated half-on-shell amplitudes displayed in Chapter 7.

Calculations were carried out for s-state to s-state scattering in

$$C^{12} + C^{13} \rightarrow C^{12} + C^{13} \ .$$

Only the core-valence particle interaction has been taken into account. The radius of the delta shell potential was, for practical reasons, fixed at .1 fm. This restricted the number of significant terms in the

factorization of the form factor. The half-on-shell amplitudes, phase shifts and cross section were obtained for centre-of-mass energies of 1, 5, 10 and 50 MeV. The binding energy was set at 2 MeV. The differential cross sections all showed two peaks, one in the forward direction and one in the backward direction. This indicated that the two competing processes: the elastic and the rearrangement scattering took place without causing much deflection. The cross section reduced for increasing energy, as the particles had less time to "see each other.

Often physical data is used to test model calculations. Since the delta shell is an idealized interaction, the need was felt to design a new solution scheme which could act as a testing ground. For this, the energy in the reaction was restricted to the adiabatic domain. The wave function, describing the particle-core subsystem was expanded in a completely discrete set of states: the Sturmian expansion. The method, which is completely rigorous, is shown to be compatible with the close-coupling scheme, where the subsystem is expanded in bound states and continuum states.

In the static limit the mass ratio $m$ of core and valence particle is assumed to be much greater than one. Under this condition the problem is formulated as a differential equation. The two approaches gave excellent agreement for different values of the delta shell radius, when the same restrictions were enforced in the integral equation.

The effects of the static and adiabatic restriction on the integral equation have been compared with the exact calculations. This shows that the static limit region sets in for $m > 30$. The comparisons did not give an indication for what range of energies the adiabatic limit would be valid. The half-on-shell amplitude is too long ranged and the interaction is not suited for this type of problem.

We have mainly concentrated our efforts in two areas. First of all: the numerical solution to an integral equation, integrating along the real line and treating carefully the singular structure of the kernel. It is this problem that most likely inhibited the use of delta shell interactions in the three-dimensional, three-body scattering problem. Secondly, we developed a different technique to test our calculations, since a comparison with a physical experiment is not possible.

In the time available we have not been able to extend the research any further than the s-state to s-state scattering for small-radius delta shell interactions. There are a number of directions the studies can go from here. A more realistic situation is obtained when the radius becomes of the order of a few fermi. This means that more terms have to be included in the factorization of the form factor, and hence the computer time will increase. The importance of multiple scattering can be studied in more realistic cases. The basic calculation of the matrix elements can be carried out by the existing program. The matrix inversion would have to be redesigned, but that is a simple excercise. The core-core interaction should be included, using the methods developed here. The intermediate level should already give some indication of the influence that these forces have on the scattering amplitude. Calculations comparing the exact amplitudes of the model with DWBA amplitudes for the model should be carried out.

## APPENDIX A

### Derivation of 2.33

$$\text{Amp} = \sum_{\alpha} \tfrac{1}{2}\{X_{1\sigma,1\alpha} + X_{2\sigma,1\alpha} + \bar{X}_{1\sigma,2\alpha} + \bar{X}_{2\sigma,2\alpha}\} .$$

$$X_{11} = Z_{12}\,\tau_2\,X_{21} + Z_{13}\,\tau_3\,X_{31} \qquad \bar{X}_{12} = Z_{12} + Z_{12}\,\tau_2\,\bar{X}_{22} + Z_{13}\,\tau_3\,\bar{X}_{32}$$

$$X_{21} = Z_{21} + Z_{21}\,\tau_1\,X_{11} + Z_{23}\,\tau_3\,X_{31} \qquad \bar{X}_{22} = Z_{21}\,\tau_1\,\bar{X}_{12} + Z_{23}\,\tau_3\,\bar{X}_{32}$$

$$X_{31} = Z_{31} + Z_{31}\,\tau_1\,X_{11} + Z_{12}\,\tau_2\,X_{21} \qquad \bar{X}_{32} = Z_{32} + Z_{31}\,\tau_1\,\bar{X}_{12} + Z_{32}\,\tau_2\,\bar{X}_{23}$$

$$A = X_{11} + \bar{X}_{12} = Z_{12} + Z_{12}\,\tau\,(X_{21} + \bar{X}_{22}) + Z_{13}\,\tau_3\,(X_{31} + \bar{X}_{32})$$

$$B = X_{21} + \bar{X}_{22} = Z_{21} + Z_{21}\,\tau\,(X_{11} + \bar{X}_{12}) + Z_{23}\,\tau_3\,(X_{31} + \bar{X}_{32})$$

$$C = X_{31} + \bar{X}_{32} = Z_{31} + Z_{32} + Z_{31}\,\tau\,(X_{11} + \bar{X}_{12}) + Z_{32}\,\tau\,(X_{21} + \bar{X}_{22})$$

$$A = Z_{12} + \sum_{\beta} Z_{12}\,\tau\,B + \sum_{\gamma} Z_{13}\,\tau_3\,C$$

$$(-)^{\sigma} B = (-)^{\alpha} Z_{12} + \sum_{\beta} (-)^{\beta} Z_{12}\,\tau\,A + \sum_{\gamma} (-)^{\gamma} Z_{13}\,\tau_3\,C$$

$\sigma$ even:

$$A + B = [1 + (-)^{\alpha}]\,Z_{12} + \sum_{\beta} (-)^{\beta} Z_{12}\,\tau\,[A + (-)^{\beta} B] + \sum_{\gamma} (-)^{\gamma} Z_{13}\,\tau_3\,[1 + (-)^{\gamma} C]$$

$$C = [1 + (-)^{\alpha}]\,Z_{31} + \sum_{\beta} Z_{31}\,\tau\,A + \sum_{\gamma} (-)^{\sigma} Z_{31}\,\tau\,(-)^{\gamma} B$$

$$(-)^{\sigma} C = [1 + (-)^{\alpha}]\,Z_{31} + \sum_{\beta} Z_{31}\,\tau\,(-)^{\beta} B + \sum_{\gamma} (-)^{\sigma} Z_{31}\,\tau\,A$$

$$[1 + (-)^{\sigma}]\,C = 2[1 + (-)^{\alpha}]\,Z_{31} + 2\sum_{\beta} Z_{31}\,\tau\,[A + (-)^{\beta}]B$$

$$D_{\sigma} = [A + (-)^{\sigma} B] = [1 + (-)^{\alpha}]\,Z_{12} + \sum_{\beta} (-)^{\beta} Z_{12}\,\tau\,[A + (-)^{\beta} B] + 2\sum_{\gamma} (-)^{\gamma} Z_{13}\,\tau_3\,[1 + (-)^{\alpha}]\,Z_{31} + 2\sum_{\gamma\beta} (-)^{\gamma} Z_{13}\,\tau_3\,Z_{31}\,\tau\,[A + (-)^{\beta} B]$$

$$D_\sigma = [1 + (-)^\alpha]\ [Z_{12} + 2 \sum_\gamma (-)^{\sigma+\gamma} Z_{13}\ \tau_3\ Z_{31}]$$

$$+ \sum_\beta (-)^\beta [Z_{12} + 2 \sum_\gamma (-)^{\beta+\gamma} Z_{13}\ \tau_3\ Z_{31}]\ \tau\ D_\beta$$

$\sigma$ odd:

$$A + B = A - (-)^\sigma B = [1 - (-)^\alpha]\ Z_{12}$$

$$- \sum_\beta (-)^\beta Z_{12}\ \tau\ [A - (-)^\beta B] - \sum_\gamma (-)^\gamma Z_{13}\ \tau_3\ [1 - (-)^\gamma]\ C$$

$$C = [1 - (-)^\alpha]\ Z_{31} + \sum_\beta Z_{31}\ \tau\ A - \sum_\gamma Z_{31}\ \tau\ (-)^\gamma B$$

$$[1 - (-)^\sigma] C = 2[1 - (-)^\alpha]\ Z_{31} + 2 \sum_\gamma Z_{31}\ \tau\ [A - (-)^\gamma] B$$

$$D_\sigma = A - (-)^\sigma B = [1 - (-)^\alpha]\ [Z_{12} - 2 \sum_\gamma (-)^\gamma Z_{13}\ \tau_3\ Z_{31}]$$

$$- \sum_\beta (-)^\beta [Z_{12} + 2 \sum_\gamma Z_{13}\ \tau_3\ (-)^{\beta+\gamma} Z_{31}]\ \tau\ D_\beta$$

$$D_\sigma = [1 + (-)^{\sigma+\alpha}]\ [Z_{12} + 2 \sum_\gamma (-)^{\sigma+\gamma} Z_{13}\ \tau_3\ Z_{31}]$$

$$+ \sum_\beta (-)^{\sigma+\beta} [Z_{12} + 2 \sum_\gamma (-)^{\beta+\gamma} Z_{13}\ \tau_3\ Z_{31}]\ \tau\ D_\beta$$

hence $\sigma$ odd and even

$$\text{Amp} = \sum_\alpha \tfrac{1}{2} [X_{1\sigma,1\alpha} + X_{2\sigma,1\alpha} + \bar{X}_{2\sigma,1\alpha} + \bar{X}_{2\sigma,2\alpha}] = \sum_\alpha \tfrac{1}{2} D_{\sigma,\alpha}$$

$$D_{\sigma,\alpha} = [1 + (-)^{\sigma+\alpha}]\ [Z_{12} + 2 \sum_\gamma (-)^{\sigma+\gamma} Z_{13}\ \tau_3\ Z_{31}]$$

$$+ \sum_\beta (-)^{\sigma+\beta} [Z_{12} + 2 \sum_\gamma (-)^{\beta+\gamma} Z_{13}\ \tau_3\ Z_{31}]\ \tau\ D_{\beta,\alpha}$$

## APPENDIX B

### Derivation of Eq. (2.43)

$$A^o_{ij} = V^o_{ij} + \sum_k V^o_{ik}\, g_o\, A^o_{kj} \tag{B1}$$

$$A_{ij} = V_{ij} + \sum_k V_{ik}\, g_o\, A_{kj} \tag{B2}$$

$$V_{ij} = V^o_{ij} + |\theta_i\rangle\ c_{ij} \langle \phi_j| \ . \tag{B3}$$

Subtracting B1 from B2

$$X_{ij} = A_{ij} - A^o_{ij} = |\theta_i\rangle c_{ij} \langle \phi_j| + \sum_k V^o_{ik}\, g_o\, X_{kj}$$

$$+ \sum_k |\theta_i\rangle c_{ij} \langle \phi_j|\, g_o\, A_{kj} \ . \tag{B4}$$

Define

$$\Omega_{ij} = (\delta_{ij} - V^o_{ij}\, g_o) = (\delta_{ij} + A_{ij}\, g_o)^{-1} \ , \tag{B5}$$

rearrange (B4) and express the last term in $X_{kj}$, then multiply from the left by $\Omega^{-1}_{\ell i}$ and sum over i:

$$X_{\ell j} = \sum_i \Omega^{-1}_{\ell i}\ |\theta_i\rangle\ c_{ik} \langle \phi_k|\ (\delta_{kj} + g_o\, A^o_{kj})$$

$$+ \sum_{ki} \Omega^{-1}_{\ell i}\ |\theta_i\rangle c_{ik} \langle \phi_k|\, g_o\, X_{kj} \ . \tag{B6}$$

Define

$$\phi_{ij} = \delta_{ij} - \sum_k \langle \phi_i|\, g_o\, \Omega^{-1}_{ik}\ |\theta_k\rangle\ c_{kj} \ . \tag{B7}$$

So

$$\langle \phi_m|\, g_o\, X_{mj} = \sum_{\ell ki} \phi^{-1}_{m\ell} \langle \phi_\ell|\, g_o\, \Omega^{-1}_{\ell i}\ |\theta_i\rangle\ c_{ik} \langle \phi_k|\ (\delta_{kj} + g_o\, A^o_{kj}) \ . \tag{B7}$$

Substitute (B5) in (B6)

$$X_{\ell j} = \sum_{ikm} \Omega^{-1}_{\ i}\ |\theta_i\rangle\ c_{ik}\ \phi^{-1}_{km} \langle \phi_m|\ (\delta_{mj} + g_o\, A^o_{mj}) \ , \tag{B9}$$

and expressed in $A^o$

$$A_{ij} = A^o + \sum_{k\ell} (\delta_{ik} + A^o{}_{ik}\, g_o)\, |\theta_k\rangle\, \Phi_{k\ell}\, \langle\phi_\ell|\, (\delta_{\ell j} + g_o\, A^o_{\ell j}) \quad , \tag{B10}$$

where

$$\Phi^{-1}_{k\ell} = c^{-1}_{k\ell} - \sum_m \langle\phi_k|\, g_o\, (\delta_{km} + A^o_{km}\, g_o\, |\theta_m\rangle \quad . \tag{B11}$$

## APPENDIX C

### Separability of the Core Induced Part of the Potential $\tilde{V}$

The integral part of the potential (c.f. 2.34) is

$$2 \sum_{\gamma} \int d^3p'' \; (-)^{\beta+\gamma} \; Z_{1\beta,3\gamma}(\vec{p}',\vec{p}'') \; \tau_{3\gamma}\left(E - \frac{p''^2}{2\mu}\right) \; Z_{3\gamma,1\alpha}(\vec{p}'',\vec{p}) \quad . \quad (C1)$$

The $Z_{3\gamma,1\alpha}$ has the same form as the $Z_{1\beta,3\gamma}$ and can be written as

$$Z_{3\gamma,1\alpha}(\vec{p}'',\vec{p}) =$$

$$f^{*}_{3\gamma}(-\vec{p} - \tfrac{1}{2}\vec{p}\,) \; \frac{1}{E - \frac{m_o + M_o}{2m_o M_o} p''^2 - \frac{p^2}{2M_o} - \frac{\vec{p}'' \cdot \vec{p}}{M_o}} \; f_{1\alpha}\left(\vec{p}'' + \frac{m_o}{m_o + M_o}\vec{p}\right) . \quad (C2)$$

Hence the initial and final momenta are coupled by the form factors and the propagators. For the delta shell interaction one can factorize the form factors (see 3.5). In the static limit (where $M_o >> m_o$) C2 reduces to

$$Z_{3\gamma,1\alpha}(\vec{p}'',\vec{p}) =$$

$$\sum_{\gamma'\gamma''} c \; f_{3\gamma'}(-\vec{p}) \; f_{3\gamma''}(-\tfrac{1}{2}p'') \; \frac{2m_o}{2m_o E - p''^2} \; f_{1\alpha}(\vec{p}'') \quad . \quad (C3)$$

Here the constant c couples the angular momentum quantum numbers and contains some normalization factors. The integration over $p''$ in C1 can be carried out under these conditions and the desired form for the integral part follows.

## APPENDIX D

### Asymptotic Behaviour of the S-Function

With the help of function

$$D_\ell(k) = k\, j_\ell(ikr_o)\, h_\ell^{(1)}(ikr_o) \tag{D1}$$

one can write the defining equation (3.14) for the $S_\ell$ as

$$S_\ell^{-2}(k) = \frac{2k_\ell}{F_\ell(k_\ell)} \frac{D_\ell(k_\ell) - D_\ell(k)}{k_\ell^2 - k^2} , \tag{D2}$$

with

$$F_\ell(k) = \frac{\partial}{\partial k} D_\ell(k) , \tag{D3}$$

where $k\ (\equiv k_i)$ and $k_\ell$ are as defined in (3.15) and (3.9). The main interest is centred in the case of $\ell = 0$. Expressing the spherical Bessel and Hankel functions in exponentials, one gets

$$D_o(k) = \frac{1}{2kr_o^2} [e^{-2kr_o} - 1] . \tag{D4}$$

In the adiabatic limit the $k^2$ is approximated by

$$k^2 \approx k_o^2 + \frac{\xi(2+\xi)}{(1+\xi)^2} p^2 \approx k_o^2 + 2\xi\, p^2 , \tag{D5}$$

for a mass ratio $m_o/M_o = \xi << 1$. The $F_o(k)$ are then expanded in

$$h = \xi \frac{p^2}{k_o} , \tag{D6}$$

around $k_o$. It is straightforward to show that

$$F_o(k) = F_o(k_o + h) = F_o(k_o) + \frac{h}{k_o} G(k_o r_o) + O(h^2) , \tag{D7}$$

with

$$G(k_o r_o) = \frac{1}{k_o r_o^2} \left(e^{-2k_o r_o} - 1\right) + \frac{2}{k_o r_o} e^{-2k_o r_o} + 2 . \tag{D8}$$

Note that G becomes zero in the limit of $r_o$ to zero. This is not unexpected since $F_o$ approaches the unit value in the same limit irrespective of the

value of k. If h is small one can reformulate D2, using D7. The $S_o$ then becomes

$$S_o^{-2}(k) = \frac{2k_o}{F_o(k_o)} \frac{1}{k + k_o + h} \left[ F_o(k) + \frac{h}{k_o} G(k_o r_o) \right] . \qquad (D9)$$

For large values of k and $r_o$ and small $k_o$ (i.e. $2kr_o > 3$, and $2k_o r_o \ll 1$) one derives, by differentiating D4 and expanding the result in $k_o r_o$, that

$$F_o(k_o) = 1 - \frac{4}{3} k_o r_o + \ldots , \qquad (D10)$$

and

$$\frac{D_o(k_o) - D_o(k)}{k_o^2 - k^2} \sim \frac{D_o(k)}{k^2} = - \frac{1}{2k^3 r_o^2} + \ldots . \qquad (D11)$$

As a result one finds the asymptotic form for the S function

$$S_o^2(r) = - (2m)^{3/2} r_o^2 \frac{p^3}{k_o} . \qquad (D12)$$

## REFERENCES


1. G. R. Satchler, Rev. of Mod. Phys., 50, 1 (1978).
2. W. Tobocman, *Theory of Direct Nuclear Reactions*, (Ocford Univ. Press, London, 1961).
3. N. Austern, *Direct Nuclear Reaction Theories*, (Wiley, Interscience, New York, 1970).
4. P. J. A. Buttle and L. J. B. Goldfarb, Nucl. Phys. 78, 409 (1966).
5. G. R. Satchler, Symposium on Heavy-Ion Transfer Reactions, Argonne, Illinois, 1973 (Argonne Physics Division, Informal Report PHY-1973B) pp. 145-159.
6. P. Braun-Munzinger and H. L. Harney, Nucl. Phys. A233, 311, 1974.
7. B. A. Robson, Int. Conference on Nuclear Reactions, Canberra 1978, Ed. B. A. Robson, (Springer-Verlag, Berlin, 1978) pp. 16-27.
8. P. S. Hauge, Nucl. Phys. A223, 394 (1974).
9. L. R. Dodd, *Nuclear Spectroscopy and Nuclear Reactions with Heavy Ions*, (LXII Corso, Editrice Compositori, Bologna, Italy, 1976) pp. 550-555.
10. R. Aaron and P. E. Shanley, Phys. Rev. 142, 608 (1966).
11. P. E. Shanley and R. Aaron, Ann. Phys. 44, 363 (1967).
12. A. S. Reiner and A. I. Jaffe, Phys. Rev. 161, 935 (1967).
13. K. King and B. H. J. McKellar, Phys. Rev. C9, 1309 (1974).
14. E. F. Redish, *Modern Three Hadron Physics*, Ed. A. W. Thomas (Springer-Verlag, Berlin, 1977).
15. H. P. Gudler, G. R. Plattner, I. Sick, A. Traber, W. Weiss, Nucl. Phys. A284, 114 (1977).
16. A. Gobbi, U. Matter, J.-L. Perrenoud, P. Marmier, Nucl. Phys. A112, 537 (1968).
17. W. von Oetzen, Nucl. Phys. A148, 529 (1970).

18. G. Bauer and C. K. Gelbke, Nucl. Phys. A204, 138 (1973).

19. G. R. Satchler, Proc. of the Int. Conference on Nuclear Physics, Munich 1973, Ed. J. de Boer and H. J. Mang, (North-Holland Publ., 1973) p. 570.

20 A. N. Mitra, Nucl. Phys. 32, 529 (1962).

21. A. N. Mitra and V. S. Bhasin, Phys. Rev. 131, 1265 (1963).

22. J. B. McGuire, Jnl. Math. Phys., 5, 622 (1964).

23. C. N. Yang, Phys. Rev. 168, 1920 (1968).

24. C. K. Majumbar, Jnl. Math. Phys., 13, 705 (1972).

25. J. B. McGuire and C. A. Hurst, Jnl. Math. Phys., 13, 1595 (1972).

26. L. R. Dodd, Austr. J. of Phys., 25, 507 (1972).

27. R. van Wageningen, J. H. Stuivenberg, J. Bruinsma, G. Evans, Proc. Int. Conference on Few Particle Problems in the Nuclear Interaction, Los Angeles, 1972, Ed. I. Slaus, S. A. Moszkowski, R. P. Haddock and W. T. H. van Oers (North-Holland Publ., 1972) p. 453.

28. R. D. Puff, Ann. of Phys., 13, 317 (1961).

29. J. Borysowicz and J. Dabrowski, Phys. Lett., 24B, 549 (1967).

30 J. Dabrowski and M. Dworzecka, Phys. Lett., 28B, 4 (1968).

31. N. M. Larson and J. H. Hetherington, Phys. Rev., C9, 699 (1974).

32. K. M. Watson and J. Nuttall, *Topics in Several Particle Dynamics*, (Holden-Day Inc., Cal., 1967), Chapter 4.

33. L. D. Faddeev, *Mathematical Aspects of the Three-Body Problem in the Quantum Scattering Theory*, (Israel Program for Scientific Translations, Jerusalem 1965).

34. C. B. Lovelace, Phys. Rev. 135, B2225 (1964).

35. R. D. Amado, Phys. Rev. 132, 485 (1963).

36. C. J. Joachain, *Quantum Collision Theory*, (North-Holland Publ., 1975), Chapter 16.6.

37. M. Rotenberg et al. *The 3-j and 6-j Symbols*, (Cambridge, M.I.T., 1959).

38. A. Messiah, *Quantum Mechanics*, (North-Holland Publ.,)

39. I. R. Afnan and A. W. Thomas, *Modern Three Hadron Physics*, Ed. A. W. Thomas, (Springer-Verlag, 1977).

40. Handbook of Mathematical Functions, ed. M. Abramowitz and I. A.Stegun, (Dover Publ. Inc., New York).

41. E. W. Schmid and H. Ziegelmann, *The Quantum Mechanical Three-Body Problem*, (Pergamon, 1974).

42. J. H. Hetherington and L. H. Schick, Phys. Rev. B137, 935 (1965).

43. R. Aaron and R. D. Amado, Phys. Rev. 150, 857 (1966).

44. R. T. Cahill and I. H. Sloan, Nucl. Phys., A165, 161 (1971).

45. Y. Avishai, Phys. Rev. D3, 3232 (1971).

46. W. Ebenhöh, Nucl. Phys., A191, 97 (1972).

47. E. W. Schmid and H. Ziegelmann, Phys. Lett., 34B, 579 (1971).

48. P. Doleshall, Nucl. Phys. A201, 264 (1973).

49. H. Antes, Num. Math., 19, 116 (1972).

50. V. I. Krylov and A. A. Pal'tsev, *Tables for Numerical Integration of Functions with Logarithmic and Power Singularities*, (Israel Program for Scientific Translation, Jerusalem, 1971).

51. G. Breit and M. E. Ebel, Phys. Rev. 103, 679 (1956).

52. T. Y. Wu and T. Ohmura, *Quantum Theory of Scattering*, (Prentice Hall, 1962), Sec. M5.

53. W. von Oetzen and H. G. Bohlen, Physics Reports, 19C, No. 1 (1975).

54. S. Weinberg, Phys. Rev. 131, 440 (1963).

55. K. Meetz, Jnl. Math. Phys., 3, 690 (1962).

56. R. Newton, *Scattering Theory of Waves and Particles*, (McGraw-Hill, New York, 1966), Chapter 9.

57. L. R. Dodd and K. J. Nieukerke, (to be published).

58. System /360. Scientific Subroutine Package, IBM Program HPCL.

59. A. C. Fonseca and P. E. Shanley, Ann. of Phys., Vol. 117, No. 2, p.268, 1979.